REHABILITATION OF BUILDING STRUCTURES WITH SOFT STORY IRREGULARITY VIA OPTIMAL VISCOUS DAMPER DISTRIBUTION

YUMUŞAK KAT DÜZENSİZLİĞİ BULUNAN YAPILARIN OPTİMAL VİSKOZ SÖNÜMLEYİCİ DAĞILIMI İLE REHABİLİTASYONU

ARCAN KÖROĞLU

ASSOC. PROF. DR. BAKİ ÖZTÜRK

Supervisor

PROF. DR. ERSİN AYDIN

2nd Supervisor

Submitted to

Graduate School of Science and Engineering of Hacettepe University

as a Partial Fulfillment to the Requirements

for the Award of the Degree of Master of Science

in Civil Engineering

May 2022

To My Mother and Father...

ABSTRACT

REHABILITATION OF BUILDING STRUCTURES WITH SOFT STORY IRREGULARITY VIA OPTIMAL VISCOUS DAMPER DISTRIBUTION

Arcan KÖROĞLU

Master of Science, Civil Engineering

Supervisor: Assoc. Prof. Dr. Baki ÖZTÜRK

2nd Supervisor: Prof. Dr. Ersin AYDIN

May 2022, 180 pages

Application of viscous dampers in structural and earthquake engineering as passive energy damping devices has become popular in last couple of decades. Research on application of viscous dampers in building structures to reduce seismic response started at 1990s. Nowadays application of viscous dampers is still an important topic in the field of structural and earthquake engineering. Viscous damper applications in building structures has two major objectives. These are designing more resilient structures and rehabilitating existing structures. Design of viscous dampers are similar to the design of the structural components of the building structures. Distribution of the viscous dampers has a great influence on seismic behavior of the structure. Viscous dampers are expensive passive energy damping devices; therefore, optimal damper distribution in building structure is an important subject. Extensive research on optimum viscous damper distribution via meta-heuristic search algorithms started at late 1990s. Application of meta-heuristic search algorithms on optimal damper distribution problems has important advantages. These are they do not require a preliminary design, they do not require gradient information, and they require significantly

low computational time when they are compared with exhaustive search methods. In this thesis work a methodology based on peak inter story drift ratios is proposed to rehabilitate building structures with soft story irregularity via optimal viscous damper distribution. Soft story structural irregularity is a type of vertical structural irregularity that is caused by abrupt stiffness changes between adjacent stories. These structures suffer from severe structural damages after earthquakes due to abnormal peak inter story drift ratios. This study proposes a methodology to keep peak inter story drift ratios in an allowable limit by optimal viscous damper distribution. Two different meta-heuristic search algorithms are utilized to find optimal viscous damper distributions. These are Differential Evolution and Particle Swarm Optimization algorithms. The suggested methodology is numerically tested on different shear buildings under different earthquake ground motion records, and results are compared with no viscous damper case and optimum damper distribution case.

Keywords: Earthquake Engineering, Meta-Heuristic Search Algorithms, Optimal Viscous Damper Distribution, Seismic Rehabilitation, Soft Story Structural Irregularity.

ÖZET

YUMUŞAK KAT DÜZENSİZLİĞİ BULUNAN YAPILARIN OPTİMAL VİSKOZ SÖNÜMLEYİCİ DAĞILIMI İLE REHABİLİTASYONU

Arcan KÖROĞLU

Yüksek Lisans, İnşaat Mühendisliği

Danışman: Doç. Dr. Baki ÖZTÜRK

Eş Danışman: Prof. Dr. Ersin AYDIN

Mayıs 2022, 180 sayfa

Yapı ve deprem mühendisliğinde viskoz sönümleyicilerin pasif enerji sönümleyici olarak uygulamaları son yıllarda popüler hale gelmiştir. Viskoz sönümleyicilerin bina türü yapılarda sismik tepkiyi azaltmak amacı ile kullanmasına ilişkin çalışmalar 1990'lı yıllarda başlamıştır. Günümüzde viskoz sönümleyicilerin kullanılması halen yapı ve deprem mühendisliğinde önemli bir konudur. Temel olarak bina türü yapılarda viskoz sönümleyici uygulamalarında iki amaç vardır. Bu amaçlardan biri daha dirençli yapılar tasarlamak diğeri ise var olan yapıları rehabilite etmektir. Bina türü yapılarda viskoz sönümleyicilerin tasarımı yapısal elemanların tasarımına oldukça benzemektedir. Yapılarda viskoz sönümleyicilerin dağılımı yapının sismik davranışını önemli bir şekilde etkilemektedir. Viskoz sönümleyiciler maliyetli pasif sönümleyici cihazlarıdır bu sebeple bina türü yapılarda viskoz sönümleyicilerin optimal dağılımı önemli bir konudur. Meta-sezgisel arama algoritmaları kullanılarak optimal viskoz sönümleyici dağılımının bulunması ile ilgili yoğun araştırmalar 1990'ların sonunda başlamıştır. Optimal viskoz sönümleyici dağılımı problemlerinde meta-sezgisel arama algoritmaları uygulamalarının önemli avantajları bulunmaktadır. Bu avantajlar şu şekildedir, bir ön tasarıma ve gradyan bilgisine ihtiyaç yoktur. Ayrıca meta-sezgisel arama yöntemleri

tam kapsamlı arama yöntemlerine kıyasla önemli ölçüde daha az hesaplama zamanına ihtiyaç duymaktadırlar. Bu tez çalışmasında katlar arası maksimum göreli kat ötelemesi oranları esas alınarak yumuşak kat yapısal düzensizliği bulunan yapıların optimal viskoz sönümleyici dağılımı ile rehabilitasyonu hedefleyen bir metodoloji önerilmiştir. Yumuşak kat düzensizliği düşeyde bir yapısal düzensizlik olup, katlar arası düzensiz ve ani rijitlik değişimleri sonucunda meydana gelmektedir. Bu tür yapılar depremler sonrasında anormal göreli kat ötelemeleri sonucunda ağır hasarlar almaktadır. Bu çalışma göreli kat ötelemesi oranlarını optimal viskoz sönümleyici dağılımı ile izin verilebilir sınırlarda tutmayı hedefleyen bir metodoloji önermektedir. Bu çalışmada optimal viskoz sönümleyici dağılımını bulmak için iki farklı meta-sezgisel arama algoritması kullanılmıştır. Bunlar Diferansiyel Evrim ve Parçacık Sürüsü Optimizasyonu algoritmalarıdır. Önerilen metodoloji farklı yapılar için farklı deprem yer hareketi kayıtları kullanılarak nümerik olarak test edilmiştir. Çalışmanın bulguları viskoz sönümleyici olmayan durum ve optimal viskoz sönümleyici dağılımı olan durum için karşılaştırılmıştır.

Keywords: Deprem Mühendisliği, Meta-Sezgisel Arama Yöntemleri, Optimal Viskoz Sönümleyici Dağılımı, Sismik Rehabilitasyon, Yumuşak Kat Yapısal Düzensizliği.

ACKNOWLEDGEMENTS

First of all, I would like to express my deepest thanks and gratitude to Assoc. Prof. Dr. Baki Öztürk, my supervisor, for the guidance, encouragement, optimism, valuable advice and continuous understanding during my thesis study. I am profoundly grateful for the lessons that I have learned from Dr. Öztürk.

Also, I would like to express my special thanks and gratitude to Prof. Dr. Ersin Aydın, my co-supervisor, for his valuable help and comments on my thesis study.

I have to give thanks to Assoc. Prof. Dr. Baki Öztürk, Prof. Dr. Ersin Aydın, Prof Dr. Safa Bozkurk Coşkun, Prof. Dr. Orhan Doğan, Assoc. Prof. Dr. Mustafa Kerem Koçkar, and Asst. Prof. Dr. Burcu Güldür Erkal for giving me the opportunity to defend my thesis.

I would like to express my sincere thanks to Prof. Dr. Mustafa Şahmaran, Assoc. Prof. Dr. Alper Aldemir, and Asst. Prof. Dr. Burcu Güldür Erkal for their continuous help and encouragement during my graduate study.

I would like to express my deepest thanks to Assoc. Prof. Dr. Saeid Kazemzadeh Azad, Asst. Prof. Dr. Ertan Sönmez, Asst. Prof. Dr. Saman Aminbakhsh, and Asst. Prof. Dr. Ebru Akış for their continuous encouragement since the day I started to my undergraduate degree.

Lastly but most importantly, I would like to thank to my mother Dilek Köroğlu and my father Gökhan Köroğlu for their endless support to me. This accomplishment would not have been possible without their limitless support.

Arcan Köroğlu

May 2022, Ankara

CONTENTS

Page

ABSTRACT i
ÖZET iii
ACKNOWLEDGEMENTS v
CONTENTS vi
TABLES x
FIGURES xii
SYMBOLS AND ABBREVIATIONS xxv
1. INTRODUCTION 1
1.1. Introduction 1
1.2. Organization 2
1.3. Previous Works 3
2. SOFT STORY STRUCTURAL IRREGULARITY 7
2.1. General Review of Soft Story Structural Irregularity 7
2.2. Soft Story Structural Irregularity in Different Earthquake Codes 9
2.2.1. ASCE 7-10 9
2.2.2. EUROCODE 8 10
2.2.3. FEMA 310 11
2.2.4. TBEC 2018 11
2.3. Soft Story Failures Due to Past Earthquakes 12
3. PASSIVE ENERGY DISSIPATION DEVICES 15
3.1. Viscous Fluid Dampers 15
3.2. Viscoelastic Dampers 16
3.3. Friction Dampers 17
3.4. Metallic Yield Dampers 19
4. DYNAMIC ANALYSIS 20
4.1. General 20
4.2. Damping in Structures 20

4.3. Construction of Damping Matrix in MDOF Structures 21
4.3.1. Rayleigh Damping 22
4.4. Newmark's Method for Solution of Equation of Motion 23
4.4.1. Stability of Newmark's Method 25
4.4.2. Application of Newmark's Method for Linear Elastic SDOF Systems 25
4.4.3. Application of Newmark's Method for Linear Elastic MDOF Systems 28
5. OPTIMIZATION ALGORITHMS 31
5.1. Differential Evolution (DE) 31
5.1.1. Mathematical Formulation and Steps of DE Algorithm 31
5.2. Particle Swarm Optimization (PSO) 33
5.2.1. Mathematical Formulation and Steps of PSO Algorithm 33
5.3. Optimization Problem 35
6. NUMERICAL EXAMPLES 37
6.1. General 37
6.1.1. Earthquake Ground Motion Data 38
6.1.2. Structure Data 39
6.2. Analysis Results for Structure1 41
6.2.1. Under RSN182 (PNF) 41
6.2.2. Under RSN821 (PNF) 45
6.2.3. Under RSN1063 (PNF) 49
6.2.4. Under RSN1605 (PNF) 53
6.2.5. Under RSN160 (NPNF) 57
6.2.6. Under RSN496 (NPNF) 61
6.2.7. Under RSN741 (NPNF) 65
6.2.8. Under RSN1004 (NPNF) 69
6.2.9. Under RSN68 (FF) 73
6.2.10. Under RSN752 (FF) 76
6.2.11. Under RSN953 (FF) 80
6.2.12. Under RSN1111 (FF) 84
6.3. Analysis Results for Structure2 88

6.3.1. Under RSN182 (PNF) 88
6.3.2. Under RSN821 (PNF) 92
6.3.3. Under RSN1063 (PNF) 96
6.3.4. Under RSN1605 (PNF) 100
6.3.5. Under RSN160 (NPNF) 104
6.3.6. Under RSN496 (NPNF) 108
6.3.7. Under RSN741 (NPNF) 112
6.3.8. Under RSN1004 (NPNF) 116
6.3.9. Under RSN68 (FF) 120
6.3.10. Under RSN752 (FF) 123
6.3.11. Under RSN953 (FF) 127
6.3.12. Under RSN1111 (FF) 131
6.4. Analysis Results for Structure3 134
6.4.1. Under RSN182 (PNF) 134
6.4.2. Under RSN821 (PNF) 138
6.4.3. Under RSN1063 (PNF) 142
6.4.4. Under RSN1605 (PNF) 146
6.4.5. Under RSN160 (NPNF) 150
6.4.6. Under RSN496 (NPNF) 154
6.4.7. Under RSN741 (NPNF) 158
6.4.8. Under RSN1004 (NPNF) 162
6.4.9. Under RSN68 (FF) 166
6.4.10. Under RSN752 (FF) 169
6.4.11. Under RSN953 (FF) 172
6.4.12. Under RSN1111 (FF) 175
7. CONCLUSIONS 178
7.1. Summary and Conclusions 178
7.2. Recommendations for Future Studies 180
REFERENCES 181

TABLES

Page

Table 4.1 Recommended Damping Values by Newmark and Hall[30] 21

Table 6.1 Pulse Near Fault (PNF) Ground Motion Data 38

Table 6.2 No Pulse Near Fault (NPNF) Ground Motion Data 38

Table 6.3 Far Fault (FF) Ground Motion Data 38

Table 6.4 V_{s30} and Soil Class Correlation in Accordance With TBEC2018 [19] .. 39

Table 6.5 Structural Properties of Structure1 39

Table 6.6 Structural Properties of Structure2 39

Table 6.7 Structural Properties of Structure3 40

Table 6.8 Structure1 Optimum viscous damper (VD) distribution Under RSN182 42

Table 6.9 Structure1 Optimum viscous damper (VD) distribution Under RSN821 46

Table 6.10 Structure1 Optimum viscous damper (VD) distribution Under RSN1063 50

Table 6.11 Structure1 Optimum viscous damper (VD) distribution Under RSN1605 54

Table 6.12 Structure1 Optimum viscous damper (VD) distribution Under RSN160 58

Table 6.13 Structure1 Optimum viscous damper (VD) distribution Under RSN496 62

Table 6.14 Structure1 Optimum viscous damper (VD) distribution Under RSN741 66

Table 6.15 Structure1 Optimum viscous damper (VD) distribution Under RSN1004 70

Table 6.16 Structure1 Optimum viscous damper (VD) distribution Under RSN752 77

Table 6.17 Structure1 Optimum viscous damper (VD) distribution Under RSN953 81

Table 6.18 Structure1 Optimum viscous damper (VD) distribution Under RSN1111 85

Table 6.19 Structure2 Optimum viscous damper (VD) distribution Under RSN182 89

Table 6.20 Structure2 Optimum viscous damper (VD) distribution Under RSN821 93

Table 6.21 Structure2 Optimum viscous damper (VD) distribution Under RSN1063 97

Table 6.22 Structure2 Optimum viscous damper (VD) distribution Under RSN1605 101

Table 6.23 Structure2 Optimum viscous damper (VD) distribution Under RSN160 105

Table 6.24 Structure2 Optimum viscous damper (VD) distribution Under RSN496 109

Table 6.25 Structure2 Optimum viscous damper (VD) distribution Under RSN741 113

Table 6.26 Structure2 Optimum viscous damper (VD) distribution Under RSN1004 117
Table 6.27 Structure2 Optimum viscous damper (VD) distribution Under RSN752 124
Table 6.28 Structure2 Optimum viscous damper (VD) distribution Under RSN953 128
Table 6.29 Structure3 Optimum viscous damper (VD) distribution Under RSN182 135
Table 6.30 Structure3 Optimum viscous damper (VD) distribution Under RSN821 139
Table 6.31 Structure3 Optimum viscous damper (VD) distribution Under RSN1063 143
Table 6.32 Structure3 Optimum viscous damper (VD) distribution Under RSN1605 147
Table 6.33 Structure3 Optimum viscous damper (VD) distribution Under RSN160 151
Table 6.34 Structure3 Optimum viscous damper (VD) distribution Under RSN496 155
Table 6.35 Structure3 Optimum viscous damper (VD) distribution Under RSN741 159
Table 6.36 Structure3 Optimum viscous damper (VD) distribution Under RSN1004 163

FIGURES

Page

Figure 2.1 Lateral Displacement Profile of a Typical Building Structure with Soft Story Structural Irregularity[15] 8

Figure 2.2 Typical Soft Story Collapse Mechanism[16] 9

Figure 2.3 Formation of a Soft Story Mechanism After Kocaeli 1999 Earthquake[20] 13

Figure 2.4 Formation of a Soft Story Mechanism After Mexico City 2007 Earthquake[21] 14

Figure 2.5 Formation of a Soft Story Mechanism After Wenchuan 2008 Earthquake[22] 14

Figure 3.1 Construction of a Typical Modern Fluid Viscous Damper [5] 16

Figure 3.2 A Typical Viscoelastic Damper[26] 17

Figure 3.3 A Typical X-Braced Friction Damper[29] 18

Figure 6.1 Structure1 Optimization History (PSO) Under RSN182 41

Figure 6.2 Structure1 Optimization History (DE) Under RSN182 42

Figure 6.3 Comparison of Maximum Acceleration Responses for Structure1 With VD and Without VD Under RSN182 43

Figure 6.4 Comparison of Maximum Velocity Responses for Structure1 With VD and Without VD Under RSN182 43

Figure 6.5 Comparison of Maximum Displacement Responses for Structure1 With VD and Without VD Under RSN182 44

Figure 6.6 Comparison of Peak IDR for Structure1 With VD and Without VD Under RSN182 44

Figure 6.7 Structure1 Optimization History (PSO) Under RSN821 45

Figure 6.8 Structure1 Optimization History (DE) Under RSN821 46

Figure 6.9 Comparison of Maximum Acceleration Responses for Structure1 With VD and Without VD Under RSN821 47

Figure 6.10 Comparison of Maximum Velocity Responses for Structure1 With VD and Without VD Under RSN821 47
Figure 6.11 Comparison of Maximum Displacement Responses for Structure1 With VD and Without VD Under RSN821 48
Figure 6.12 Comparison of Peak IDR for Structure1 With VD and Without VD Under RSN821 48
Figure 6.13 Structure1 Optimization History (PSO) Under RSN1063..... 49
Figure 6.14 Structure1 Optimization History (DE) Under RSN1063 50
Figure 6.15 Comparison of Maximum Acceleration Responses for Structure1 With VD and Without VD Under RSN1063 51
Figure 6.16 Comparison of Maximum Velocity Responses for Structure1 With VD and Without VD Under RSN1063 51
Figure 6.17 Comparison of Maximum Displacement Responses for Structure1 With VD and Without VD Under RSN1063 52
Figure 6.18 Comparison of Peak IDR for Structure1 With VD and Without VD Under RSN1063 52
Figure 6.19 Structure1 Optimization History (PSO) Under RSN1605..... 53
Figure 6.20 Structure1 Optimization History (DE) Under RSN1605 54
Figure 6.21 Comparison of Maximum Acceleration Responses for Structure1 With VD and Without VD Under RSN1605 55
Figure 6.22 Comparison of Maximum Velocity Responses for Structure1 With VD and Without VD Under RSN1605 55
Figure 6.23 Comparison of Maximum Displacement Responses for Structure1 With VD and Without VD Under RSN1605 56
Figure 6.24 Comparison of Peak IDR for Structure1 With VD and Without VD Under RSN1605 56
Figure 6.25 Structure1 Optimization History (PSO) Under RSN160 57
Figure 6.26 Structure1 Optimization History (DE) Under RSN160 58
Figure 6.27 Comparison of Maximum Acceleration Responses for Structure1 With VD and Without VD Under RSN160 59

Figure 6.28 Comparison of Maximum Velocity Responses for Structure1 With VD and Without VD Under RSN160 59
Figure 6.29 Comparison of Maximum Displacement Responses for Structure1 With VD and Without VD Under RSN160 60
Figure 6.30 Comparison of Peak IDR for Structure1 With VD and Without VD Under RSN160 60
Figure 6.31 Structure1 Optimization History (PSO) Under RSN496 61
Figure 6.32 Structure1 Optimization History (DE) Under RSN496 62
Figure 6.33 Comparison of Maximum Acceleration Responses for Structure1 With VD and Without VD Under RSN496 63
Figure 6.34 Comparison of Maximum Velocity Responses for Structure1 With VD and Without VD Under RSN496 63
Figure 6.35 Comparison of Maximum Displacement Responses for Structure1 With VD and Without VD Under RSN496 64
Figure 6.36 Comparison of Peak IDR for Structure1 With VD and Without VD Under RSN496 64
Figure 6.37 Structure1 Optimization History (PSO) Under RSN741 65
Figure 6.38 Structure1 Optimization History (DE) Under RSN741 66
Figure 6.39 Comparison of Maximum Acceleration Responses for Structure1 With VD and Without VD Under RSN741 67
Figure 6.40 Comparison of Maximum Velocity Responses for Structure1 With VD and Without VD Under RSN741 67
Figure 6.41 Comparison of Maximum Displacement Responses for Structure1 With VD and Without VD Under RSN741 68
Figure 6.42 Comparison of Peak IDR for Structure1 With VD and Without VD Under RSN741 68
Figure 6.43 Structure1 Optimization History (PSO) Under RSN1004..... 69
Figure 6.44 Structure1 Optimization History (DE) Under RSN1004 70
Figure 6.45 Comparison of Maximum Acceleration Responses for Structure1 With VD and Without VD Under RSN1004 71

Figure 6.46 Comparison of Maximum Velocity Responses for Structure1 With VD and Without VD Under RSN1004 71
Figure 6.47 Comparison of Maximum Displacement Responses for Structure1 With VD and Without VD Under RSN1004 72
Figure 6.48 Comparison of Peak IDR for Structure1 With VD and Without VD Under RSN1004 72
Figure 6.49 Comparison of Maximum Acceleration Responses for Structure1 With VD and Without VD Under RSN68 73
Figure 6.50 Comparison of Maximum Velocity Responses for Structure1 With VD and Without VD Under RSN68 74
Figure 6.51 Comparison of Maximum Displacement Responses for Structure1 With VD and Without VD Under RSN68 74
Figure 6.52 Comparison of Peak IDR for Structure1 With VD and Without VD Under RSN68 75
Figure 6.53 Structure1 Optimization History (PSO) Under RSN752 76
Figure 6.54 Structure1 Optimization History (DE) Under RSN752 77
Figure 6.55 Comparison of Maximum Acceleration Responses for Structure1 With VD and Without VD Under RSN752 78
Figure 6.56 Comparison of Maximum Velocity Responses for Structure1 With VD and Without VD Under RSN752 78
Figure 6.57 Comparison of Maximum Displacement Responses for Structure1 With VD and Without VD Under RSN752 79
Figure 6.58 Comparison of Peak IDR for Structure1 With VD and Without VD Under RSN752 79
Figure 6.59 Structure1 Optimization History (PSO) Under RSN953 80
Figure 6.60 Structure1 Optimization History (DE) Under RSN953 81
Figure 6.61 Comparison of Maximum Acceleration Responses for Structure1 With VD and Without VD Under RSN953 82
Figure 6.62 Comparison of Maximum Velocity Responses for Structure1 With VD and Without VD Under RSN953 82

Figure 6.63 Comparison of Maximum Displacement Responses for Structure1 With VD and Without VD Under RSN953 83
Figure 6.64 Comparison of Peak IDR for Structure1 With VD and Without VD Under RSN953 83
Figure 6.65 Structure1 Optimization History (PSO) Under RSN1111..... 84
Figure 6.66 Structure1 Optimization History (DE) Under RSN1111 85
Figure 6.67 Comparison of Maximum Acceleration Responses for Structure1 With VD and Without VD Under RSN1111 86
Figure 6.68 Comparison of Maximum Velocity Responses for Structure1 With VD and Without VD Under RSN1111 86
Figure 6.69 Comparison of Maximum Displacement Responses for Structure1 With VD and Without VD Under RSN1111 87
Figure 6.70 Comparison of Peak IDR for Structure1 With VD and Without VD Under RSN1111..... 87
Figure 6.71 Structure2 Optimization History (PSO) Under RSN182 88
Figure 6.72 Structure2 Optimization History (DE) Under RSN182 89
Figure 6.73 Comparison of Maximum Acceleration Responses for Structure2 With VD and Without VD Under RSN182 90
Figure 6.74 Comparison of Maximum Velocity Responses for Structure2 With VD and Without VD Under RSN182 90
Figure 6.75 Comparison of Maximum Displacement Responses for Structure2 With VD and Without VD Under RSN182 91
Figure 6.76 Comparison of Peak IDR for Structure2 With VD and Without VD Under RSN182 91
Figure 6.77 Structure2 Optimization History (PSO) Under RSN821 92
Figure 6.78 Structure2 Optimization History (DE) Under RSN821 93
Figure 6.79 Comparison of Maximum Acceleration Responses for Structure2 With VD and Without VD Under RSN821 94
Figure 6.80 Comparison of Maximum Velocity Responses for Structure2 With VD and Without VD Under RSN821 94

Figure 6.81 Comparison of Maximum Displacement Responses for Structure2 With VD and Without VD Under RSN821 95
Figure 6.82 Comparison of Peak IDR for Structure2 With VD and Without VD Under RSN821 95
Figure 6.83 Structure2 Optimization History (PSO) Under RSN1063..... 96
Figure 6.84 Structure2 Optimization History (DE) Under RSN1063 97
Figure 6.85 Comparison of Maximum Acceleration Responses for Structure2 With VD and Without VD Under RSN1063 98
Figure 6.86 Comparison of Maximum Velocity Responses for Structure2 With VD and Without VD Under RSN1063 98
Figure 6.87 Comparison of Maximum Displacement Responses for Structure2 With VD and Without VD Under RSN1063 99
Figure 6.88 Comparison of Peak IDR for Structure2 With VD and Without VD Under RSN1063..... 99
Figure 6.89 Structure2 Optimization History (PSO) Under RSN1605..... 100
Figure 6.90 Structure2 Optimization History (DE) Under RSN1605 101
Figure 6.91 Comparison of Maximum Acceleration Responses for Structure2 With VD and Without VD Under RSN1605 102
Figure 6.92 Comparison of Maximum Velocity Responses for Structure2 With VD and Without VD Under RSN1605 102
Figure 6.93 Comparison of Maximum Displacement Responses for Structure2 With VD and Without VD Under RSN1605 103
Figure 6.94 Comparison of Peak IDR for Structure2 With VD and Without VD Under RSN1605..... 103
Figure 6.95 Structure2 Optimization History (PSO) Under RSN160 104
Figure 6.96 Structure2 Optimization History (DE) Under RSN160 105
Figure 6.97 Comparison of Maximum Acceleration Responses for Structure2 With VD and Without VD Under RSN160 106
Figure 6.98 Comparison of Maximum Velocity Responses for Structure2 With VD and Without VD Under RSN160 106

Figure 6.99 Comparison of Maximum Displacement Responses for Structure2 With VD and Without VD Under RSN160 107
Figure 6.100 Comparison of Peak IDR for Structure2 With VD and Without VD Under RSN160 107
Figure 6.101 Structure2 Optimization History (PSO) Under RSN496 108
Figure 6.102 Structure2 Optimization History (DE) Under RSN496 109
Figure 6.103 Comparison of Maximum Acceleration Responses for Structure2 With VD and Without VD Under RSN496 110
Figure 6.104 Comparison of Maximum Velocity Responses for Structure2 With VD and Without VD Under RSN496 110
Figure 6.105 Comparison of Maximum Displacement Responses for Structure2 With VD and Without VD Under RSN496 111
Figure 6.106 Comparison of Peak IDR for Structure2 With VD and Without VD Under RSN496 111
Figure 6.107 Structure2 Optimization History (PSO) Under RSN741 112
Figure 6.108 Structure2 Optimization History (DE) Under RSN741 113
Figure 6.109 Comparison of Maximum Acceleration Responses for Structure2 With VD and Without VD Under RSN741 114
Figure 6.110 Comparison of Maximum Velocity Responses for Structure2 With VD and Without VD Under RSN741 114
Figure 6.111 Comparison of Maximum Displacement Responses for Structure2 With VD and Without VD Under RSN741 115
Figure 6.112 Comparison of Peak IDR for Structure2 With VD and Without VD Under RSN741 115
Figure 6.113 Structure2 Optimization History (PSO) Under RSN1004..... 116
Figure 6.114 Structure2 Optimization History (DE) Under RSN1004 117
Figure 6.115 Comparison of Maximum Acceleration Responses for Structure2 With VD and Without VD Under RSN1004 118
Figure 6.116 Comparison of Maximum Velocity Responses for Structure2 With VD and Without VD Under RSN1004 118

Figure 6.117 Comparison of Maximum Displacement Responses for Structure2 With VD and Without VD Under RSN1004 119
Figure 6.118 Comparison of Peak IDR for Structure2 With VD and Without VD Under RSN1004 119
Figure 6.119 Comparison of Maximum Acceleration Responses for Structure2 With VD and Without VD Under RSN68 120
Figure 6.120 Comparison of Maximum Velocity Responses for Structure2 With VD and Without VD Under RSN68 121
Figure 6.121 Comparison of Maximum Displacement Responses for Structure2 With VD and Without VD Under RSN68 121
Figure 6.122 Comparison of Peak IDR for Structure2 With VD and Without VD Under RSN68 122
Figure 6.123 Structure2 Optimization History (PSO) Under RSN752 123
Figure 6.124 Structure2 Optimization History (DE) Under RSN752 124
Figure 6.125 Comparison of Maximum Acceleration Responses for Structure2 With VD and Without VD Under RSN752 125
Figure 6.126 Comparison of Maximum Velocity Responses for Structure2 With VD and Without VD Under RSN752 125
Figure 6.127 Comparison of Maximum Displacement Responses for Structure2 With VD and Without VD Under RSN752 126
Figure 6.128 Comparison of Peak IDR for Structure2 With VD and Without VD Under RSN752 126
Figure 6.129 Structure2 Optimization History (PSO) Under RSN953 127
Figure 6.130 Structure2 Optimization History (DE) Under RSN953 128
Figure 6.131 Comparison of Maximum Acceleration Responses for Structure2 With VD and Without VD Under RSN953 129
Figure 6.132 Comparison of Maximum Velocity Responses for Structure2 With VD and Without VD Under RSN953 129
Figure 6.133 Comparison of Maximum Displacement Responses for Structure2 With VD and Without VD Under RSN953 130

Figure 6.134 Comparison of Peak IDR for Structure2 With VD and Without VD Under RSN953 130
Figure 6.135 Comparison of Maximum Acceleration Responses for Structure2 With VD and Without VD Under RSN1111 131
Figure 6.136 Comparison of Maximum Velocity Responses for Structure2 With VD and Without VD Under RSN1111 132
Figure 6.137 Comparison of Maximum Displacement Responses for Structure2 With VD and Without VD Under RSN1111 132
Figure 6.138 Comparison of Peak IDR for Structure2 With VD and Without VD Under RSN1111 133
Figure 6.139 Structure3 Optimization History (PSO) Under RSN182 134
Figure 6.140 Structure3 Optimization History (DE) Under RSN182 135
Figure 6.141 Comparison of Maximum Acceleration Responses for Structure3 With VD and Without VD Under RSN182 136
Figure 6.142 Comparison of Maximum Velocity Responses for Structure3 With VD and Without VD Under RSN182 136
Figure 6.143 Comparison of Maximum Displacement Responses for Structure3 With VD and Without VD Under RSN182 137
Figure 6.144 Comparison of Peak IDR for Structure3 With VD and Without VD Under RSN182 137
Figure 6.145 Structure3 Optimization History (PSO) Under RSN821 138
Figure 6.146 Structure3 Optimization History (DE) Under RSN821 139
Figure 6.147 Comparison of Maximum Acceleration Responses for Structure3 With VD and Without VD Under RSN821 140
Figure 6.148 Comparison of Maximum Velocity Responses for Structure3 With VD and Without VD Under RSN821 140
Figure 6.149 Comparison of Maximum Displacement Responses for Structure3 With VD and Without VD Under RSN821 141
Figure 6.150 Comparison of Peak IDR for Structure3 With VD and Without VD Under RSN821 141

Figure 6.151 Structure3 Optimization History (PSO) Under RSN1063 142
Figure 6.152 Structure3 Optimization History (DE) Under RSN1063 143
Figure 6.153 Comparison of Maximum Acceleration Responses for Structure3 With VD and Without VD Under RSN1063 144
Figure 6.154 Comparison of Maximum Velocity Responses for Structure3 With VD and Without VD Under RSN1063 144
Figure 6.155 Comparison of Maximum Displacement Responses for Structure3 With VD and Without VD Under RSN1063 145
Figure 6.156 Comparison of Peak IDR for Structure3 With VD and Without VD Under RSN1063 145
Figure 6.157 Structure3 Optimization History (PSO) Under RSN1605 146
Figure 6.158 Structure3 Optimization History (DE) Under RSN1605 147
Figure 6.159 Comparison of Maximum Acceleration Responses for Structure3 With VD and Without VD Under RSN1605 148
Figure 6.160 Comparison of Maximum Velocity Responses for Structure3 With VD and Without VD Under RSN1605 148
Figure 6.161 Comparison of Maximum Displacement Responses for Structure3 With VD and Without VD Under RSN1605 149
Figure 6.162 Comparison of Peak IDR for Structure3 With VD and Without VD Under RSN1605 149
Figure 6.163 Structure3 Optimization History (PSO) Under RSN160 150
Figure 6.164 Structure3 Optimization History (DE) Under RSN160 151
Figure 6.165 Comparison of Maximum Acceleration Responses for Structure3 With VD and Without VD Under RSN160 152
Figure 6.166 Comparison of Maximum Velocity Responses for Structure3 With VD and Without VD Under RSN160 152
Figure 6.167 Comparison of Maximum Displacement Responses for Structure3 With VD and Without VD Under RSN160 153
Figure 6.168 Comparison of Peak IDR for Structure3 With VD and Without VD Under RSN160 153

Figure 6.169 Structure3 Optimization History (PSO) Under RSN496 154
Figure 6.170 Structure3 Optimization History (DE) Under RSN496 155
Figure 6.171 Comparison of Maximum Acceleration Responses for Structure3 With VD and Without VD Under RSN496 156
Figure 6.172 Comparison of Maximum Velocity Responses for Structure3 With VD and Without VD Under RSN496 156
Figure 6.173 Comparison of Maximum Displacement Responses for Structure3 With VD and Without VD Under RSN496 157
Figure 6.174 Comparison of Peak IDR for Structure3 With VD and Without VD Under RSN496 157
Figure 6.175 Structure3 Optimization History (PSO) Under RSN741 158
Figure 6.176 Structure3 Optimization History (DE) Under RSN741 159
Figure 6.177 Comparison of Maximum Acceleration Responses for Structure3 With VD and Without VD Under RSN741 160
Figure 6.178 Comparison of Maximum Velocity Responses for Structure3 With VD and Without VD Under RSN741 160
Figure 6.179 Comparison of Maximum Displacement Responses for Structure3 With VD and Without VD Under RSN741 161
Figure 6.180 Comparison of Peak IDR for Structure3 With VD and Without VD Under RSN741 161
Figure 6.181 Structure3 Optimization History (PSO) Under RSN1004..... 162
Figure 6.182 Structure3 Optimization History (DE) Under RSN1004 163
Figure 6.183 Comparison of Maximum Acceleration Responses for Structure3 With VD and Without VD Under RSN1004 164
Figure 6.184 Comparison of Maximum Velocity Responses for Structure3 With VD and Without VD Under RSN1004 164
Figure 6.185 Comparison of Maximum Displacement Responses for Structure3 With VD and Without VD Under RSN1004 165
Figure 6.186 Comparison of Peak IDR for Structure3 With VD and Without VD Under RSN1004 165

Figure 6.187 Comparison of Maximum Acceleration Responses for Structure3 With VD and Without VD Under RSN68 166
Figure 6.188 Comparison of Maximum Velocity Responses for Structure3 With VD and Without VD Under RSN68 167
Figure 6.189 Comparison of Maximum Displacement Responses for Structure3 With VD and Without VD Under RSN68 167
Figure 6.190 Comparison of Peak IDR for Structure3 With VD and Without VD Under RSN68 168
Figure 6.191 Comparison of Maximum Acceleration Responses for Structure3 With VD and Without VD Under RSN752 169
Figure 6.192 Comparison of Maximum Velocity Responses for Structure3 With VD and Without VD Under RSN752 170
Figure 6.193 Comparison of Maximum Displacement Responses for Structure3 With VD and Without VD Under RSN752 170
Figure 6.194 Comparison of Peak IDR for Structure3 With VD and Without VD Under RSN752 171
Figure 6.195 Comparison of Maximum Acceleration Responses for Structure3 With VD and Without VD Under RSN953 172
Figure 6.196 Comparison of Maximum Velocity Responses for Structure3 With VD and Without VD Under RSN953 173
Figure 6.197 Comparison of Maximum Displacement Responses for Structure3 With VD and Without VD Under RSN953 173
Figure 6.198 Comparison of Peak IDR for Structure3 With VD and Without VD Under RSN953 174
Figure 6.199 Comparison of Maximum Acceleration Responses for Structure3 With VD and Without VD Under RSN1111 175
Figure 6.200 Comparison of Maximum Velocity Responses for Structure3 With VD and Without VD Under RSN1111 176
Figure 6.201 Comparison of Maximum Displacement Responses for Structure3 With VD and Without VD Under RSN1111 176

Figure 6.202 Comparison of Peak IDR for Structure3 With VD and Without VD Under RSN1111 177

SYMBOLS AND ABBREVIATIONS

Symbols

a_0, a_1	:	Rayleigh's Method Constants
C	:	Structure Damping Matrix
C_{AD}	:	Damping Damping Matrix of Added Viscous Dampers
CR	:	Crossover Rate
c	:	Damping Coefficient
$c_{AD,i}$	:	Damping Coefficient of Added Viscous Damper at i^{th} Story
c_1, c_2	:	Acceleration Parameters
F	:	Mutation Factor
$f(X)$	:	Objective Function
G	:	Global Best Position
h	:	Height
K	:	Stiffness Matrix
k	:	Stiffness
M	:	Mass Matrix
m	:	Mass
P	:	External Force in Dynamic Analysis,Particle Best Position in PSO
q	:	Modal Coordinate Vector
Sa	:	Spectral Acceleration
Sd	:	Spectral Displacement
Sv	:	Spectral Velocity
T	:	Period
T_i	:	Undamped Natural Period of the i^{th} Mode of Vibration
T_n	:	Undamped Natural Period
t	:	Time
$\vec{U}$	:	Trail Vector

u	:	Displacement
$\dot{u}$	:	Velocity
$\ddot{u}$	:	Acceleration
u_g	:	Ground Displacement
$\dot{u}_g$	:	Ground Velocity
$\ddot{u}_g$	:	Ground Acceleration
$\vec{V}$	:	Mutant Vector in DE, Velocity Vector in PSO
w	:	Inertia Weight
X^T	:	Design Vector
$\vec{X}$	:	Target Vector in DE, Position Vector in PSO
β, γ	:	Newmark's Method Constants
Δ_i	:	Relative Displacement
Δ_t	:	Time Step
η_{ki}	:	Rigidity Irregularity Factor
ξ	:	Damping Ratio
ξ_i	:	Modal Damping Ratio of the i^{th} Mode of Vibration
ϕ_i	:	Mode Shape Vector of the i^{th} Mode of Vibration
ω_n	:	Undamped Natural Frequency
ω_i	:	Undamped Natural Frequency of the i^{th} Mode of Vibration

Abbreviations

avg	:	Average
DE	:	Differential Evolution
FF	:	Far Fault
GM	:	Ground Motion
IDR	:	Inter Story Drift Ratio
LB	:	Lower Bound
MDOF	:	Multi Degree of Freedom
NP	:	Number of Population
NPNF	:	No Pulse Near Fault

PNF	:	Pulse Near Fault
PSO	:	Particle Swarm Optimization
SDOF	:	Single Degree of Freedom
UB	:	Upper Bound

1. INTRODUCTION

1.1. Introduction

Soft story structural irregularity is a type of vertical structural irregularity that has adverse impact on earthquake performance of building structures. The main cause of the soft story structural irregularity is abrupt changes in stiffness between adjacent stories of the building structure or involve a story that relatively less stiffness than average stiffness of the stories of the building. Soft story behavior causes severe structural damages or soft story collapse mechanism after earthquakes due to abnormal inter story drift ratios.

After the major earthquakes in the past (such as Loma Prieta 1989, Earthquake Northridge 1994 Earthquake, and Kocaeli 1999 Earthquake) collapses and unrepairable severe structural damages observed. Therefore, rehabilitation of building structures with soft story irregularity is an important subject to prevent big economic losses, and more importantly life losses.

The main problem in soft story structural irregularity is abnormal inter story drift ratios and abrupt change in inter story drift ratios between adjacent stories of the building that is caused by abrupt change in stiffness between adjacent stories of the building. These structures can be rehabilitated by conventional methods. Besides conventional methods, viscous damper applications can be used in order to rehabilitate these structures. Viscous dampers are remarkably effective passive energy dissipation devices to absorb harmless seismic energy and reduce dynamic response of the structures. Additionally, viscous dampers can be used to reduce inter story drifts. However, viscous dampers are expensive devices because of that reason optimum distribution of viscous dampers is vital.

The aim and scope of this thesis is to propose a methodology to rehabilitate existing building structures with soft story structural irregularity based on peak inter story drift ratios via optimum viscous damper distribution using two different meta-heuristic search algorithms. These are Differential Evolution (DE) and Particle Swarm Optimization (PSO) algorithms. Thus, peak inter story drift ratios will not exceed allowable limits via optimal viscous damper

allocation. Proposed methodology is proposed on three different shear buildings under twelve different earthquake ground motion records. Ground motion data sets involve twelve Pulse Near Fault (PNF), No Pulse Near Fault (NPNF), and Far Fault (FF) records. Results of this study is reported and compared to both without viscous damper case and optimal viscous damper distribution case.

1.2. Organization

Chapter 1 gives a simple idea of proposed methodology and gives information about previous works with related subject.

Chapter 2 gives a detailed information about soft story structural irregularity and investigates soft story behavior in different earthquake codes and guidelines.

Chapter 3 gives information about different passive energy dissipation devices. In this chapter, role of passive damping devices in structural and earthquake engineering is explained. Besides that, working principle and background information about passive damping devices are simply covered.

Chapter 4 explains the selected dynamic analysis method of shear buildings with and without viscous damper under earthquake ground motions.

Chapter 5 gives information about optimization methods, including their background, inspiration sources, mathematical formulations, and flowcharts. This chapter also explains the formulation of the optimization problem.

Chapter 6 gives numerical examples related to proposed methodology. This chapter gives numerical examples on different shear building structures under different earthquake ground motion data.

Chapter 7 gives a brief conclusion about this thesis work and explains outcomes of this thesis works.

1.3. Previous Works

Viscous fluid dampers are passive damping devices such that they absorb the harmless shock or vibration energy. The absorbed energy is transferred into heat energy by viscous fluid dampers. There are various applications of viscous fluid dampers in order to dissipate shock or vibration energy in different engineering products. The common use of viscous fluid dampers in civil structures started in mid 1990s [1]. The aim of using viscous fluid dampers in civil structures is, designing more resilient structures and rehabilitating existing structures [2]. Fluid viscous dampers are absorbing the seismic vibration energy and transferring seismic vibration energy to heat energy during earthquakes.

Constantinou and Symans investigated both analytical and experimental behavior of structures that are equipped with supplemental passive energy dissipation devices. It is observed that supplementally added passive energy dissipation systems in civil structures have an important influence on structures' performance during seismic excitations [3].

Constantinou et al. investigated application of fluid viscous dampers as a passive energy dissipation device for seismic isolation of structures. In that study effect of viscous fluid dampers on buildings and bridges was investigated both analytically and experimentally for seismic protection. In accordance with this study, viscous fluid dampers are remarkably effective energy dissipation devices to reduce dynamic response of buildings and bridges that they are attached [4]. This study also shows that viscous fluid dampers have a significant influence on story drifts in building structures. From the experimental results of this study, it can be observed that, it is possible to reduce story drifts by using supplementally added viscous fluid dampers. In this regard, viscous fluid dampers are remarkably effective passive energy dissipation devices for seismic protection and rehabilitation of structures.

Symans and Constantinou experimentally tested passive viscous fluid dampers for seismic energy dissipation also experimental results compared with analytical results. In this experimental research work, a three-story scaled moment-resisting frame structure tested with no damper, two dampers, four dampers and six dampers, and experimental test results

compared with analytical results. Experimental works through the study proves the analytical models for dynamic response of scaled structure. This study clearly shows that viscous dampers are capable to absorb significant amount of energy which is greater than energy absorption of the frame due hysteric action [5]. Further, in scope of this research temperature effects on viscous fluid dampers are investigated, and it is concluded that there is no momentous change in viscous fluid dampers' performance range between temperatures 0°C to 50°C [5].

Optimization of viscous fluid dampers are another crucial point for the design since their locations and damping capacities greatly affect seismic performance of structures under earthquake excitation. In this regard, optimal allocation of viscous fluid dampers is an important subject in terms of seismic performance of structures. In the literature, there are many research studies on optimization of fluid viscous dampers in order to increase the seismic performance of the structures.

Constantinou and Tadjbakhsh investigated the optimum damping coefficient for the first story damping systems. In this research, a methodology is developed by Constantinou and Tadjbakhsh for the optimum design of the damping systems in multi-story shear building under random earthquake excitation [6].

Gurgoze and Muller investigated optimum positioning of viscous dampers in multi-degree-of-freedom systems. In this study, a numerical approach is proposed in order to find optimal positioning of viscous dampers [7].

Takewaki developed a procedure for optimal damper positioning in planar building frames. The aim of this study is, minimizing the dynamic compliance of planar building with an optimum damper allocation. Steepest direction search algorithm is proposed in order to find the optimum damper allocation in planar building frames [8].

Bishop and Striz proposed a meta-heuristic approach in order to find optimum damper allocation in space trusses. In this study, genetic algorithm is employed to find optimum design of dampers in space trusses with different structural configurations [9].

Aydın developed a new strategy to find optimum viscous damper allocation in planar steel building frames [10]. The proposed methodology is based on the elastic base moment. In this research, the objective function is taken as the transfer function amplitude of elastic base moment and subjected to minimization by using an optimum damper allocation[10]. The optimum size and location of viscous dampers are investigated to minimize the selected objective function.

Aydin et al. investigated optimal viscous damper distribution in multi-story shear buildings. The aim of this study is, to reduce the dynamic response of the multi-story shear buildings with an optimum viscous damper distribution. Objective function is selected as summation of the damping coefficients of additionally added viscous dampers in each floor and subjected to minimize via different meta-heuristic optimization algorithms [11].

Cetin et al. investigated optimal viscous damper distribution in multi-story shear buildings under seismic excitation. Differential Evolution (DE) algorithm is employed to find optimum design and distribution of additionally added viscous dampers. From this research it is observed that reduction in dynamic response in multi-story shear building under seismic excitation is possible. It can be concluded that proposed method is highly effective to reduce IDR in multi-story story shear buildings subjected to ground excitation. Also, Differential Evolution (DE) algorithm can be employed to find optimum viscous damper allocation in multi-story shear building under seismic ground motions [12].

Aydin et al. investigated influence of soil-structure interaction (SSI) on optimal viscous damper distribution building structures. Optimum damper design is performed under different soil conditions and different earthquake records. Optimum design of viscous dampers is determined by using different meta-heuristic optimization algorithms. This study shows that soil-structure interaction (SSI) has an important influence on optimum damper allocation in building structures. Proposed method clearly shows that the negative impact of sandy soils can be eliminated by optimum viscous damper allocation without any ground improvement[13]. Furthermore, it can be concluded that proposed methodology is

very efficient for reducing the IDR in different soil conditions, and different earthquake records[13].

2. SOFT STORY STRUCTURAL IRREGULARITY

2.1. General Review of Soft Story Structural Irregularity

Soft structural irregularity, known as rigidity irregularity, is a type of vertical irregularity in building structures. Basically, soft story structural irregularity refers to abrupt stiffness change between adjacent stories or involving a story that have a significantly less stiffness when it is compared with average stiffness of other stories.

Ideally, engineers should avoid from any type of structural irregularities while design stage of structure. The reason is structural irregularities make structures seismically vulnerable. Unfortunately, soft story structural irregularity may cause severe damages during earthquakes or local collapse mechanism during seismic loading.

Due to lateral loading, such as earthquake loads, acting on the building structures, plastic hinges are formed at the structural members. In general, building codes or guidelines aim to spread plastic hinges that are formed under lateral loads. This is one of the fundamental approaches of the modern earthquake-resistant design philosophy. The main reason behind this approach is, increasing the dissipated energy during the seismic loads. Plastic hinges may be localized at some points, if the structure has a soft story structural irregularity. In this case, structure fails with a local collapse mechanism without dissipate significant amount of seismic energy.

Soft stories are generally observed in very first stories in building structures. This causes significantly large inner-story drifts in the first story when it is compared with the other stories' inner-story drifts, and this situation increases secondary effects. Plastic hinges are localized at first story structural members under seismic loading in such structures. Due to that reason, lateral loads acting on the building structure cannot be well-distributed along the height of the building. Finally, all these inevitable consequences ended up with severe damages at specific stories or local collapse mechanisms. Soft story behavior clearly

contradicts with modern earthquake-resistant design philosophy since structure fails without absorbing significant amount of seismic energy due to soft stories.

All these reasons make building structures, with soft story structural irregularity, seismically vulnerable due to abrupt changes in peak inter-story drift ratios. Soft story behavior causes severe structural damages or local collapse mechanisms especially after a demanding earthquake. Soft story structural irregularity is more critical for building structures particularly located in near fault regions since near fault ground motions have peculiar characteristics [14].

In Figure 2.1 [15], lateral displacement profile of a typical building structure with soft story structural irregularity is shown below.

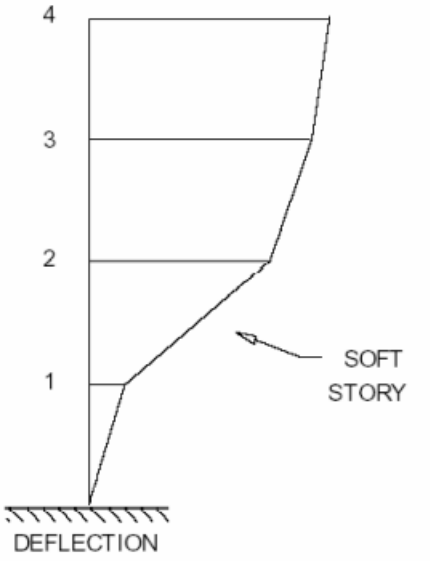

Figure 2.1 Lateral Displacement Profile of a Typical Building Structure with Soft Story Structural Irregularity[15]

In Figure 2.2 [16], a typical soft story collapse mechanism is shown below.

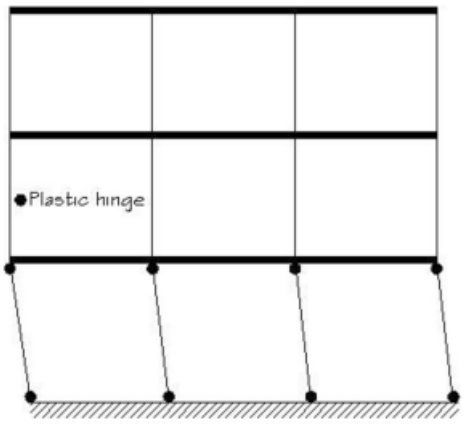

Figure 2.2 Typical Soft Story Collapse Mechanism[16]

2.2. Soft Story Structural Irregularity in Different Earthquake Codes

Soft structural irregularity basically refers to abrupt stiffness change between adjacent stories or involving a story that has a significantly less stiffness when it is compared with average stiffness of other stories. In this section, definition of story structural irregularity in different earthquake codes and guidelines will be discussed briefly.

2.2.1. ASCE 7-10

ASCE 7-10 investigates soft-story structural irregularity in two branches. These are soft story and extreme soft story. These two cases are both referring to rigidity structural irregularity in vertical axis of the building structure. The case of extreme soft story irregularity can be considered as exaggerated version of soft story irregularity which is defined in ASCE 7-10.

ASCE 7-10 defines soft story structural irregularity as, “Stiffness-soft storey irregularity is defined to exist where there is a story in which the lateral stiffness is less than 70% of that in the story above or less than 80% of the average stiffness of the three stories above[17]”.

The case of extreme soft story structural irregularity defined in ASCE 7-10 as, “Stiffness–extreme soft storey irregularity is defined to exist where there is a story in which

the lateral stiffness is less than 60% of that in the story above or less than 70% of the average stiffness of the three stories above [17]".

ASCE 7-10 prevents abrupt stiffness changes along the height of the building structures by these requirements. Therefore, ASCE 7-10 prohibits soft story failure mechanism risk.

2.2.2. EUROCODE 8

In EUROCODE 8, there is no factor or rigidity criteria to define soft stories. In accordance with EUROCODE 8, global and local ductility conditions should be satisfied. In other words, both all the structural elements and the structure as a whole should have enough ductility [18]. EUROCODE 8 mainly focus on preventing soft story failure mechanisms by capacity design principles. EUROCODE 8 aims to prevent brittle failures by using capacity design principles.

Local ductility demands for building structures with soft story may not be satisfied, and it may lead to soft story collapse mechanisms. Therefore, EUROCODE 8 requires that all beam and columns in the structure should satisfy the following criteria:

$$\sum M_{Rc} \geq 1.3 \sum M_{Rb} \tag{2.1}$$

Where:
M_{Rc} is the summation of the design moment values of the columns which are connected to specified joint of the frame.
M_{Rb} is the summation of the design moment values of the beams which are connected to specified joint of the frame.

EUROCODE 8 requires that the criteria given in Equation 2.1 should be satisfied in two orthogonal directions of the earthquake.

2.2.3. FEMA 310

FEMA 310 is a guiding document for structural engineers, and FEMA 310 covers seismic evaluation of building structures. FEMA 310 defines soft story structural irregularity as "The stiffness of the lateral-force-resisting system in any story shall not be less than 70% of the stiffness in an adjacent story above or below or less than 80% of the average stiffness of three stories above or below for Life-Safety and Immediate Occupancy[15]".

These requirements are similar with the requirements stated in ASCE 7-10. FEMA 310 prevents abrupt stiffness changes along the height of the building structures by these requirements, thus the risk of soft story failure mechanism will be prohibited.

2.2.4. TBEC 2018

Turkish Building Earthquake Code (TBEC 2018) defines a rigidity irregularity factor (η_{ki}) to define soft stories in the building structures. This stiffness irregularity factor (η_{ki}) must be checked for two orthogonal earthquake directions.

Turkish Building Earthquake Code (TBEC 2018) defines stiffness irregularity factor (η_{ki}) as ratio of the inter-story drift ratios of two adjacent stories. In accordance with TBEC 2018, soft story is a condition that stiffness irregularity factor (η_{ki}) is greater than 2 [19].

Stiffness irregularity factor (η_{ki}) can be more explicitly written as

$$\eta_{ki} = (\Delta_i/h_i)_{avg}/(\Delta_{i+1}/h_{i+1})_{avg} \tag{2.2}$$

or

$$\eta_{ki} = (\Delta_{i+1}/h_{i+1})_{avg}/(\Delta_i/h_i)_{avg} \tag{2.3}$$

This requirement prevents abrupt changes in inter-story drift ratios of the two adjacent stories of the building structure. Thus, Turkish Building Earthquake Code (TBDY 2018) prevents severe structural damages due to soft-story failure mechanism.

2.3. Soft Story Failures Due to Past Earthquakes

As it mentioned beginning of this chapter building structures with soft story structural irregularity, are seismically vulnerable due to abrupt changes in peak inter-story drift ratios between adjacent stories. Abrupt changes in peak inter-story drift ratios between adjacent stories may cause severe damages or soft story collapse mechanism.

Building structures suffer from unrepairable severe structural damages or collapses due to soft story mechanism after the past earthquakes. This section of this thesis includes images of structural damages and collapses from past earthquakes due to soft story behavior.

Figure 2.3 shows the formation of a soft story mechanism in building structure after Kocaeli 1999 earthquake [20].

Figure 2.3 Formation of a Soft Story Mechanism After Kocaeli 1999 Earthquake[20]

Figure 2.4 shows the formation of a soft story mechanism in different building structures after Mexico City 2017 earthquake[21].

Figure 2.4 Formation of a Soft Story Mechanism After Mexico City 2007 Earthquake[21]

Figure 2.5 shows the formation of a soft story mechanism in building structure from different point views after Wenchuan 2008 earthquake[22].

Figure 2.5 Formation of a Soft Story Mechanism After Wenchuan 2008 Earthquake[22]

3. PASSIVE ENERGY DISSIPATION DEVICES

3.1. Viscous Fluid Dampers

There are various application of viscous fluid dampers in engineering to dissipate shock or vibration energy in different engineering products such as guns, aerospace structures, military defense systems, various civil structures etc. The main objective is, dissipating the harmless shock or vibration energy. This dissipated shock/vibration energy is transferred to heat energy by viscous fluid dampers. The operation principle of viscous fluid damper is based on fluid flow through the orifices, viscous fluid dampers were firstly used in French artillery field guns in 1987 to reduce the guns' recoil[23].

Applications of viscous fluid dampers as passive vibration/shock absorber devices in different engineering disciplines started at 1980s. The implementations of viscous fluid dampers in various civil structures as seismic energy absorbers widely started at mid-1990s [1]. The aim of using fluid viscous dampers in earthquake engineering is, reducing the dynamic response of the structure during the earthquake-excitation.

Fluid viscous dampers absorbs the energy during the earthquake and transfers this energy to heath energy. By this way, harmless vibration seismic energy, generated by ground, is dissipated by viscous fluid dampers, and transformed into heat energy. Typical parts of viscous fluid damper are a stainless-steel piston with a bronze orifice head and accumulator. Viscous fluid dampers are filled with a viscous oil, generally silicone oil, and generally operating temperatures of viscous fluid dampers are around -40°C to 70°C [5].

Construction of a typical modern fluid viscous damper is given below in Figure 3.1 [5].

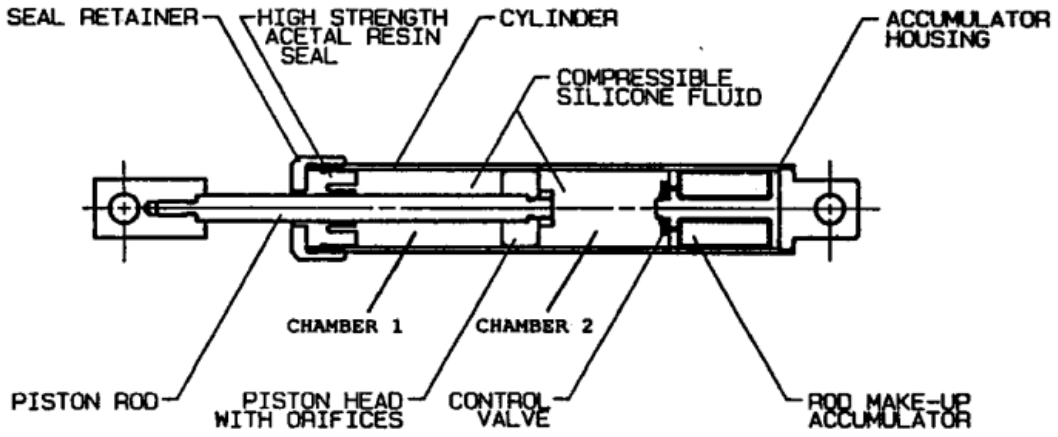

Figure 3.1 Construction of a Typical Modern Fluid Viscous Damper [5]

3.2. Viscoelastic Dampers

Viscoelastic dampers are passive energy dissipation devices that use the shear deformation of viscoelastic materials. There are various applications of viscoelastic dampers in different engineering fields. Viscoelastic dampers were first used in aircrafts as an energy dissipation device in order control the vibration in 1950s.

Applications of viscoelastic dampers in structural engineering as a passive energy dissipation device date back to 1960s. The first structural engineering application of viscoelastic dampers to mitigate wind-induced vibrations in World Trade Center Towers in New York City in 1969. Viscoelastic dampers are remarkably successful to reduce vibration energy in tall buildings due wind induced vibrations[24]. Research on seismic response of building structures with viscoelastic dampers started in 1987[25]. In 1993 Chang et al. tested 5 story 2/5 scaled steel framed structure with viscoelastic dampers under seismic ground excitations[26]. The first application of viscoelastic dampers in earthquake engineering started in 1993 to rehabilitate Santa Clara County Building in in San Jose, California.

Working principle of viscoelastic dampers is converting the shear deformation of the viscoelastic materials. After the shear deformation, viscoelastic material returns its original

shape. Strain and kinetic energy transferred into heat energy during this process. Amount of dissipated energy through the viscoelastic dampers depends on displacement and velocity.

Besides the energy dissipation, viscoelastic dampers offer additional stiffness, and change the natural period of the structure. As a result, viscoelastic dampers provide remarkable advantages to the structure, and these advantages are beneficial for the performance of the structure under seismic ground motions.

A typical viscoelastic damper is shown below in Figure 3.2 [26].

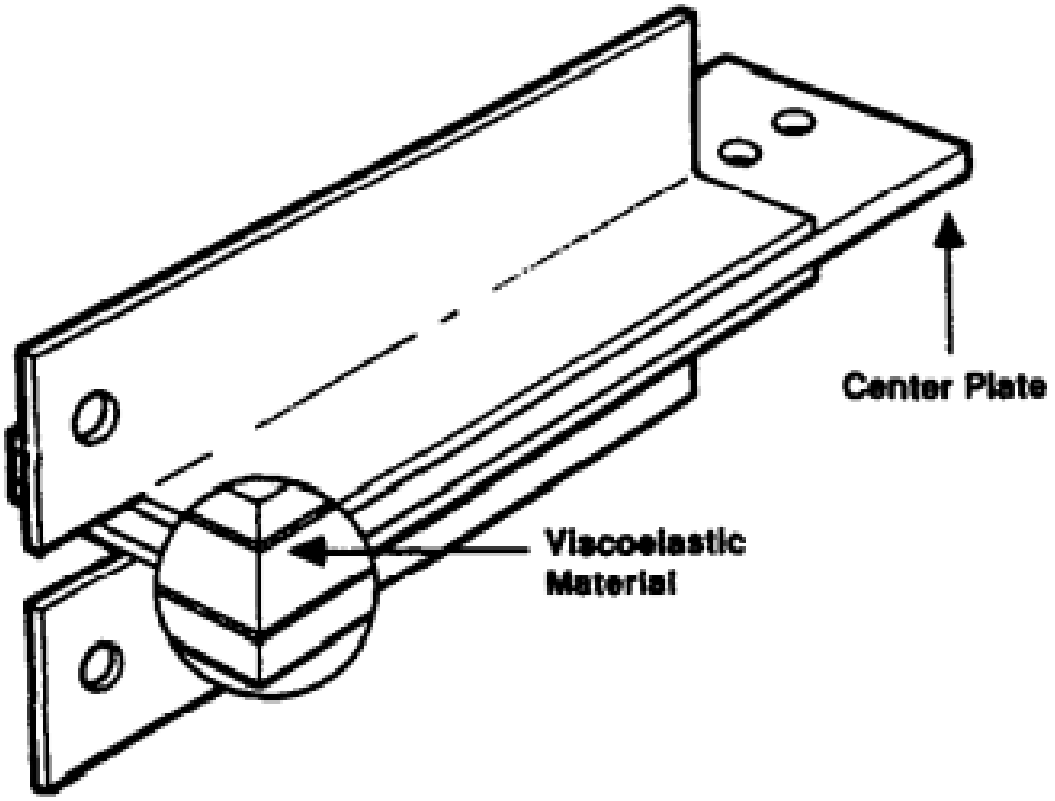

Figure 3.2 A Typical Viscoelastic Damper[26]

3.3. Friction Dampers

Passive friction dampers are a type of hysteretic dampers. Sliding of the surfaces of the surfaces of the friction dampers dissipates the kinetic energy. Surfaces of the friction dampers made by high frictions coefficient materials. Friction dampers can absorb significant amount

of energy through friction mechanism of the solid surfaces. This effect is triggered by relative sliding between the layers of the friction dampers. This mechanism is very close to the friction brake mechanism in trains to stop motion of the train.

In 1975 Mayes and Mowbray investigate response of multi-degree-of freedom system with friction dampers [27]. In 1977 Keightley studied on response of building structures friction dampers[28]. In 1996 Pall et al. investigated applications of friction dampers in earthquake engineering[29]. They made extensive research on seismic behavior of the building structures equipped with friction dampers. They utilized friction dampers for new designed structures. Besides that, they utilized friction dampers to rehabilitate existing structures. Friction dampers provide more economical design of new building structures also friction dampers provide economical solutions of rehabilitation of existing building structures[29].

In Figure 3.3 [29] a typical X-Braced friction damper is shown below.

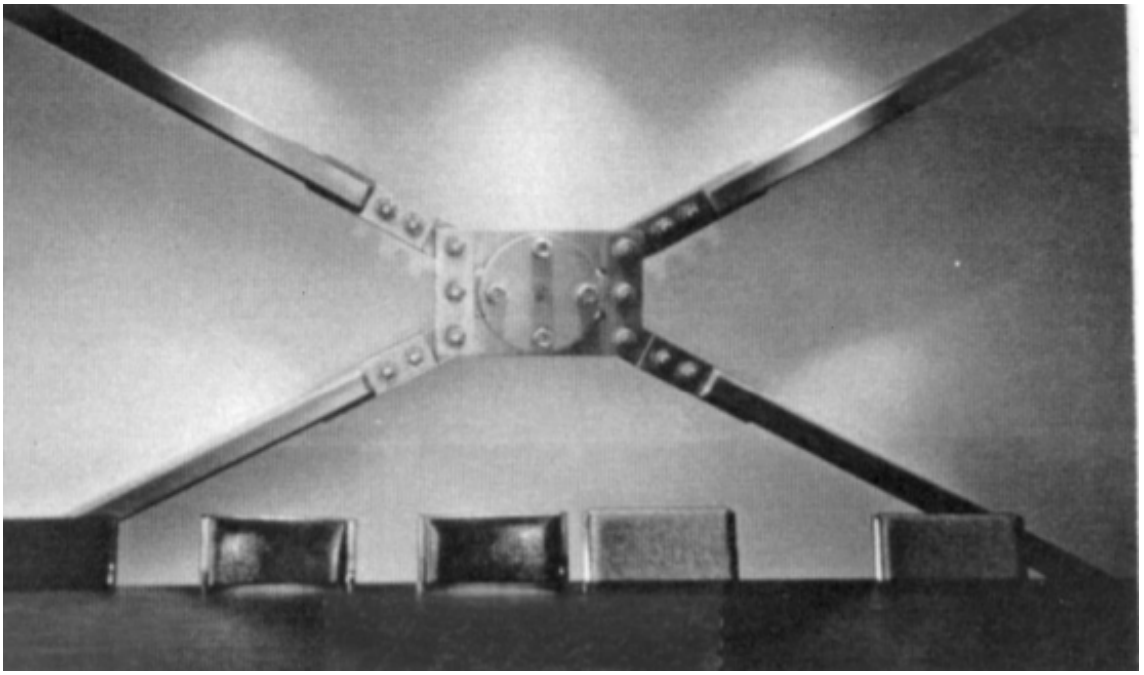

Figure 3.3 A Typical X-Braced Friction Damper[29]

3.4. Metallic Yield Dampers

Metallic yield dampers are passive energy dissipation devices that use hysteretic behavior of metals. Metallic yield dampers absorb significant amount energy under an arbitrary load due to hysteretic properties of metals that used in metallic yield dampers. Mild steel is commonly employed for construction of metallic yield damper [23]. Metallic yield dampers are advantageous passive energy dissipation devices in the field of earthquake engineering. Under demanding earthquakes, metallic yield dampers act like passive energy dissipation systems; however, metallic yield dampers resist to deformations and behave as stiff members under moderate earthquake levels [23]. Because of that reason metallic yield dampers can be employed as both stiff resisting members and passive energy dissipation devices in structures.

4. DYNAMIC ANALYSIS

4.1. General

In scope of this thesis, different MDOF shear buildings are analyzed under earthquake ground motions. A linear elastic procedure is employed to conduct dynamic analysis under earthquake ground motions. Newmark's β linear acceleration method is utilized to solve differential equation of equation of motion of MDOF systems numerically. Rayleigh's method is utilized to obtain damping matrices of MDOF structures. In this chapter of the thesis, damping in structures, Rayleigh's method, and Newmark's β method are explained briefly.

4.2. Damping in Structures

Ideally damping in structures can be computed via experiment; however, it is not feasible. Experimental test for evaluating modal damping consumes great budget and time. Therefore, determining modal damping ratios by experiments is impractical. In engineering practice, the modal damping ratios are determined by taking into consideration literature and building codes.

Recommended damping values by Newmark and Hall for damping values is given below in Table 4.1 [30].

Table 4.1 Recommended Damping Values by Newmark and Hall[30]

Stress Level	**Type and Condition of Structure**	**Critical Damping (%)**
Working Stress, no more than about $1/2$ of yield point	Vital Piping	1 to 2
	Welded steel, prestressed concrete, well reinforced concrete (only slight cracking)	2 to 3
	Reinforced concrete with considerable cracking	3 to 5
	Bolted and/or riveted steel, wood structures nailed or bolted joints	5 to 7
At or just below yield point	Vital Piping	2 to 3
	Welded steel, prestressed concrete (without complete loss in prestress),	5 to 7
	Prestressed concrete with no prestress left	7 to 10
	Reinforced concrete	7 to 10
	Bolted and/or riveted steel	10 to 15
	Wood structures with bolted joints	15 to 20

4.3. Construction of Damping Matrix in MDOF Structures

In MDOF systems damping matrix is not completely needed if response of the structure can be solved by classical modal analysis. However, in some cases classical modal analysis is not applicable. Providing that the response of the structure is nonlinear or the structure has non-proportional damping, it is necessary to express the damping matrix of the structure [31]. In these cases, the damping matrix should be expressed completely in order to determine structural response under dynamic loading. It is impractical to compute damping matrix from dimensions of structural members, member sizes of structural elements or damping of the materials that are used in the structure [32]. Therefore, Rayleigh Damping is a practical choice to express mass and stiffness proportional damping matrix in structures.

4.3.1. Rayleigh Damping

As it is discussed previously in Section 4.3., a complete damping matrix should be expressed when the classical modal analysis is not applicable. In such cases Rayleigh Damping is a good way to express both stiffness and mass proportional damping matrix in MDOF structures in case several modal damping ratios and modal damping frequencies are known. Formulation of Rayleigh Damping method is given below [32].

The mass-proportional damping matrix can be expressed as follows,

$$C = a_0 M \tag{4.1}$$

The stiffness-proportional damping matrix can be expressed as follows,

$$C = a_1 K \tag{4.2}$$

The Rayleigh Damping matrix can be expressed as follows,

$$C = a_0 M + a_1 K \tag{4.3}$$

Damping ratio of n^{th} mode of vibration of a MDOF system can be expressed as follows,

$$\xi_n = \frac{a_0}{2}\frac{1}{\omega_n} + \frac{a_1}{2}\omega_n \tag{4.4}$$

Coefficients a_0 and a_1 can be determined by using two selected damping ratios. Let the selected modes be i^{th} and j^{th} modes then corresponding damping ratios are ξ_i and ξ_j respectively.

Equation 4.4 can be expressed in a matrix equation form for i^{th} and j^{th} modes of vibration as follows,

$$0.5 \begin{bmatrix} \frac{1}{\omega_i} & \omega_i \\ \frac{1}{\omega_j} & \omega_j \end{bmatrix} \begin{Bmatrix} a_0 \\ a_1 \end{Bmatrix} = \begin{Bmatrix} \xi_i \\ \xi_j \end{Bmatrix} \tag{4.5}$$

Assume that $\xi_i = \xi_j = \xi$, and solve the Equation 4.5 for a_0 and a_1. Then, a_0 and a_1 can be solved as follows,

$$a_0 = \xi \frac{2\omega_i \omega_j}{2\omega_i + \omega_j} \tag{4.6}$$

$$a_1 = \xi \frac{2}{\omega_i + \omega_j} \tag{4.7}$$

In this procedure, Rayleigh Damping, selection of the modal damping ratios at i^{th} and j^{th} modes of vibration is an important issue. While performing the selection of modal damping ratios, it should be considered that all modes significantly contribute to the dynamic response of the structure [32].

4.4. Newmark's Method for Solution of Equation of Motion

Analytical solution of equation of motion of a MDOF system is not always applicable. If the externally applied dynamic force varies with time arbitrarily or the MDOF system is subjected to arbitrary ground excitation (i.e., earthquake excitation) it is generally impossible to solve differential equation of the equation of motion. In such cases numerical approaches can be employed to solve differential equation of the equation of motion. There are numerous numerical methods in literature for solving differential equations. One of the most well-known numerical approach for solving the differential equation of the equation motion is Newmark's β Method.

Newmark's Method, as known as Newmark's β Method, was developed by Nathan M. Newmark in 1959. Newmark's Method is a time-stepping method, and can be employed

to numerically solve differential equation of the equation of motion under different dynamic loading. Newmark's Method is still widely used numerical approach in order to evaluate the dynamic response of structures under various dynamic loading.Newmark's Method can be investigated in two special cases which are commonly used. Constant average acceleration method, unconditionally stable, and linear acceleration method, conditionally stable, are the two special cases of the Newmark's Method.

Newmark's method is based on following equations.

$$\dot{u}_{i+1} = \dot{u}_i + [(1-\gamma)\Delta_t]\ddot{u}_i + (\gamma\Delta_t)\ddot{u}_{i+1} \tag{4.8}$$

and

$$u_{i+1} = u_i + (\Delta_t)\dot{u}_i + [(0.5-\beta)(\Delta_t)^2]\ddot{u}_i + [\beta(\Delta_t)^2]\ddot{u}_{i+1} \tag{4.9}$$

Where:

γ and β are acceleration variation parameters over a time step. γ and β parameters have an important influence on accuracy and stability of the method.

- For constant average acceleration case $\gamma = \frac{1}{2}$ and $\beta = \frac{1}{4}$.
- For linear acceleration case $\gamma = \frac{1}{2}$ and $\beta = \frac{1}{6}$.

4.4.1. Stability of Newmark's Method

Stability conditions of Newmark's method is given below [32].

Newmark's Method is stable proving that the following condition satisfied,

$$\frac{\Delta_t}{T_n} \leq \frac{1}{\pi\sqrt{2}} \frac{1}{\sqrt{\gamma - 2\beta}} \tag{4.10}$$

For the constant average acceleration method,$\gamma = 1/2$ and $\beta = 1/4$. Put $\gamma = 1/2$ and $\beta = 1/4$ into Equation 4.10 then the stability condition becomes,

$$\frac{\Delta_t}{T_n} \leq \infty \tag{4.11}$$

Equation 4.11 shows that constant average acceleration method is unconditionally stable.

For the linear acceleration method,$\gamma = 1/2$ and $\beta = 1/6$. Put $\gamma = 1/2$ and $\beta = 1/6$ into Equation 4.12 then the stability condition becomes,

$$\frac{\Delta_t}{T_n} \leq 0.551 \tag{4.12}$$

Equation 4.12 shows that linear acceleration method is conditionally stable. $\frac{\Delta_t}{T_n}$ must be smaller than 0.551 while using linear acceleration method.

4.4.2. Application of Newmark's Method for Linear Elastic SDOF Systems

Application of Newmark's Method for linear elastic SDOF systems is summarized below [32].

Equation of motion of a SDOF structure can be written as follows.

$$m\ddot{u}(t) + c\dot{u}(t) + ku(t) = p(t) \tag{4.13}$$

Equation of motion of a SDOF structure with additional viscous damper can be written as follows.

$$m\ddot{u}(t) + (c_S + c_{AD})\dot{u}(t) + ku(t) = p(t) \tag{4.14}$$

For base excited SDOF systems $p(t)$ can be written as follows.

$$p(t) = m(-1)\ddot{u}_g \tag{4.15}$$

Assume that the SDOF system has zero (at rest) initial conditions such that $\dot{u}(0) = 0$ and $u(0) = 0$.

Equation 4.8 and Equation 4.9 can be modified as follows.

$$m\ddot{u}_i + c\dot{u}_i + ku_i = p_i \tag{4.16}$$

Equation 4.9 can be manipulated to obtain $\ddot{u}_{i+1}$ in terms of u_{i+1} as follows.

$$\ddot{u}_{i+1} = \frac{1}{\beta(\Delta_t)^2}(u_{i+1} - u_i) - \frac{1}{\beta}\Delta_t - \Big(\frac{1}{2\beta} - 1\Big)\ddot{u}_i \tag{4.17}$$

Put Equation 4.16 into Equation 4.8 to obtain $\dot{u}_{i+1}$ in terms of u_{i+1} as follows.

$$\dot{u}_{i+1} = \frac{\gamma}{\beta\Delta_t}(u_{i+1} - u_i) + \Big(1 - \frac{\gamma}{\beta}\Big)\dot{u}_i + \Delta_t\Big(1 - \frac{\gamma}{2\beta}\Big)\ddot{u}_i \tag{4.18}$$

Put Equation 4.17 and Equation 4.18 into Equation 4.8 at the time step $i+1$, and Equation 4.8 becomes

$$\hat{k}u_{i+1} = \hat{p}u_{i+1} \tag{4.19}$$

Where

$$\hat{k} = k + \frac{\gamma}{\beta\Delta_t}c + \frac{1}{\beta(\Delta_t)^2}m \tag{4.20}$$

and

$$\begin{aligned}\hat{p} = p_{i+1} + \Big[\frac{1}{\beta(\Delta_t)^2}m + \frac{\gamma}{\beta(\Delta_t)^2}c\Big]u_i + \Big[\frac{1}{\beta\Delta_t}m + \Big(\frac{\gamma}{\beta} - 1\Big)c\Big]\dot{u}_i \\ + \Big[\Big(\frac{1}{2\beta} - 1\Big)m + \Delta_t\Big(\frac{\gamma}{2\beta} - 1\Big)c\Big]\ddot{u}_i\end{aligned} \tag{4.21}$$

In this case $\hat{k}$ and $\hat{p}_{i+1}$ can be computed from structural properties (such as m,c,and k), and Newmark's method constants (such as γ and β) in accordance with selected special Newmark's method case.

Displacement of the structure at time step $i+1$ can be calculated as follows.

$$u_{i+1} = \frac{\hat{p}_{i+1}}{\hat{k}} \tag{4.22}$$

Displacement of the structure at time step $i+1$ can be computed from Equation 4.22.Velocity of the structure at time step $i+1$ can be computed from Equation 4.18. Acceleration of the structure at time step $i+1$ can be computed from Equation 4.17.

To start the iterative procedure acceleration at t=0 can be calculated from equation motion providing that initial condition for velocity and acceleration are known. Equation for $\ddot{u}_0$ is shown below.

$$\ddot{u}_{t=0} = \frac{p_{t=1} - c\dot{u}_{t=1} - ku_{t=1}}{m} \tag{4.23}$$

4.4.3. Application of Newmark's Method for Linear Elastic MDOF Systems

Application of Newmark's Method for linear elastic MDOF systems is summarized below [32].

Equation of motion of a MDOF structure can be written as follows.

$$M\ddot{u}(t) + C\dot{u}(t) + Ku(t) = P(t) \tag{4.24}$$

If the structure has additional viscous damper, damping matrix can be expressed as follows.

$$C = (C_S + C_{AD}) \tag{4.25}$$

For base excited MDOF systems $P(t)$ can be written as follows.

$$P(t) = M\{-1\}\ddot{u}_g \tag{4.26}$$

Modal expansion of $u(t)$ is given below.

$$u = \sum_{n=1}^{N} \phi_n q_n \tag{4.27}$$

Modal expansion of $\dot{u}(t)$ is given below.

$$\dot{u} = \sum_{n=1}^{N} \phi_n \dot{q}_n \tag{4.28}$$

Modal expansion of $\ddot{u}(t)$ is given below.

$$\ddot{u} = \sum_{n=1}^{N} \phi_n \ddot{q}_n \tag{4.29}$$

Put equations 4.27,4.28,and 4.29 into equation 4.24, then pre-multiply it with the transpose of r^{th} mode shape vector (ϕ_r^T).

$$\phi_r^T M \sum_{n=1}^{N} \phi_n q_n + \phi_r^T C \sum_{n=1}^{N} \phi_n \dot{q}_n + \phi_r^T K \sum_{n=1}^{N} \phi_n \ddot{q}_n = \phi_r^T P \tag{4.30}$$

Orthogonality conditions are given below.

$$\phi_r^T M \phi_n = 0 \;\; for \;\; n \neq r \tag{4.31}$$

$$\phi_r^T C \phi_n = 0 \;\; for \;\; n \neq r \tag{4.32}$$

$$\phi_r^T K \phi_n = 0 \;\; for \;\; n \neq r \tag{4.33}$$

Apply orthogonality conditions to Equation 4.30. Then Equation 4.30 can be written as follows.

$$M_n\ddot{q}_n + C_n\dot{q}_n + K_n q_n = P_n \tag{4.34}$$

Equation 4.34 represents n^{th} mode of vibration of MDOF system. By using modal expansions and orthogonality conditions, Equation 4.34 is transferred to a set of second order differential equations. Each differential equation represents equation of motion of a SDOF system. By this way, Newmark's method stated in the Section 4.4.2. can be easily applied to a MDOF structure.

5. OPTIMIZATION ALGORITHMS

5.1. Differential Evolution (DE)

Differential Evolution (DE) algorithm is a population based meta-heuristic search algorithm that uses the evolutionary process.DE algorithm was proposed by Storn and Price in 1997.Inspiration of the DE algorithm is evolutionary process of the nature. DE algorithm consists of three main operators. These operators are mutation, crossover, and selection. DE algorithm is simple and effective algorithm especially for continuous optimization problems [33].

5.1.1. Mathematical Formulation and Steps of DE Algorithm

Mathematical formulation and steps of Differential Evolution algorithm is summarized below [33].

i^{th} target vector of G^{th} generation can be represented as follows.

$$\vec{X}^{i}_{i,G} = \{X^{G}_{1,i}, X^{G}_{2,i}, ..., X^{G}_{D,i}\}, i = 1, 2, ..., NP \tag{5.1}$$

i^{th} mutant vector of G^{th} generation can be represented as follows.

$$\vec{V}^{i}_{i,G} = \{V^{G}_{1,i}, X^{G}_{2,i}, ..., V^{G}_{D,i}\}, i = 1, 2, ..., NP \tag{5.2}$$

i^{th} trial vector of G^{th} generation can be represented as follows.

$$\vec{U}^{i}_{i,G} = \{U^{G}_{1,i}, U^{G}_{2,i}, ..., U^{G}_{D,i}\}, i = 1, 2, ..., NP \tag{5.3}$$

D stands for the dimension of the optimization problem, and NP stands for the population size.

Step 1: Initialization

Set the parameters of the DE algorithm. Randomly create an initial population by taking in account of Lower Bound (LB) and Upper Bound (UB) of the optimization problem. Then evaluate fitness of the initial population by using the fitness function.

Step 2: Mutation

Randomly select three target vectors such that $\vec{X}_{r1,G}$, $\vec{X}_{r2,G}$, and $\vec{X}_{r3,G}$. $r1$, $r2$, and $r3$ are different random integer indexes.$r1$, $r2$, and $r3 \in \{1, 2, ..., NP\}$ are determined stochastically from population. Mutant vector is created via three randomly selected target vectors as follows.

$$\vec{V}_{i,G+1} = \vec{X}_{r1,G} + F.(\vec{X}_{r2,G} - \vec{X}_{r3,G}) \tag{5.4}$$

In Equation 5.4 F is called as mutation factor. F is a real and constant vector $\in [0, 2]$.

Step 3: Crossover Crossover operator generates trial vector. Trial vector is formed as follows.

$$\vec{U}_{ji,G+1} = \begin{cases} \vec{V}_{ji,G+1}, & if \quad (randb(j) \leq CR) \quad or \quad j = rnbr(i) \\ \vec{X}_{ji,G}, & otherwise \end{cases} \tag{5.5}$$

In Equation 5.5 $randb(j)$ is the randomly generated number at the j_{th} evaluation. $randb(j)$ $\in [0, 1]$. $rbnr(i)$ is a stochastically chosen index $\in 1, 2, ..., D$. $CR \in [0, 1]$ is the crossover rate.

Step 4: Selection Selection operator compares trial vector $\vec{U}_{i,G+1}$ and target vector $\vec{X}_{i,G}$. This operator selects the superior one. After this step, go back to Step 2 and repeat the

process until the stopping criterion is satisfied. In the scope of this thesis study, the stopping criterion is based on maximum iteration termination.

5.2. Particle Swarm Optimization (PSO)

Particle Swarm Optimization (PSO) algorithm is a population based meta-heuristic search algorithm that uses the swarm intelligence. PSO is a nature inspired meta-heuristic search algorithm. PSO algorithm mimics the navigation or foraging behavior of flock of birds or fishes. PSO algorithm is firstly proposed by Kennedy and Eberhart in 1995 [34]. Then PSO algorithm is modified by Shi and Eberhart in 1998 to increase the performance of PSO algorithm. This modification introduced inertia weight (w) term. Inertia weight can be a positive constant. Besides that, inertia weight can be expressed as positive linear or nonlinear function of iteration[35].

5.2.1. Mathematical Formulation and Steps of PSO Algorithm

Mathematical formulation and steps of Particle Swarm Optimization algorithm is summarized below [35].

i^{th} position vector can be represented as follows.

$$\vec{X_i} = \{X_{i,1}, X_{i,2}, ..., X_{i,D}\}, i = 1, 2, ..., NP \tag{5.6}$$

i^{th} velocity vector can be represented as follows.

$$\vec{V_i} = \{V_{i,1}, V_{i,2}, ..., V_{i,D}\}, i = 1, 2, ..., NP \tag{5.7}$$

D stands for the dimension of the optimization problem, and NP stands for the population size.

Step 1: Initialization

Set the parameters of the PSO algorithm. Randomly create an initial population by taking in account of Lower Bound (LB) and Upper Bound (UB) of the optimization problem. Evaluate fitness of the initial population by using the fitness function. Determine best position of each particle (P), and global best position (G).

Step 2: Update Velocity Vector

Update the velocity vector as follows.

$$\vec{V}_i^{t+1} = w\vec{V}_i^t + c_1 r_1 \left(\vec{P}_i^t - \vec{X}_i^t\right) + c_2 r_2 \left(\vec{G}^t - \vec{X}_i^t\right) \tag{5.8}$$

Where:

c_1 and c_2 are acceleration factors.

r_1 and $r_2 \in [0, 1]$ are randomly generated numbers.

w is the inertia weight.

P is the particle best position.

G is the global best position.

Step 3: Update Position Vector

Update the position vector as follows.

$$\vec{X}_i^{t+1} = \vec{X}_i^t + \vec{V}_i^{t+1} \tag{5.9}$$

Step 4: Update Global Best and Particle Best

Evaluate fitness of each particle by using fitness function and update particle best position and global best position. After this step, go back to Step 2 and repeat the process until the stopping criterion is satisfied. In the scope of this thesis study, the stopping criterion is based on maximum iteration termination.

5.3. Optimization Problem

Design variables of the optimization are damping coefficients of the added viscous damper at each story. Design vector (X^T) is given below.

$$X^T = [c_{AD,1}, c_{AD,2}, c_{AD,3}, ..., c_{AD,i-1}, c_{AD,i}] \tag{5.10}$$

Optimization problem is a continues type optimization problem. Lower Bound (LB) and Upper Bound (UB) values are decided by taking into account the literature [13]. Lower Bound (LB) and Upper Bound (UB) of the optimization problem is given below.

$$0 \leq c_{AD,N} \leq 2 \times 10^4 \ kN.s/m \tag{5.11}$$

Objective function subjected to minimize is summation of the damping coefficients of the added viscous dampers at all stories of the shear building. Objective function $f(X)$ is given below.

$$f(X) = \sum_{N=0}^{i} c_{AD,N} \tag{5.12}$$

Optimization problem is based on IDR constraints. Peak IDR should not exceed allowable limit. Allowable peak IDR is 0.01 for each story [36]. Constraint of the optimization problem is given below.

$$Peak\ IDR_N \leq 0.01\ \ [36] \tag{5.13}$$

6. NUMERICAL EXAMPLES

6.1. General

In this chapter, dynamic behavior of three different shear buildings are investigated under twelve different earthquake ground motion records. All shear buildings have structural rigidity irregularity at first story. Shear buildings are rehabilitated with optimum viscous damper distribution via Differential Evolution (DE) and Particle Swarm Optimization (PSO) in case rehabilitation is needed under specific earthquake ground motion data.

The structural data obtained from Cetin et al [12], and ground motion data obtained from PEER Ground Motion Database [37] are used. Ground motions are selected from FEMA P695 data set [38]. For each structure stiffness of first story is reduced by 20%. Twelve earthquake ground motions are used in numerical examples for all shear buildings. Earthquake ground motions consist of four Pulse Near Fault (PNF), four No Pulse Near Fault (NPNF), and four Far Fault (FF) records to analyze dynamic response of the shear building under various ground motion data [39]. It is assumed that $\xi_1 = \xi_2 = 0.02$ for all shear buildings in order to construct damping matrix via Rayleigh's method [12].

In all shear buildings, first story stiffness is reduced by 20% to cause soft story structural irregularity in accordance with ASCE 7-10 [17] and FEMA 310 [15] standards.ASCE 7-10 and FEMA 310 standards for soft story structural irregularity are explained in detail in Section 2.2.1. and Section 2.2.3. of this thesis. It is observed that in most of the numerical examples, 20% stiffness reduction in first story cause abnormal peak IDR values. In this chapter of the thesis, three different shear building are analyzed under twelve different earthquake ground motion data. Structures are rehabilitated by an optimum viscous damper (VD) distribution in case it is needed. Acceptance criteria for peak IDR limit is taken from literature, and allowable IDR limit for each story is 0.01 [13]. In numerical examples, lower bound (LB) and upper bound (UB) value for added dampers are indicated in Section 5.3.. Upper bound (UB) value for added dampers is increased in case it is needed, and it is indicated at the beginning of the example.

6.1.1. Earthquake Ground Motion Data

Pulse Near Fault (PNF) ground motion data are given below in Table 6.1.

Table 6.1 Pulse Near Fault (PNF) Ground Motion Data

Pulse Near Fault (PNF)				
RSN No	Name	Magnitude	V_{s30}(m/s)	Used Component
182	Imperial Valley-06	6.53	210.51	RSN182_IMPVALL.H_H-E07140
821	Erzincan,Turkey	6.69	352.05	RSN821_ERZINCAN_ERZ-EW
1063	Northridge-01	6.69	282.25	RSN1063_NORTHR_RRS228
1605	Duzce,Turkey	7.14	281.86	RSN1605_DUZCE_DZC180

No Pulse Near Fault (NPNF) ground motion data are given below in Table 6.2.

Table 6.2 No Pulse Near Fault (NPNF) Ground Motion Data

No Pulse Near Fault (NPNF)				
RSN No	Name	Magnitude	V_{s30} (m/s)	Used Component
160	Imperial Valley-06	6.61	316.46	RSN160_IMPVALL.H_H-BCR140
496	Nahanni,Canada	6.76	605.04	RSN496_NAHANNI_S2240
741	Loma Prieta	6.93	476.54	RSN741_LOMAP_BRN000
1004	Northridge-01	6.69	380.06	RSN1004_NORTHR_SPV360

Far Fault (FF) ground motion data are given below in Table 6.3.

Table 6.3 Far Fault (FF) Ground Motion Data

No Pulse Near Fault (NPNF)				
RSN No	Name	Magnitude	V_{s30} (m/s)	Used Component
68	San Fernando	6.53	220.03	RSN68_SFERN_PEL180
752	Loma Prieta	6.93	288.62	RSN752_LOMAP_CAP090
953	Northridge	6.69	355.81	RSN953_NORTHR_MUL009
1111	Kobe,Japan	6.9	609	RSN1111_KOBE_NIS000

Correlation between V_{s30} and soil class in accordance with TBEC2018 is given below in Table 6.4 [19].

Table 6.4 V_{s30} and Soil Class Correlation in Accordance With TBEC2018 [19]

Site Soil Class	**Definition**	V_{s30} **(m/s)**
ZA	Hard rock	> 1500
ZB	Medium rock	$760 - 1500$
ZC	Dense sand,gravel,very stiff clay,soft rock	$360 - 760$
ZD	Medium dense sand,gravel, stiff clay	$180 - 360$
ZE	Loose sand,gravel,medium to stiff clay	< 180
ZF	Site specific research required	

6.1.2. Structure Data

Structural properties of Structure1 is given below in Table 6.5.

Table 6.5 Structural Properties of Structure1

Structural Properties of Structure1			
Story No	Stiffness(kN/m)	Mass(tons)	Height(m)
1	2×10^4	120	3
2	2.5×10^4	120	3
3	2.5×10^4	120	3
4	2.5×10^4	120	3

Structural properties of Structure2 is given below in Table 6.6.

Table 6.6 Structural Properties of Structure2

Structural Properties of Structure2			
Story No	Stiffness(kN/m)	Mass(tons)	Height(m)
1	2×10^4	120	3
2	2.5×10^4	120	3
3	2.5×10^4	120	3
4	2.5×10^4	120	3
5	2.5×10^4	120	3
6	2.5×10^4	120	3
7	2.5×10^4	120	3

Structural properties of Structure3 is given below in Table 6.7.

Table 6.7 Structural Properties of Structure3

Structural Properties of Structure3			
Story No	Stiffness(kN/m)	Mass(tons)	Height(m)
1	2×10^4	120	3
2	2.5×10^4	120	3
3	2.5×10^4	120	3
4	2.5×10^4	120	3
5	2.5×10^4	120	3
6	2.5×10^4	120	3
7	2.5×10^4	120	3
8	2.5×10^4	120	3
9	2.5×10^4	120	3
10	2.5×10^4	120	3

6.2. Analysis Results for Structure1

6.2.1. Under RSN182 (PNF)

Particle Swarm Optimization (PSO) optimization history for Structure1 under RSN182 is given below in Figure 6.1.

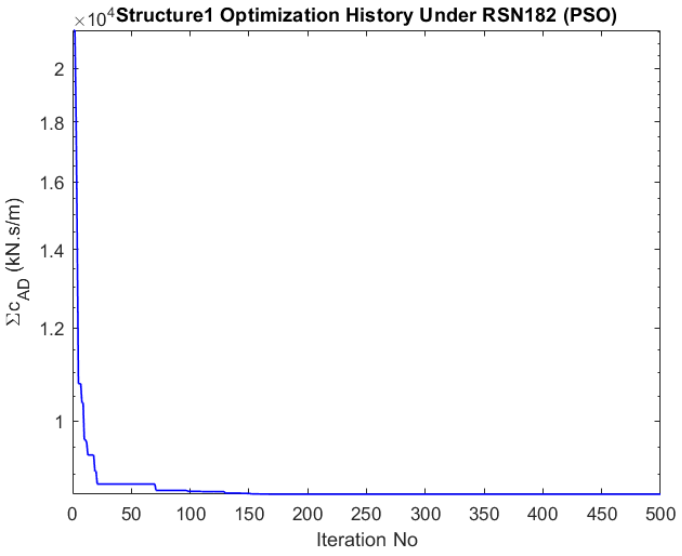

Figure 6.1 Structure1 Optimization History (PSO) Under RSN182

Differential Evolution (DE) optimization history for Structure1 under RSN182 is given below in Figure 6.1.

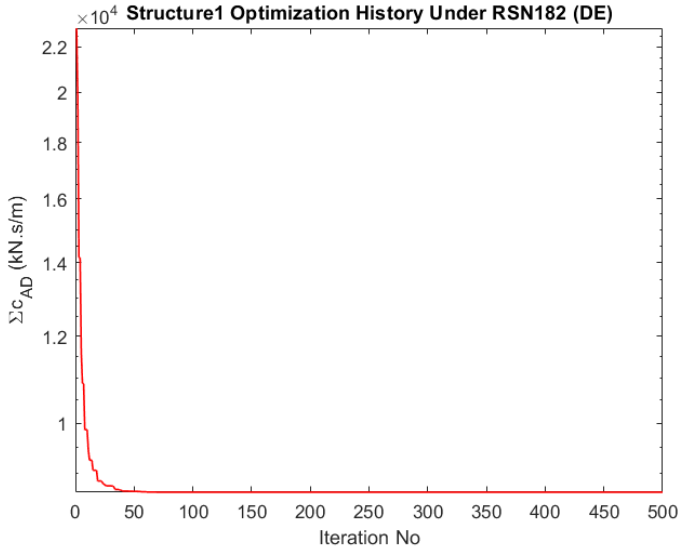

Figure 6.2 Structure1 Optimization History (DE) Under RSN182

Optimum viscous damper (VD) distribution for Structure1 Under RSN182 is given below in Table 6.8.

Table 6.8 Structure1 Optimum viscous damper (VD) distribution Under RSN182

Structure1 Optimum viscous damper (VD) distribution Under RSN182		
Story No	Added Damper PSO (kN.s/m)	Added Damper DE (kN.s/m)
1	4737.487	4716.202
2	3183.411	3154.095
3	734.310	783.910
4	0.000	0.000
Total Global Best	8655.209	8654.207

Comparison of maximum acceleration responses for Structure1 without VD and with optimum VD under RSN182 is given below in Figure 6.3.

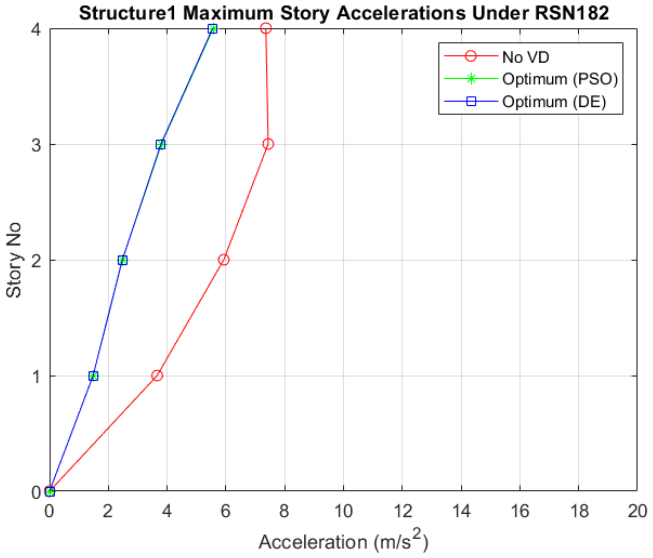

Figure 6.3 Comparison of Maximum Acceleration Responses for Structure1 With VD and Without VD Under RSN182

Comparison of maximum velocity responses for Structure1 without VD and with optimum VD under RSN182 is given below in Figure 6.3.

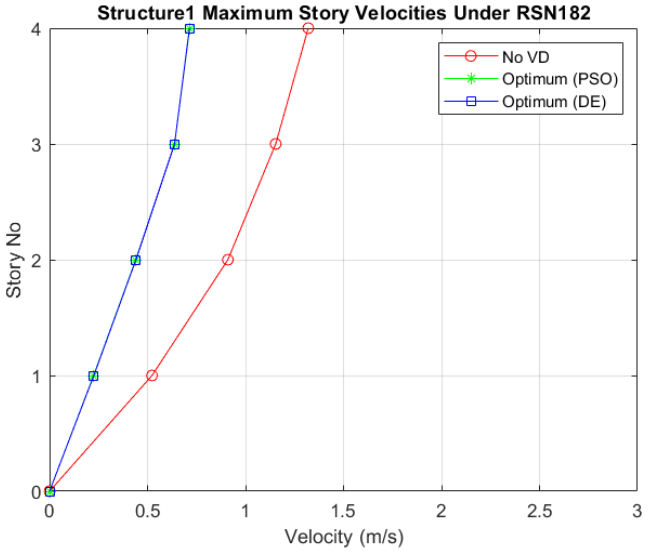

Figure 6.4 Comparison of Maximum Velocity Responses for Structure1 With VD and Without VD Under RSN182

Comparison of maximum displacement responses for Structure1 without VD and with optimum VD under RSN182 is given below in Figure 6.5.

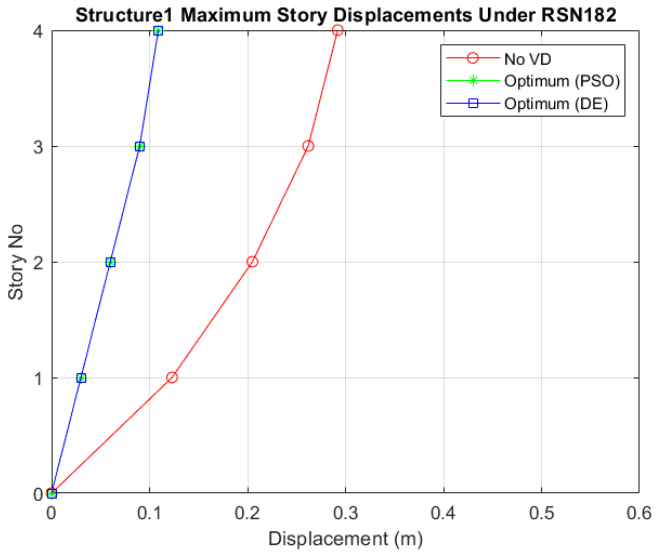

Figure 6.5 Comparison of Maximum Displacement Responses for Structure1 With VD and Without VD Under RSN182

Comparison of peak IDR for Structure1 without VD and with optimum VD under RSN182 is given below in Figure 6.6.

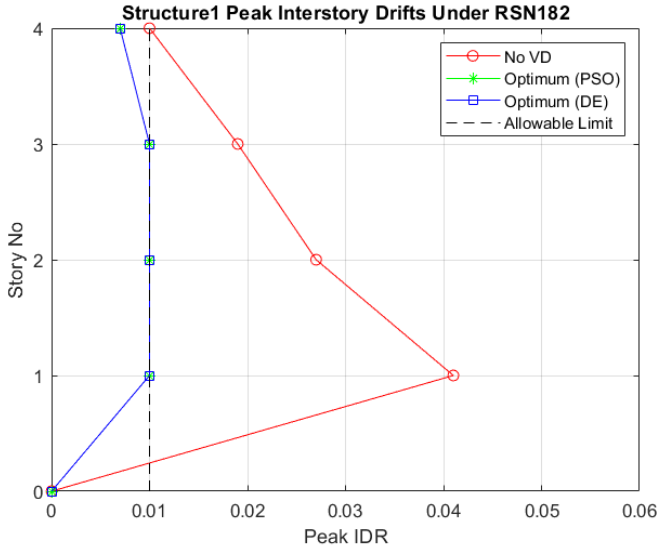

Figure 6.6 Comparison of Peak IDR for Structure1 With VD and Without VD Under RSN182

6.2.2. Under RSN821 (PNF)

Particle Swarm Optimization (PSO) optimization history for Structure1 under RSN821 is given below in Figure 6.7.

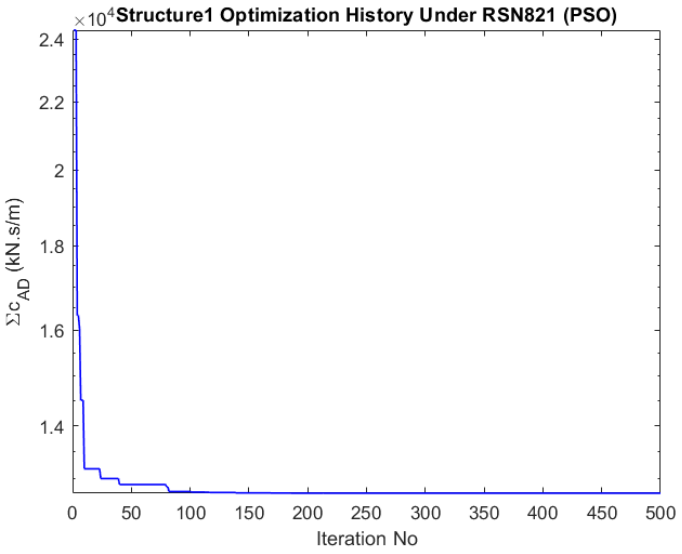

Figure 6.7 Structure1 Optimization History (PSO) Under RSN821

Differential Evolution (DE) optimization history for Structure1 under RSN821 is given below in Figure 6.8.

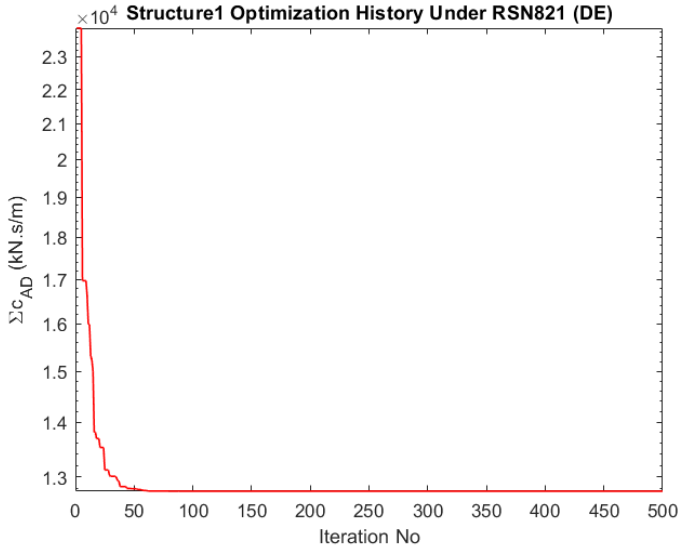

Figure 6.8 Structure1 Optimization History (DE) Under RSN821

Optimum viscous damper (VD) distribution for Structure1 Under RSN821 is given below in Table 6.9.

Table 6.9 Structure1 Optimum viscous damper (VD) distribution Under RSN821

Structure1 Optimum viscous damper (VD) distribution Under RSN821		
Story No	Added Damper PSO (kN.s/m)	Added Damper DE (kN.s/m)
1	7994.710	7994.710
2	4169.185	4169.185
3	580.806	580.806
4	0.000	0.000
Total Global Best	12744.701	12744.701

Comparison of maximum acceleration responses for Structure1 without VD and with optimum VD under RSN821 is given below in Figure 6.9.

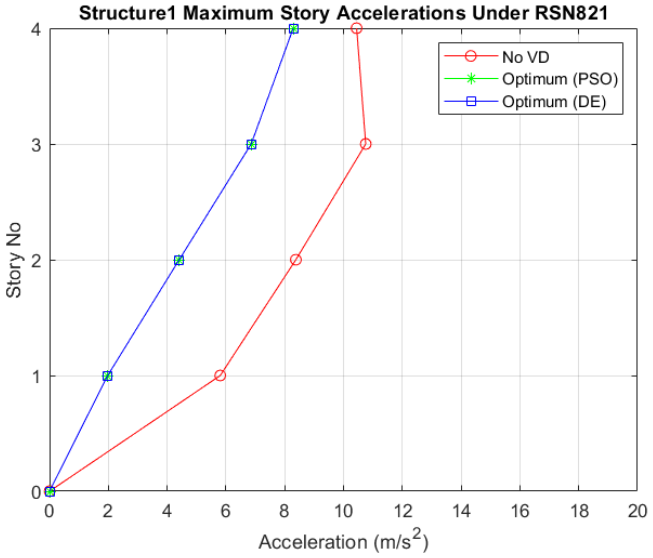

Figure 6.9 Comparison of Maximum Acceleration Responses for Structure1 With VD and Without VD Under RSN821

Comparison of maximum velocity responses for Structure1 without VD and with optimum VD under RSN821 is given below in Figure 6.10.

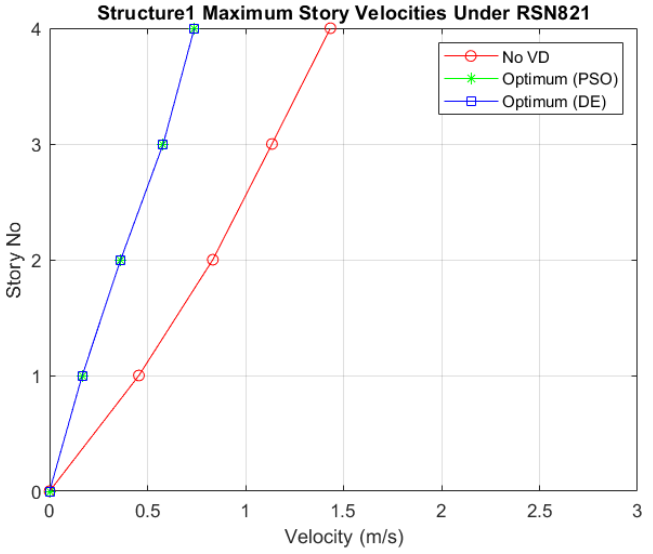

Figure 6.10 Comparison of Maximum Velocity Responses for Structure1 With VD and Without VD Under RSN821

Comparison of maximum displacement responses for Structure1 without VD and with optimum VD under RSN821 is given below in Figure 6.11.

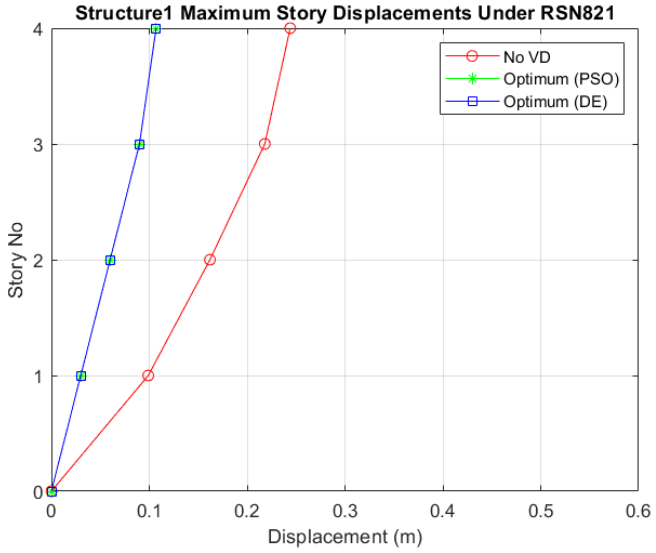

Figure 6.11 Comparison of Maximum Displacement Responses for Structure1 With VD and Without VD Under RSN821

Comparison of peak IDR for Structure1 without VD and with optimum VD under RSN821 is given below in Figure 6.12.

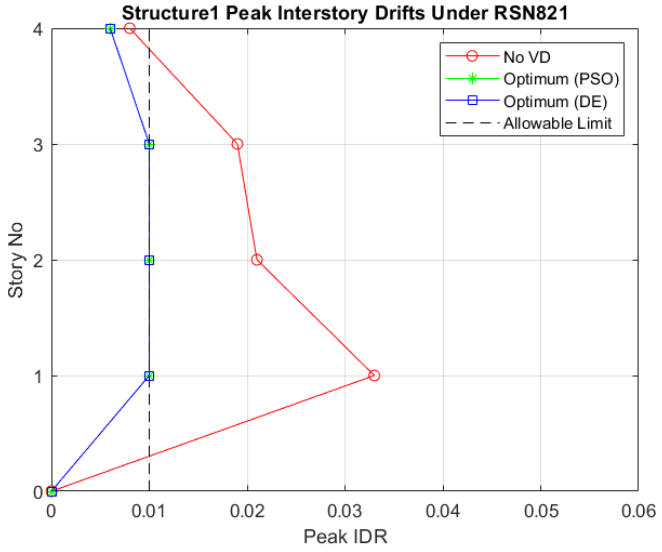

Figure 6.12 Comparison of Peak IDR for Structure1 With VD and Without VD Under RSN821

6.2.3. Under RSN1063 (PNF)

Particle Swarm Optimization (PSO) optimization history for Structure1 under RSN1063 is given below in Figure 6.13.

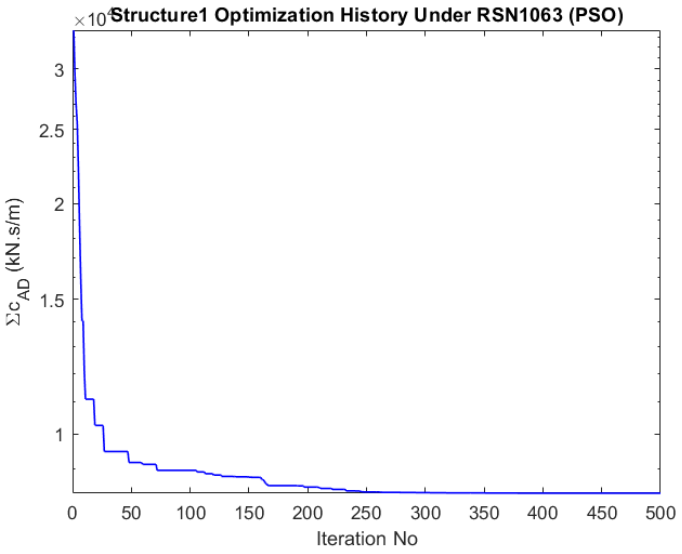

Figure 6.13 Structure1 Optimization History (PSO) Under RSN1063

Differential Evolution (DE) optimization history for Structure1 under RSN1063 is given below in Figure 6.14.

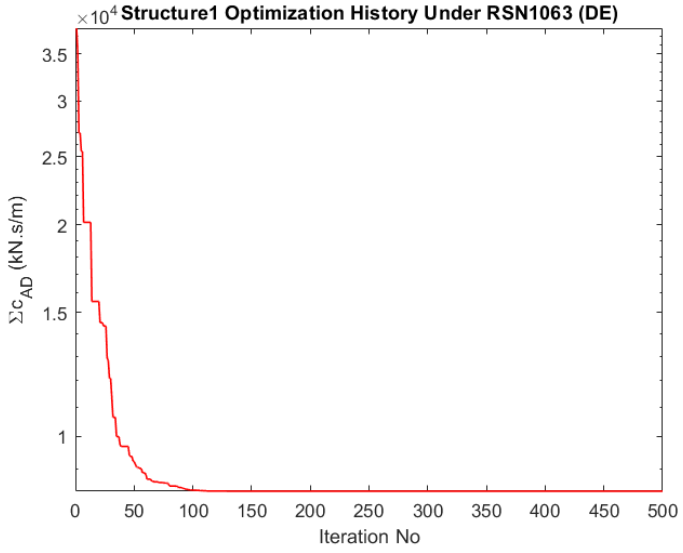

Figure 6.14 Structure1 Optimization History (DE) Under RSN1063

Optimum viscous damper (VD) distribution for Structure1 Under RSN1063 is given below in Table 6.10.

Table 6.10 Structure1 Optimum viscous damper (VD) distribution Under RSN1063

Structure1 Optimum viscous damper (VD) distribution Under RSN1063		
Story No	Added Damper PSO (kN.s/m)	Added Damper DE (kN.s/m)
1	4926.990	4926.990
2	2210.611	2210.611
3	688.120	688.120
4	534.626	534.626
Total Global Best	8360.347	8360.347

Comparison of maximum acceleration responses for Structure1 without VD and with optimum VD under RSN1063 is given below in Figure 6.15.

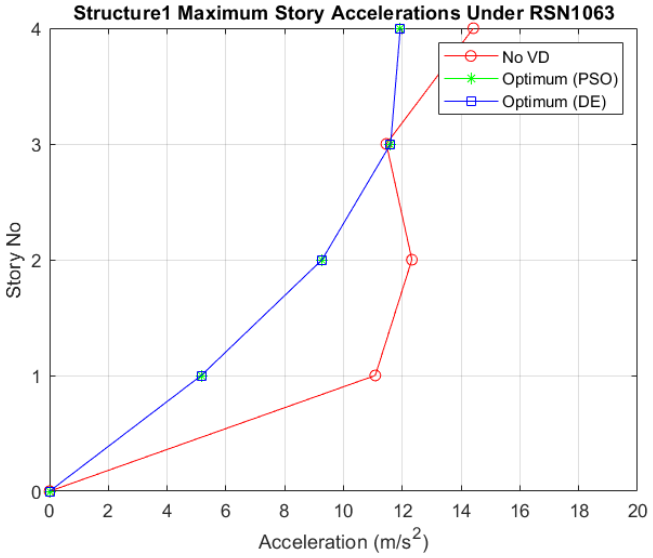

Figure 6.15 Comparison of Maximum Acceleration Responses for Structure1 With VD and Without VD Under RSN1063

Comparison of maximum velocity responses for Structure1 without VD and with optimum VD under RSN1063 is given below in Figure 6.16.

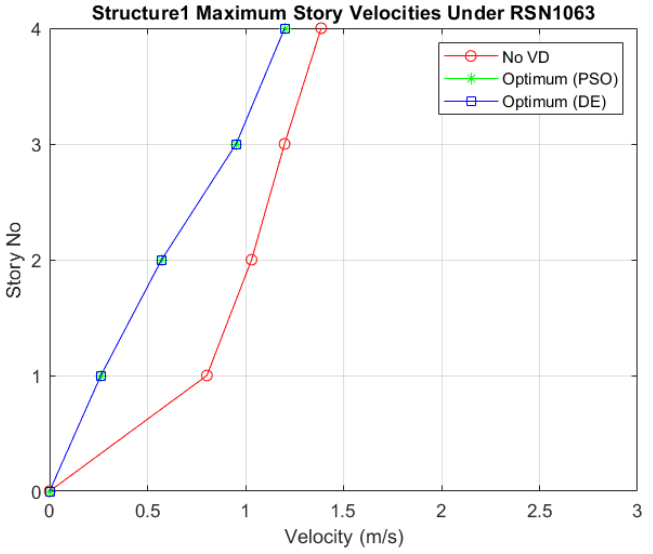

Figure 6.16 Comparison of Maximum Velocity Responses for Structure1 With VD and Without VD Under RSN1063

Comparison of maximum displacement responses for Structure1 without VD and with optimum VD under RSN1063 is given below in Figure 6.17.

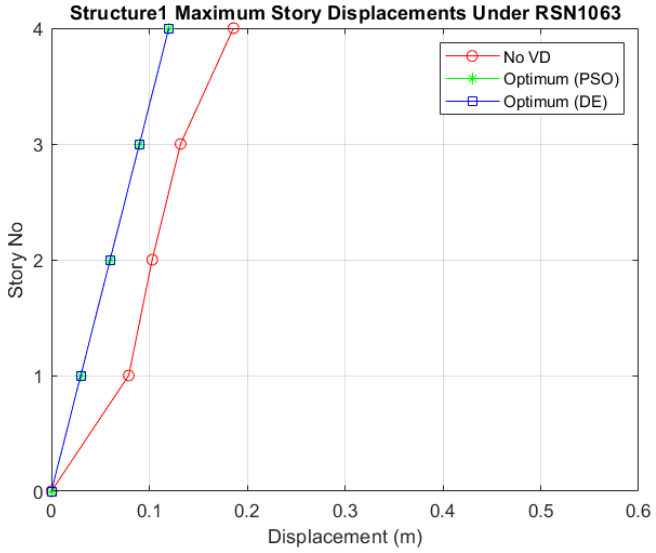

Figure 6.17 Comparison of Maximum Displacement Responses for Structure1 With VD and Without VD Under RSN1063

Comparison of peak IDR for Structure1 without VD and with optimum VD under RSN1063 is given below in Figure 6.18.

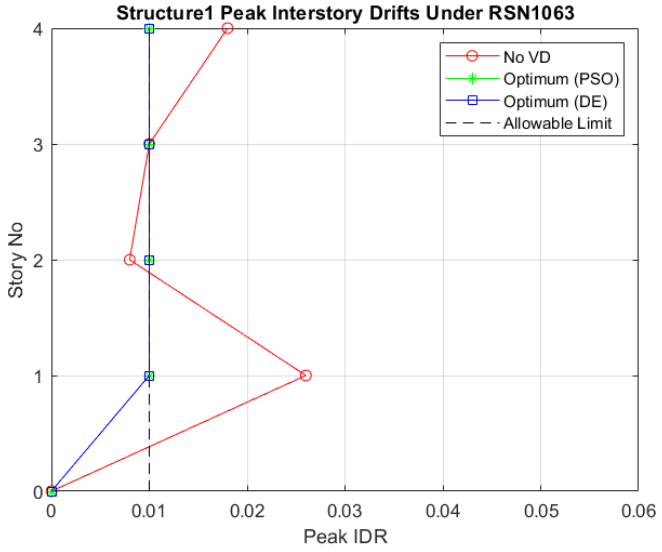

Figure 6.18 Comparison of Peak IDR for Structure1 With VD and Without VD Under RSN1063

6.2.4. Under RSN1605 (PNF)

Particle Swarm Optimization (PSO) optimization history for Structure1 under RSN1605 is given below in Figure 6.19.

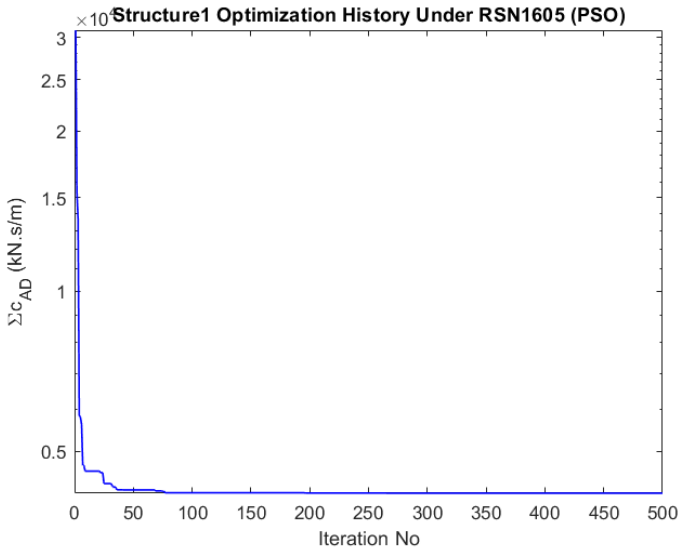

Figure 6.19 Structure1 Optimization History (PSO) Under RSN1605

Differential Evolution (DE) optimization history for Structure1 under RSN1605 is given below in Figure 6.20.

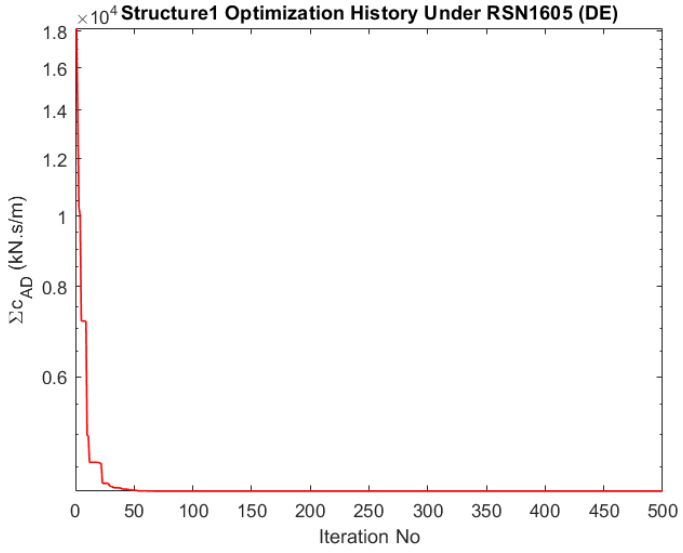

Figure 6.20 Structure1 Optimization History (DE) Under RSN1605

Optimum viscous damper (VD) distribution for Structure1 Under RSN1605 is given below in Table 6.11.

Table 6.11 Structure1 Optimum viscous damper (VD) distribution Under RSN1605

Structure1 Optimum viscous damper (VD) distribution Under RSN1605		
Story No	Added Damper PSO (kN.s/m)	Added Damper DE (kN.s/m)
1	2610.828	2610.828
2	622.412	622.412
3	937.040	937.040
4	0.000	0.000
Total Global Best	4170.280	4170.280

Comparison of maximum acceleration responses for Structure1 without VD and with optimum VD under RSN1605 is given below in Figure 6.21.

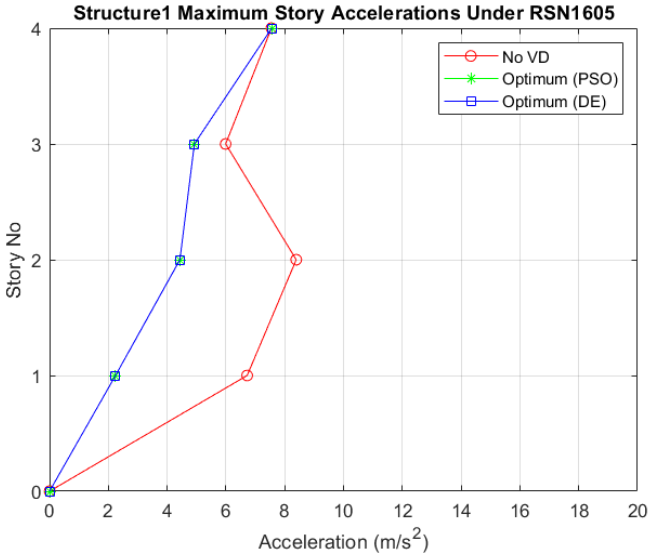

Figure 6.21 Comparison of Maximum Acceleration Responses for Structure1 With VD and Without VD Under RSN1605

Comparison of maximum velocity responses for Structure1 without VD and with optimum VD under RSN1605 is given below in Figure 6.22.

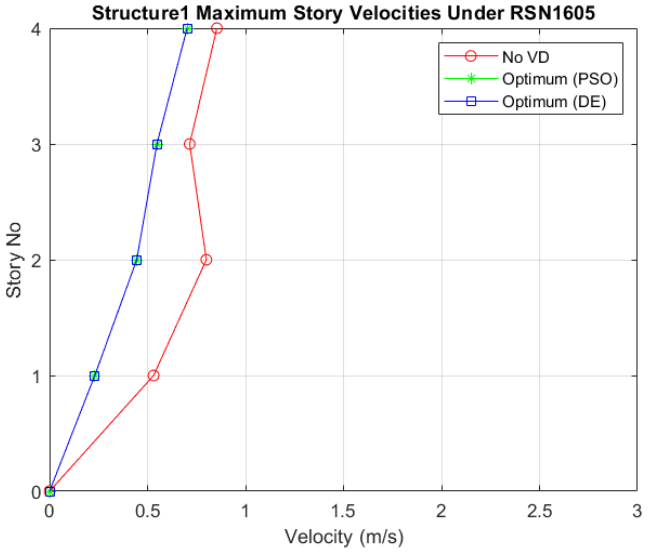

Figure 6.22 Comparison of Maximum Velocity Responses for Structure1 With VD and Without VD Under RSN1605

Comparison of maximum displacement responses for Structure1 without VD and with optimum VD under RSN1605 is given below in Figure 6.23.

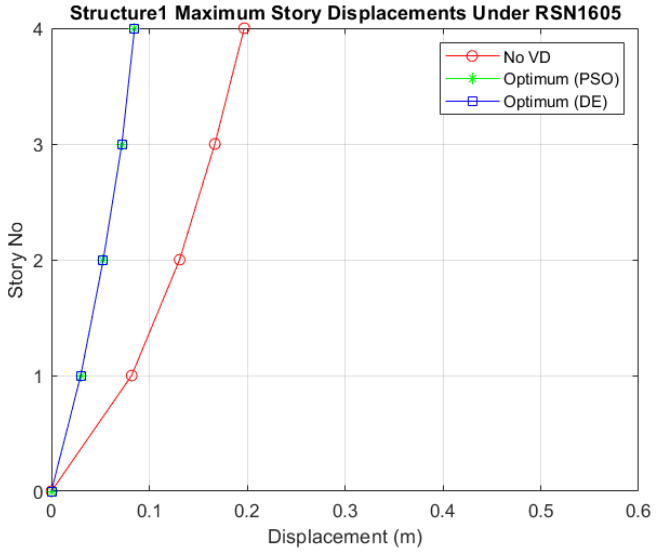

Figure 6.23 Comparison of Maximum Displacement Responses for Structure1 With VD and Without VD Under RSN1605

Comparison of peak IDR for Structure1 without VD and with optimum VD under RSN1605 is given below in Figure 6.24.

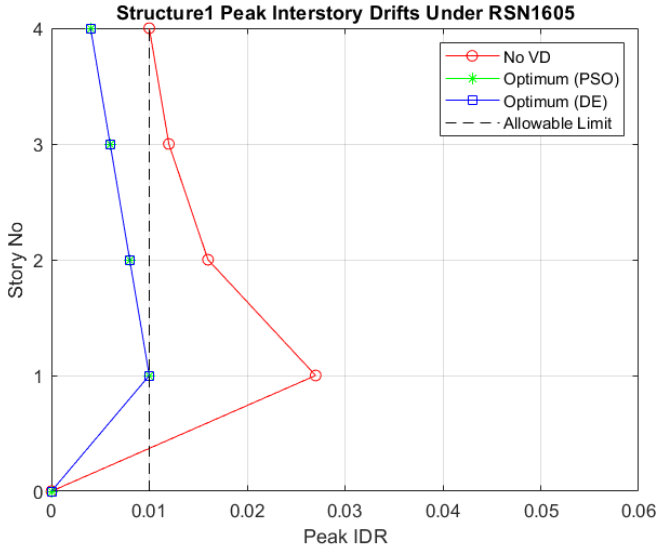

Figure 6.24 Comparison of Peak IDR for Structure1 With VD and Without VD Under RSN1605

6.2.5. Under RSN160 (NPNF)

Particle Swarm Optimization (PSO) optimization history for Structure1 under RSN160 is given below in Figure 6.25.

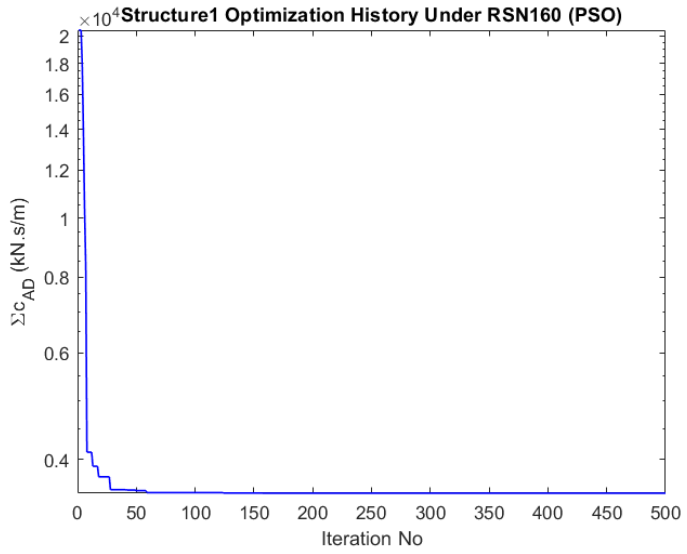

Figure 6.25 Structure1 Optimization History (PSO) Under RSN160

Differential Evolution (DE) optimization history for Structure1 under RSN160 is given below in Figure 6.26.

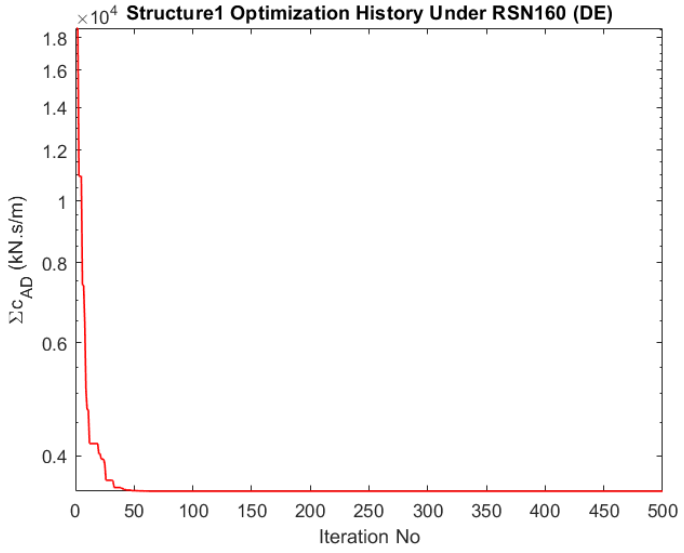

Figure 6.26 Structure1 Optimization History (DE) Under RSN160

Optimum viscous damper (VD) distribution for Structure1 Under RSN160 is given below in Table 6.12.

Table 6.12 Structure1 Optimum viscous damper (VD) distribution Under RSN160

Structure1 Optimum viscous damper (VD) distribution Under RSN160		
Story No	Added Damper PSO (kN.s/m)	Added Damper DE (kN.s/m)
1	2671.568	2671.568
2	848.414	848.414
3	0.000	0.000
4	0.000	0.000
Total Global Best	3519.982	3519.982

Comparison of maximum acceleration responses for Structure1 without VD and with optimum VD under RSN160 is given below in Figure 6.27.

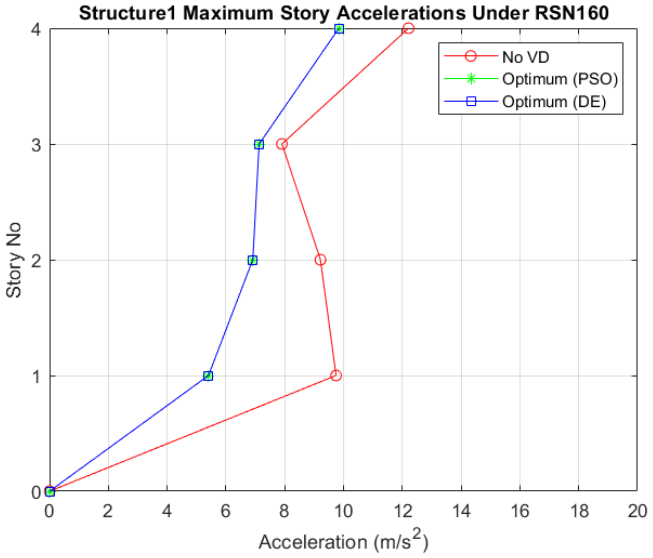

Figure 6.27 Comparison of Maximum Acceleration Responses for Structure1 With VD and Without VD Under RSN160

Comparison of maximum velocity responses for Structure1 without VD and with optimum VD under RSN160 is given below in Figure 6.28.

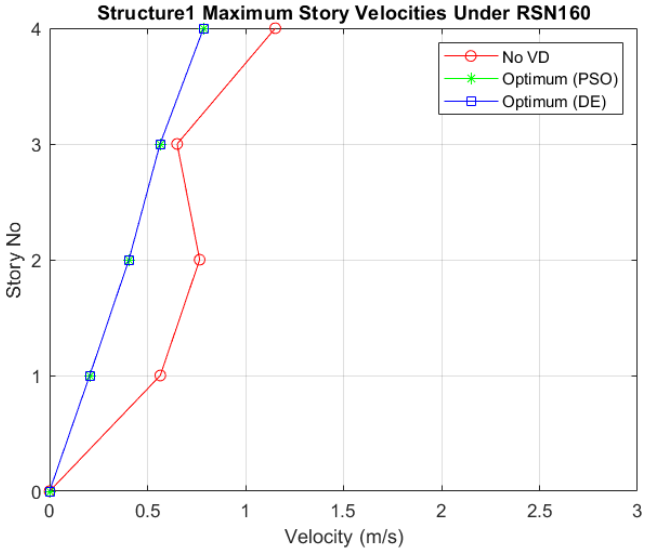

Figure 6.28 Comparison of Maximum Velocity Responses for Structure1 With VD and Without VD Under RSN160

Comparison of maximum displacement responses for Structure1 without VD and with optimum VD under RSN160 is given below in Figure 6.29.

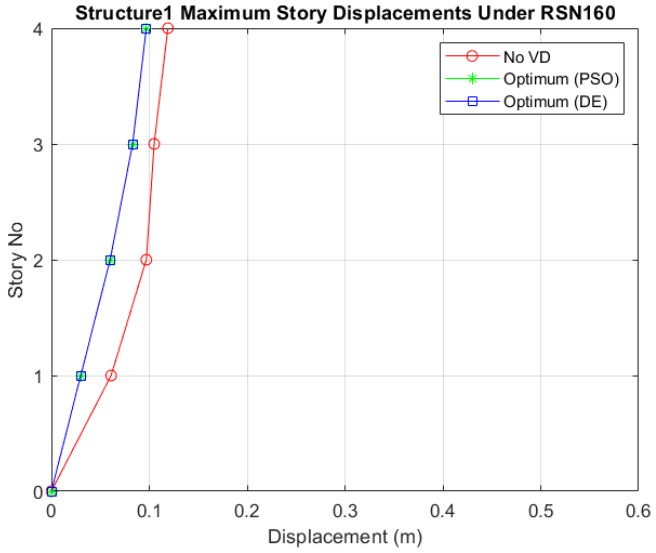

Figure 6.29 Comparison of Maximum Displacement Responses for Structure1 With VD and Without VD Under RSN160

Comparison of peak IDR for Structure1 without VD and with optimum VD under RSN160 is given below in Figure 6.30.

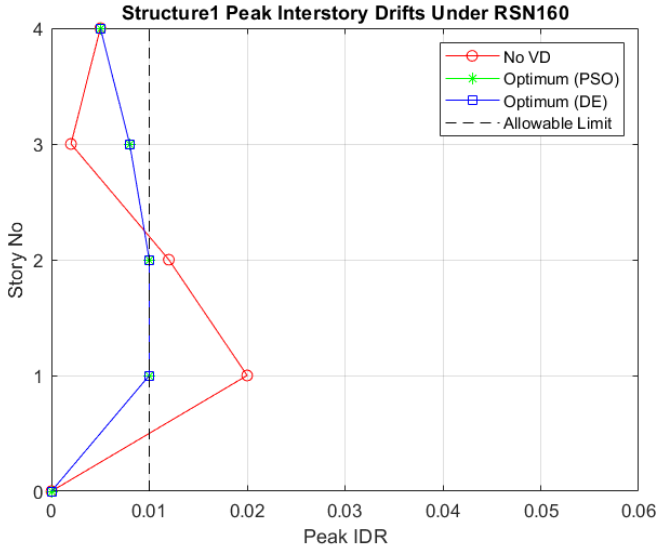

Figure 6.30 Comparison of Peak IDR for Structure1 With VD and Without VD Under RSN160

6.2.6. Under RSN496 (NPNF)

Particle Swarm Optimization (PSO) optimization history for Structure1 under RSN496 is given below in Figure 6.31.

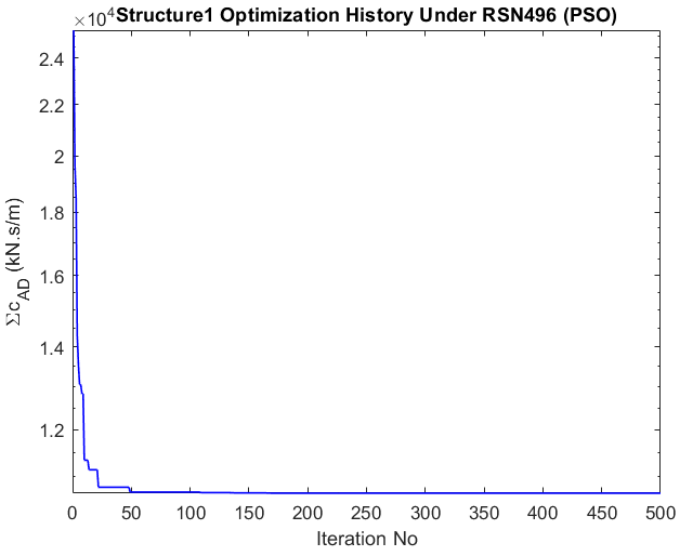

Figure 6.31 Structure1 Optimization History (PSO) Under RSN496

Differential Evolution (DE) optimization history for Structure1 under RSN496 is given below in Figure 6.32.

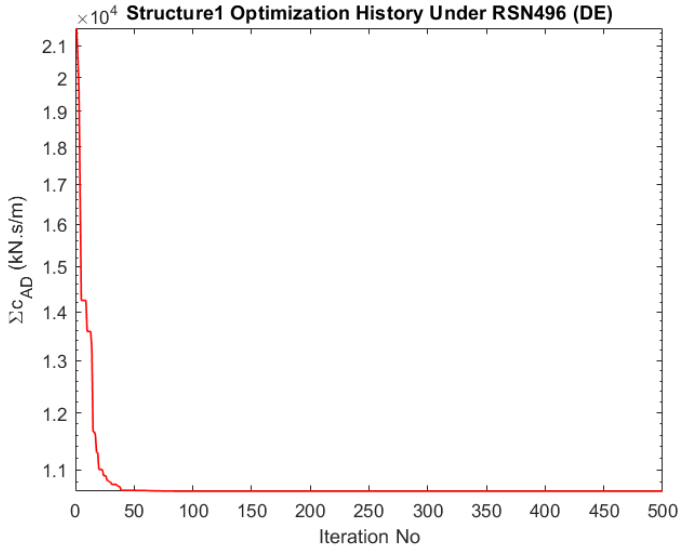

Figure 6.32 Structure1 Optimization History (DE) Under RSN496

Optimum viscous damper (VD) distribution for Structure1 Under RSN496 is given below in Table 6.13.

Table 6.13 Structure1 Optimum viscous damper (VD) distribution Under RSN496

Structure1 Optimum viscous damper (VD) distribution Under RSN496		
Story No	Added Damper PSO (kN.s/m)	Added Damper DE (kN.s/m)
1	5844.313	5900.028
2	3444.854	3531.880
3	1369.190	1220.064
4	0.000	0.000
Total Global Best	10658.357	10651.972

Comparison of maximum acceleration responses for Structure1 without VD and with optimum VD under RSN496 is given below in Figure 6.33.

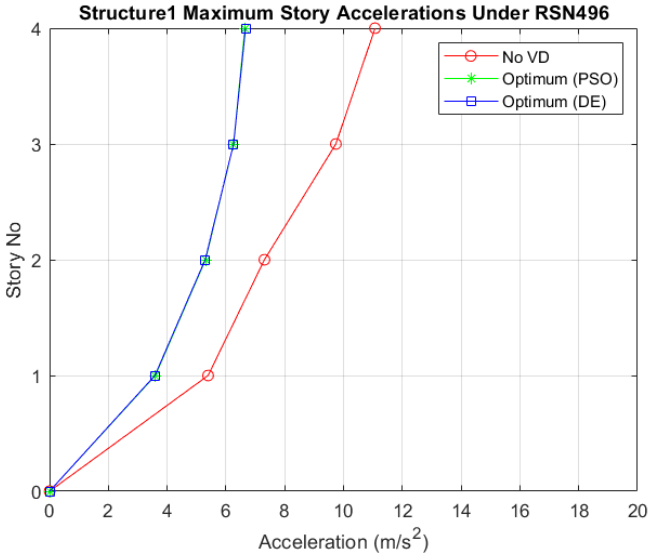

Figure 6.33 Comparison of Maximum Acceleration Responses for Structure1 With VD and Without VD Under RSN496

Comparison of maximum velocity responses for Structure1 without VD and with optimum VD under RSN496 is given below in Figure 6.34.

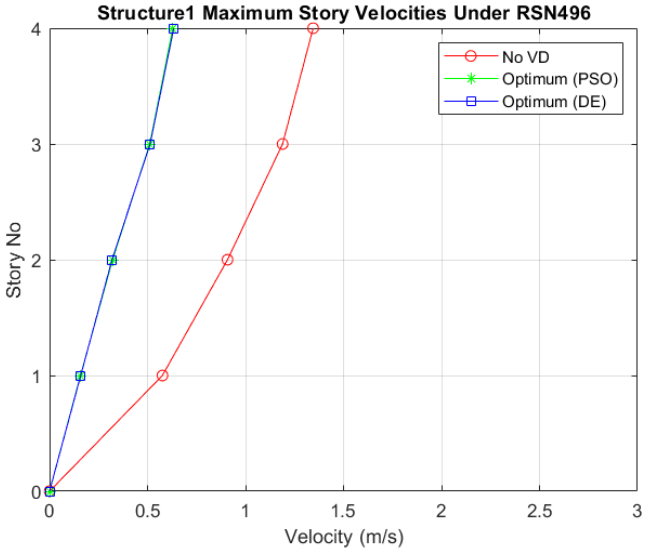

Figure 6.34 Comparison of Maximum Velocity Responses for Structure1 With VD and Without VD Under RSN496

Comparison of maximum displacement responses for Structure1 without VD and with optimum VD under RSN496 is given below in Figure 6.35.

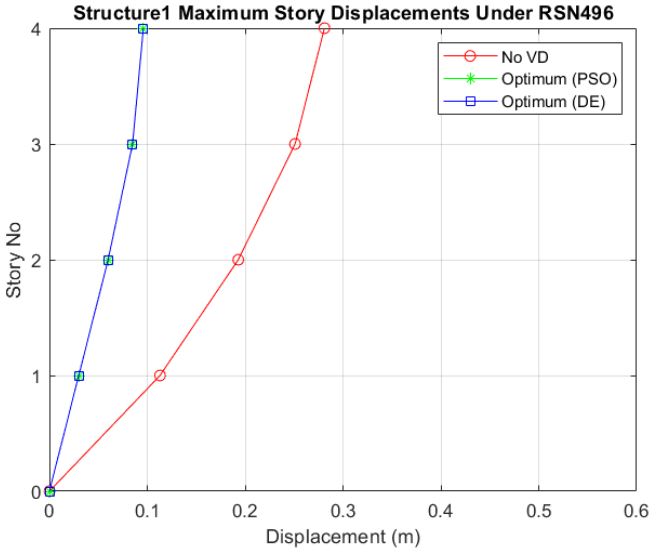

Figure 6.35 Comparison of Maximum Displacement Responses for Structure1 With VD and Without VD Under RSN496

Comparison of peak IDR for Structure1 without VD and with optimum VD under RSN496 is given below in Figure 6.36.

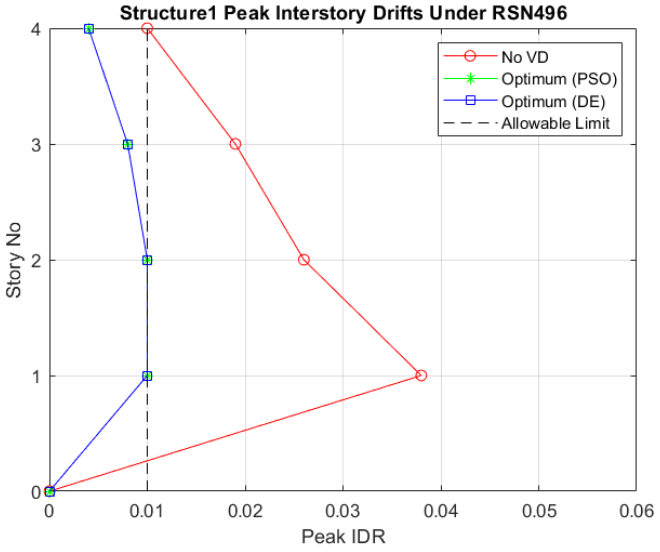

Figure 6.36 Comparison of Peak IDR for Structure1 With VD and Without VD Under RSN496

6.2.7. Under RSN741 (NPNF)

Particle Swarm Optimization (PSO) optimization history for Structure1 under RSN741 is given below in Figure 6.37.

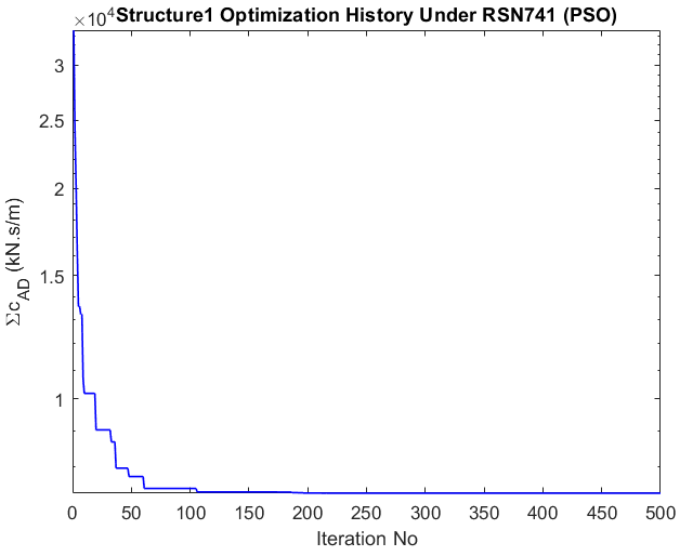

Figure 6.37 Structure1 Optimization History (PSO) Under RSN741

Differential Evolution (DE) optimization history for Structure1 under RSN741 is given below in Figure 6.38.

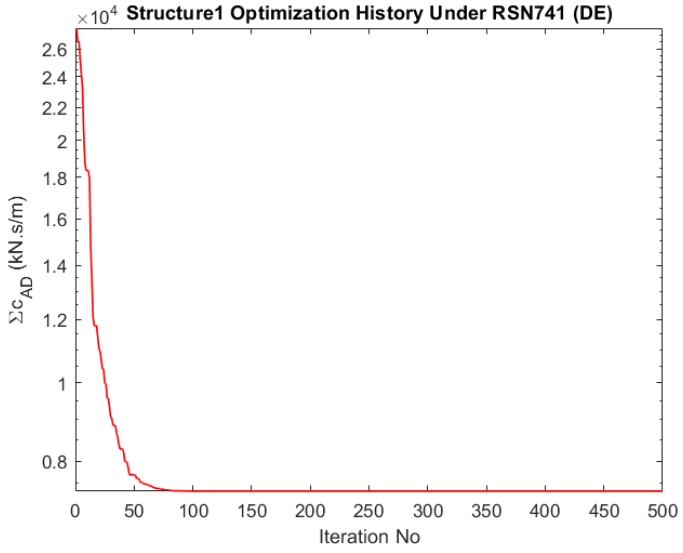

Figure 6.38 Structure1 Optimization History (DE) Under RSN741

Optimum viscous damper (VD) distribution for Structure1 Under RSN741 is given below in Table 6.14.

Table 6.14 Structure1 Optimum viscous damper (VD) distribution Under RSN741

Structure1 Optimum viscous damper (VD) distribution Under RSN741		
Story No	Added Damper PSO (kN.s/m)	Added Damper DE (kN.s/m)
1	4528.131	4528.131
2	1689.315	1689.315
3	1120.067	1120.067
4	0.000	0.000
Total Global Best	7337.514	7337.514

Comparison of maximum acceleration responses for Structure1 without VD and with optimum VD under RSN741 is given below in Figure 6.39.

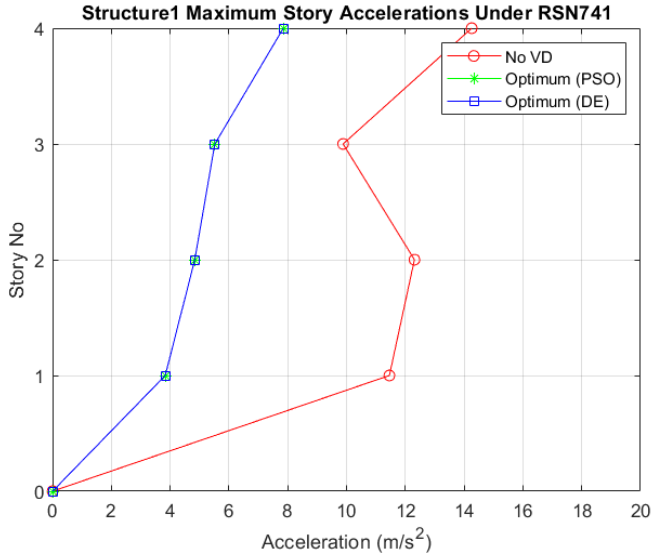

Figure 6.39 Comparison of Maximum Acceleration Responses for Structure1 With VD and Without VD Under RSN741

Comparison of maximum velocity responses for Structure1 without VD and with optimum VD under RSN741 is given below in Figure 6.40.

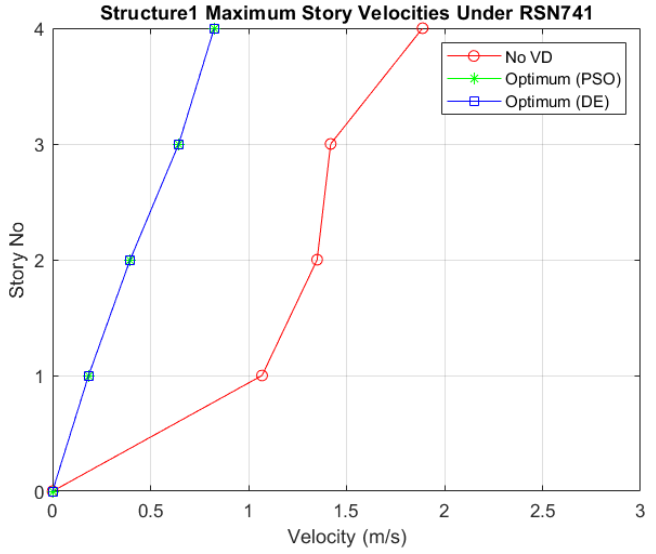

Figure 6.40 Comparison of Maximum Velocity Responses for Structure1 With VD and Without VD Under RSN741

Comparison of maximum displacement responses for Structure1 without VD and with optimum VD under RSN741 is given below in Figure 6.41.

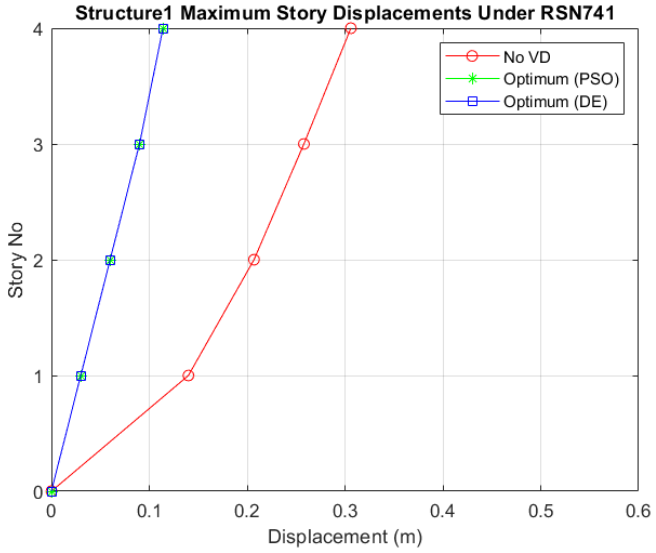

Figure 6.41 Comparison of Maximum Displacement Responses for Structure1 With VD and Without VD Under RSN741

Comparison of peak IDR for Structure1 without VD and with optimum VD under RSN741 is given below in Figure 6.42.

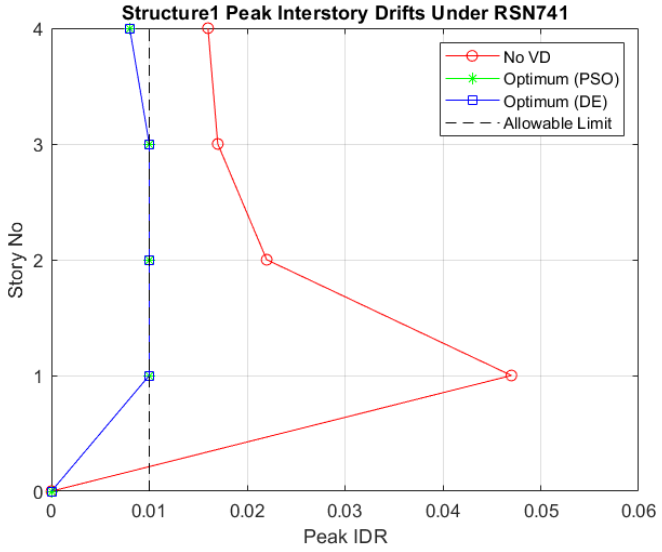

Figure 6.42 Comparison of Peak IDR for Structure1 With VD and Without VD Under RSN741

6.2.8. Under RSN1004 (NPNF)

Particle Swarm Optimization (PSO) optimization history for Structure1 under RSN1004 is given below in Figure 6.43.

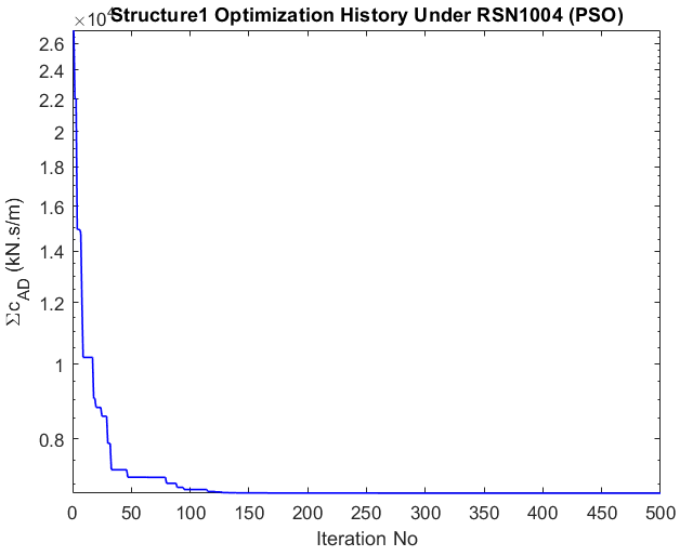

Figure 6.43 Structure1 Optimization History (PSO) Under RSN1004

Differential Evolution (DE) optimization history for Structure1 under RSN1004 is given below in Figure 6.44.

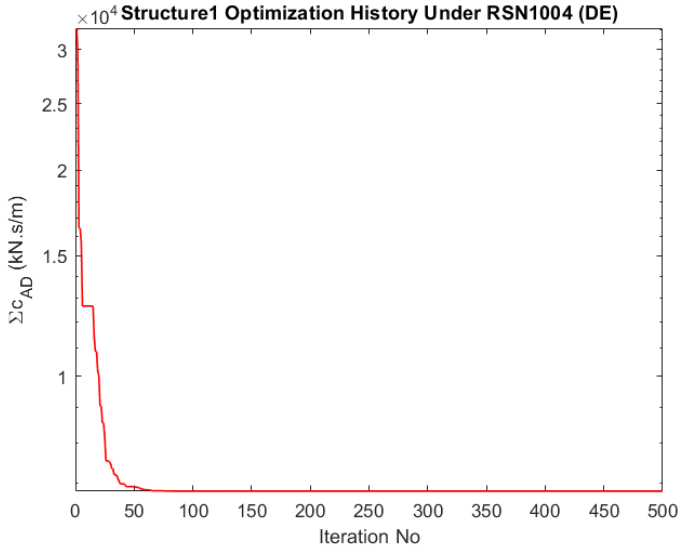

Figure 6.44 Structure1 Optimization History (DE) Under RSN1004

Optimum viscous damper (VD) distribution for Structure1 Under RSN1004 is given below in Table 6.15.

Table 6.15 Structure1 Optimum viscous damper (VD) distribution Under RSN1004

Structure1 Optimum viscous damper (VD) distribution Under RSN1004		
Story No	Added Damper PSO (kN.s/m)	Added Damper DE (kN.s/m)
1	4305.402	4307.965
2	1459.828	1455.055
3	1038.218	1039.567
4	0.000	0.000
Total Global Best	6803.449	6802.588

Comparison of maximum acceleration responses for Structure1 without VD and with optimum VD under RSN1004 is given below in Figure 6.45.

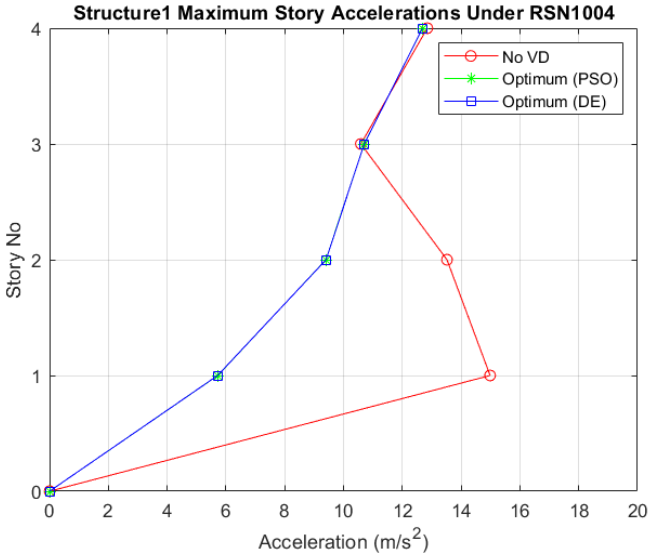

Figure 6.45 Comparison of Maximum Acceleration Responses for Structure1 With VD and Without VD Under RSN1004

Comparison of maximum velocity responses for Structure1 without VD and with optimum VD under RSN1004 is given below in Figure 6.46.

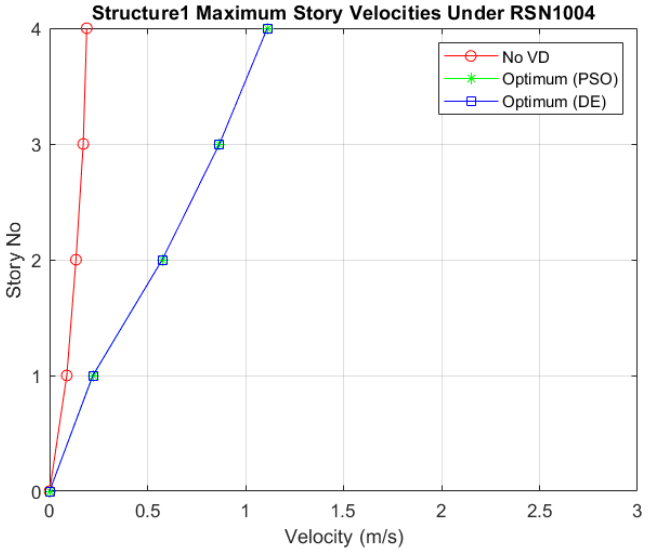

Figure 6.46 Comparison of Maximum Velocity Responses for Structure1 With VD and Without VD Under RSN1004

Comparison of maximum displacement responses for Structure1 without VD and with optimum VD under RSN1004 is given below in Figure 6.47.

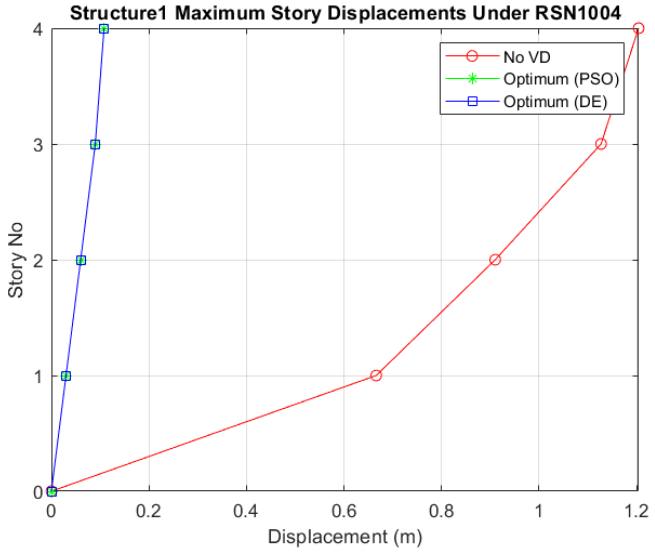

Figure 6.47 Comparison of Maximum Displacement Responses for Structure1 With VD and Without VD Under RSN1004

Comparison of peak IDR for Structure1 without VD and with optimum VD under RSN1004 is given below in Figure 6.48.

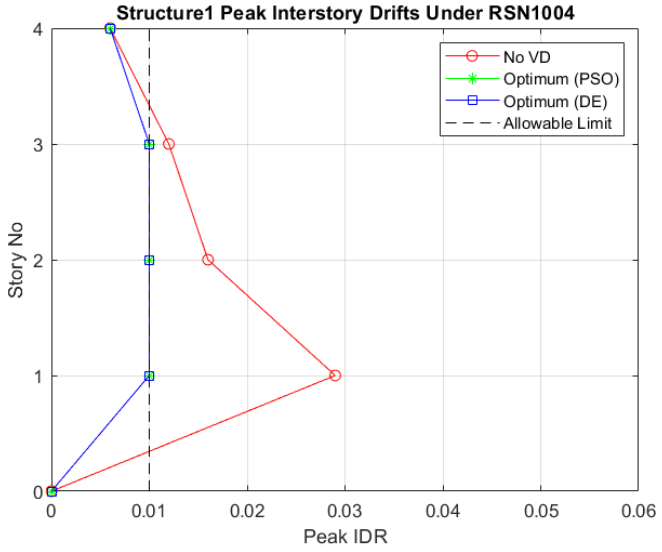

Figure 6.48 Comparison of Peak IDR for Structure1 With VD and Without VD Under RSN1004

6.2.9. Under RSN68 (FF)

Under this earthquake ground motion data, peak IDR of each story is lower than allowable limit. Because of that reason, Structure1 does not need additional VD under RSN68.

Comparison of maximum acceleration responses for Structure1 without VD and with optimum VD under RSN68 is given below in Figure 6.49.

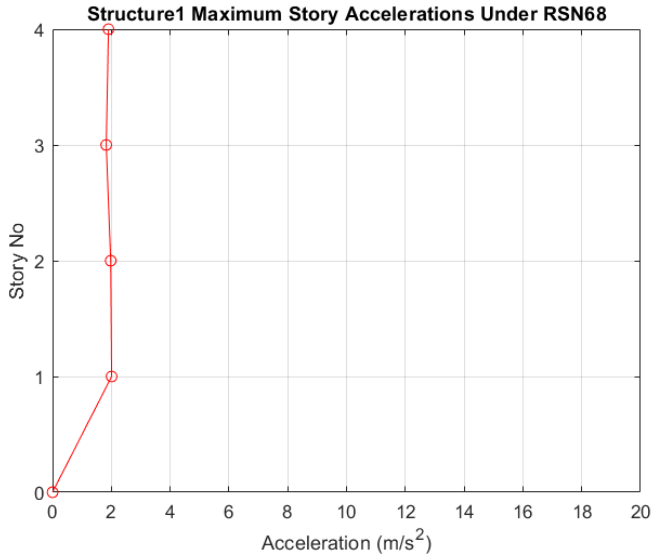

Figure 6.49 Comparison of Maximum Acceleration Responses for Structure1 With VD and Without VD Under RSN68

Comparison of maximum velocity responses for Structure1 without VD and with optimum VD under RSN68 is given below in Figure 6.50.

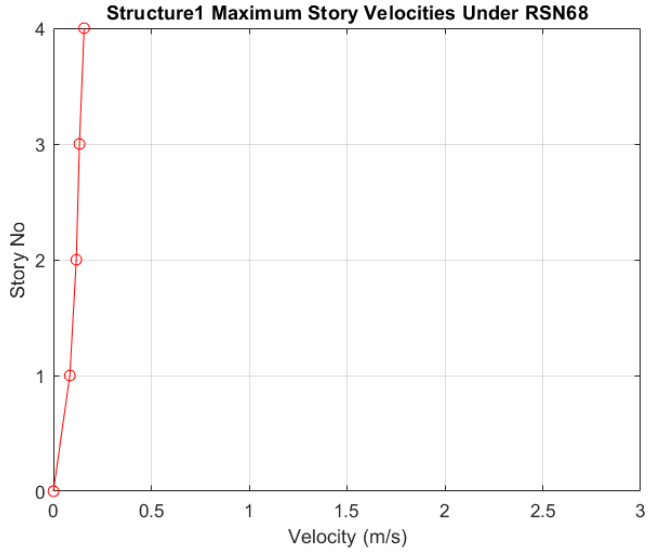

Figure 6.50 Comparison of Maximum Velocity Responses for Structure1 With VD and Without VD Under RSN68

Comparison of maximum displacement responses for Structure1 without VD and with optimum VD under RSN68 is given below in Figure 6.51.

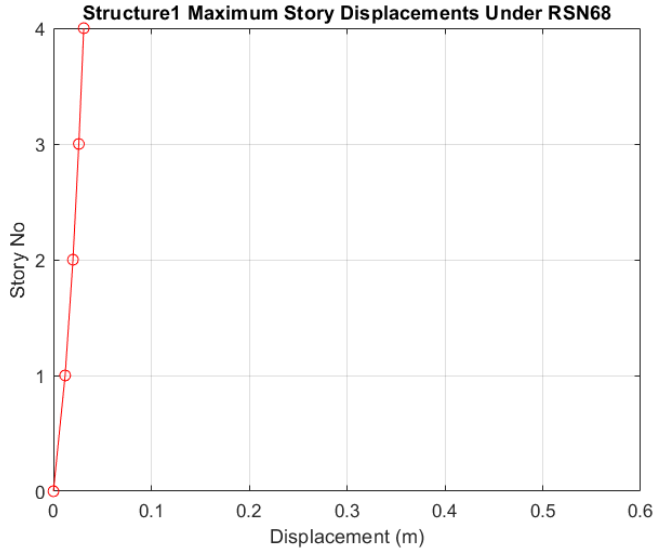

Figure 6.51 Comparison of Maximum Displacement Responses for Structure1 With VD and Without VD Under RSN68

Comparison of peak IDR for Structure1 without VD and with optimum VD under RSN68 is given below in Figure 6.52.

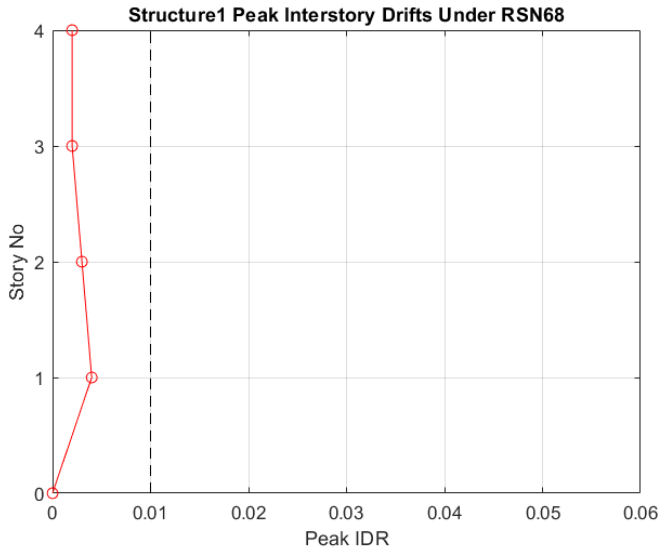

Figure 6.52 Comparison of Peak IDR for Structure1 With VD and Without VD Under RSN68

6.2.10. Under RSN752 (FF)

Particle Swarm Optimization (PSO) optimization history for Structure1 under RSN752 is given below in Figure 6.53.

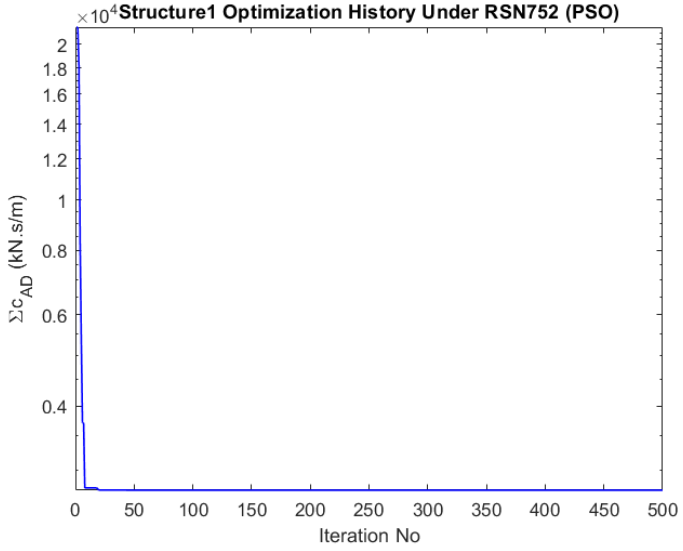

Figure 6.53 Structure1 Optimization History (PSO) Under RSN752

Differential Evolution (DE) optimization history for Structure1 under RSN752 is given below in Figure 6.54.

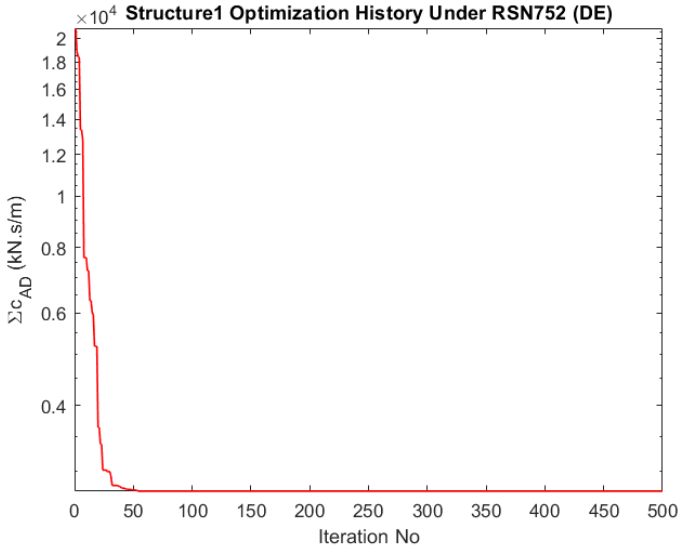

Figure 6.54 Structure1 Optimization History (DE) Under RSN752

Optimum viscous damper (VD) distribution for Structure1 Under RSN752 is given below in Table 6.16.

Table 6.16 Structure1 Optimum viscous damper (VD) distribution Under RSN752

Structure1 Optimum viscous damper (VD) distribution Under RSN752		
Story No	Added Damper PSO (kN.s/m)	Added Damper DE (kN.s/m)
1	2749.494	2749.494
2	0.000	0.000
3	0.000	0.000
4	0.000	0.000
Total Global Best	2749.494	2749.494

Comparison of maximum acceleration responses for Structure1 without VD and with optimum VD under RSN752 is given below in Figure 6.55.

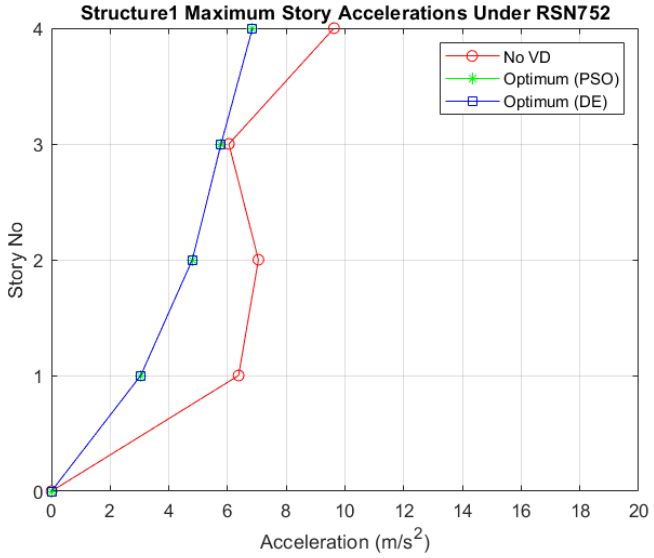

Figure 6.55 Comparison of Maximum Acceleration Responses for Structure1 With VD and Without VD Under RSN752

Comparison of maximum velocity responses for Structure1 without VD and with optimum VD under RSN752 is given below in Figure 6.56.

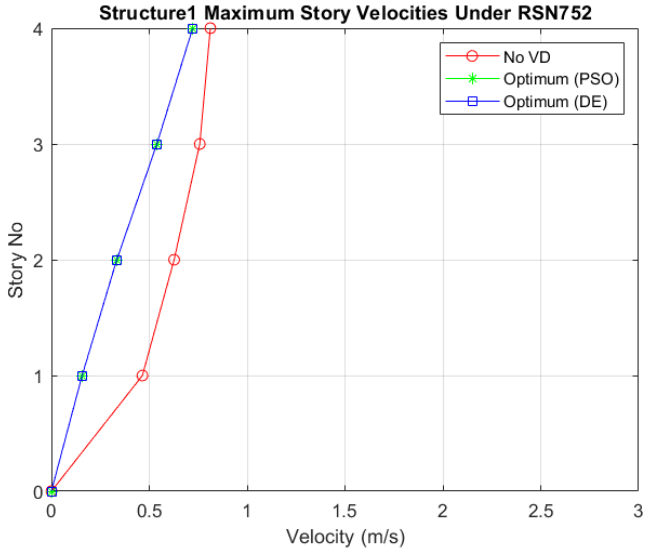

Figure 6.56 Comparison of Maximum Velocity Responses for Structure1 With VD and Without VD Under RSN752

Comparison of maximum displacement responses for Structure1 without VD and with optimum VD under RSN752 is given below in Figure 6.57.

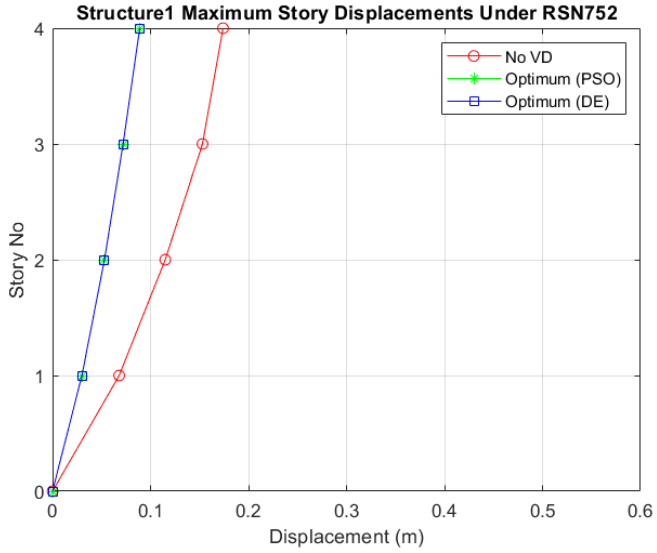

Figure 6.57 Comparison of Maximum Displacement Responses for Structure1 With VD and Without VD Under RSN752

Comparison of peak IDR for Structure1 without VD and with optimum VD under RSN752 is given below in Figure 6.58.

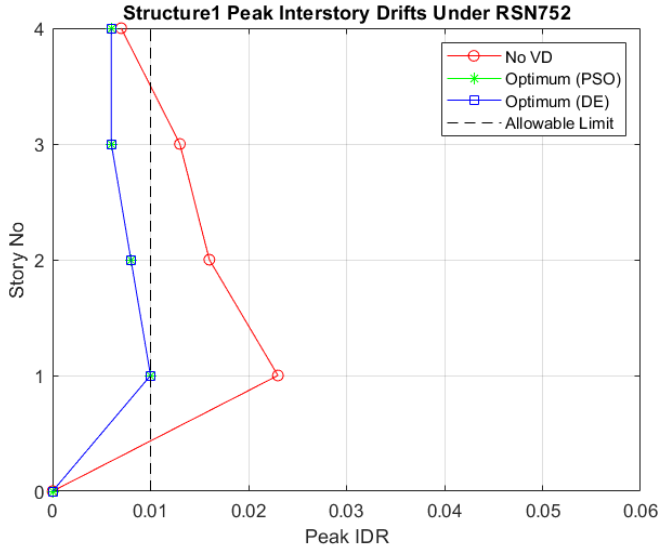

Figure 6.58 Comparison of Peak IDR for Structure1 With VD and Without VD Under RSN752

6.2.11. Under RSN953 (FF)

Particle Swarm Optimization (PSO) optimization history for Structure1 under RSN953 is given below in Figure 6.59.

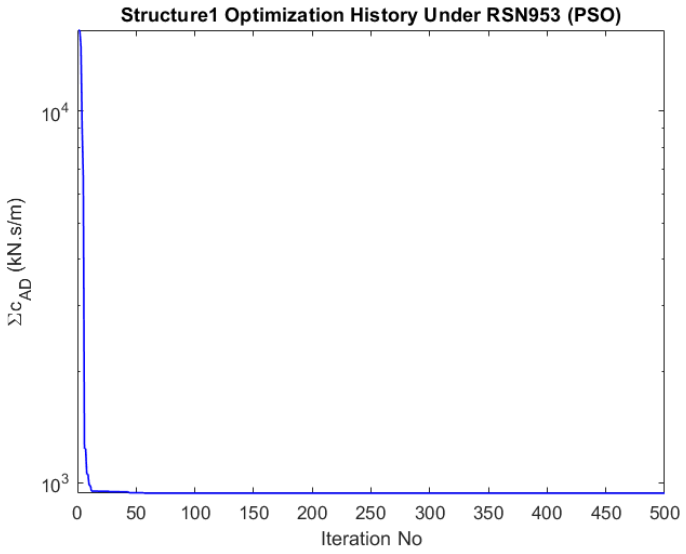

Figure 6.59 Structure1 Optimization History (PSO) Under RSN953

Differential Evolution (DE) optimization history for Structure1 under RSN953 is given below in Figure 6.60.

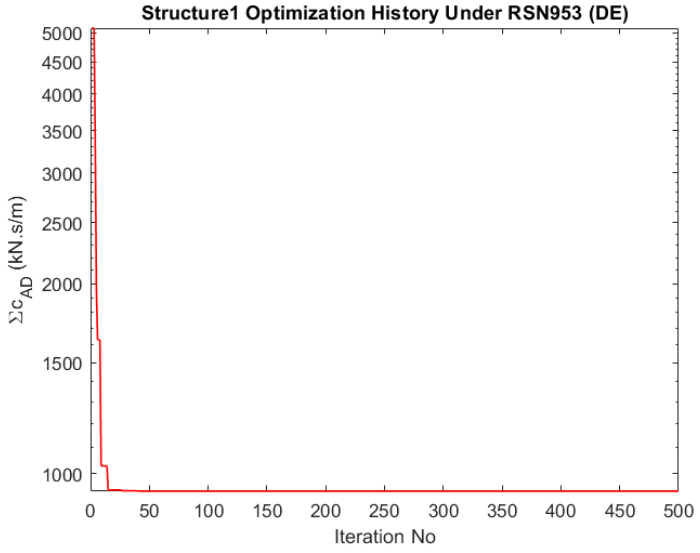

Figure 6.60 Structure1 Optimization History (DE) Under RSN953

Optimum viscous damper (VD) distribution for Structure1 Under RSN953 is given below in Table 6.17.

Table 6.17 Structure1 Optimum viscous damper (VD) distribution Under RSN953

Structure1 Optimum viscous damper (VD) distribution Under RSN953		
Story No	Added Damper PSO (kN.s/m)	Added Damper DE (kN.s/m)
1	937.833	937.833
2	0.000	0.000
3	0.000	0.000
4	0.000	0.000
Total Global Best	937.833	937.833

Comparison of maximum acceleration responses for Structure1 without VD and with optimum VD under RSN953 is given below in Figure 6.61.

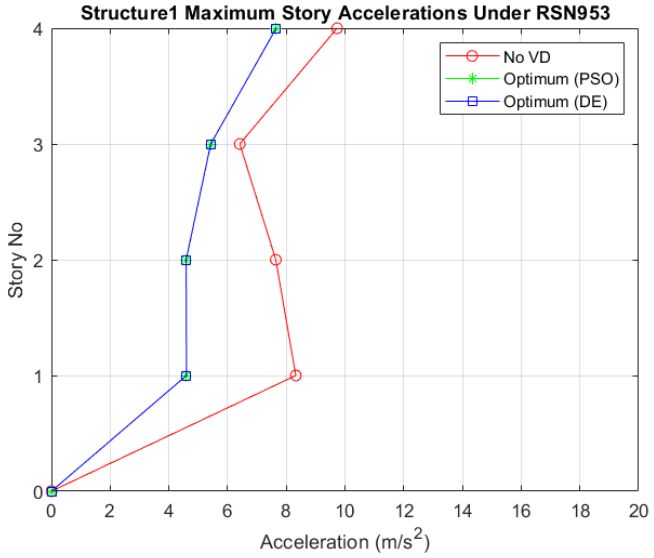

Figure 6.61 Comparison of Maximum Acceleration Responses for Structure1 With VD and Without VD Under RSN953

Comparison of maximum velocity responses for Structure1 without VD and with optimum VD under RSN953 is given below in Figure 6.62.

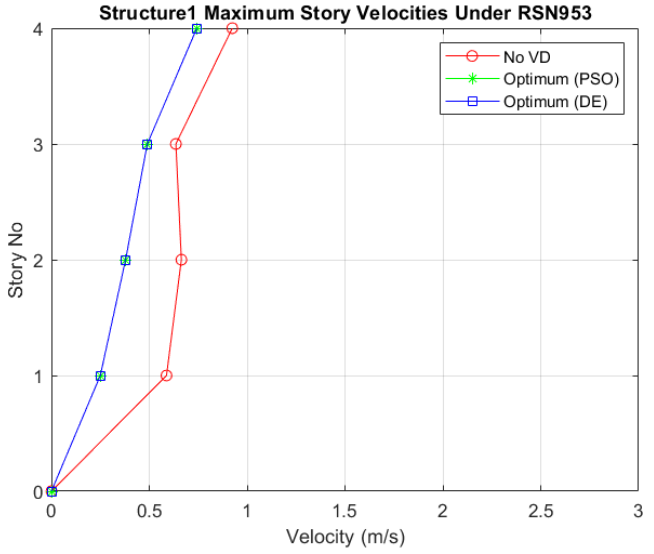

Figure 6.62 Comparison of Maximum Velocity Responses for Structure1 With VD and Without VD Under RSN953

Comparison of maximum displacement responses for Structure1 without VD and with optimum VD under RSN953 is given below in Figure 6.63.

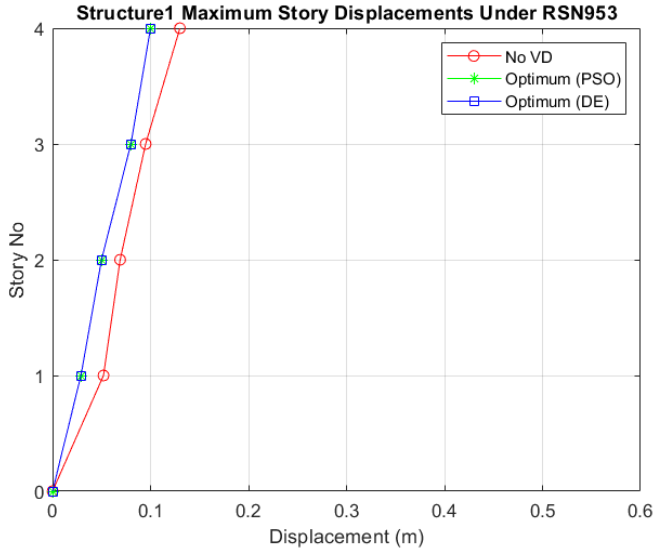

Figure 6.63 Comparison of Maximum Displacement Responses for Structure1 With VD and Without VD Under RSN953

Comparison of peak IDR for Structure1 without VD and with optimum VD under RSN953 is given below in Figure 6.64.

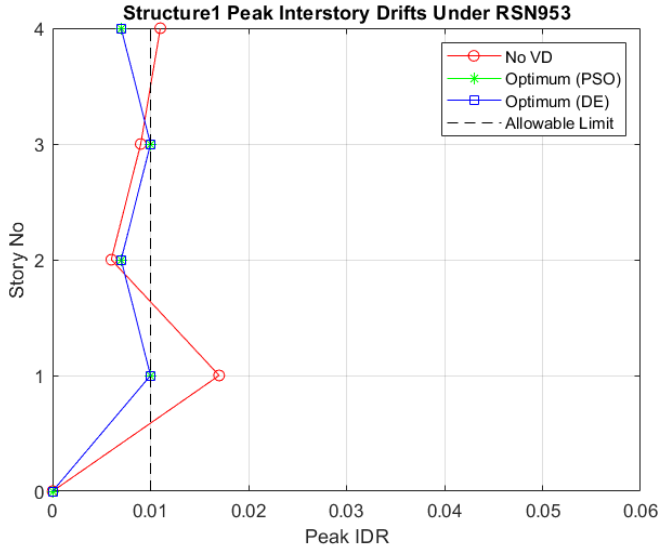

Figure 6.64 Comparison of Peak IDR for Structure1 With VD and Without VD Under RSN953

6.2.12. Under RSN1111 (FF)

Particle Swarm Optimization (PSO) optimization history for Structure1 under RSN1111 is given below in Figure 6.65.

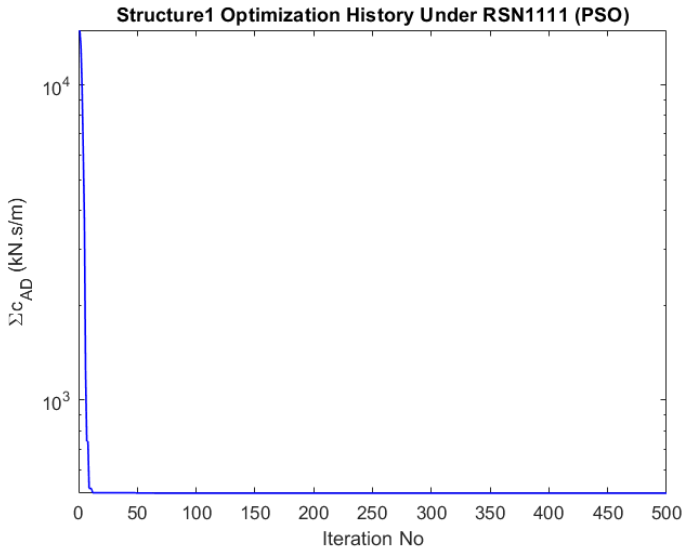

Figure 6.65 Structure1 Optimization History (PSO) Under RSN1111

Differential Evolution (DE) optimization history for Structure1 under RSN1111 is given below in Figure 6.66.

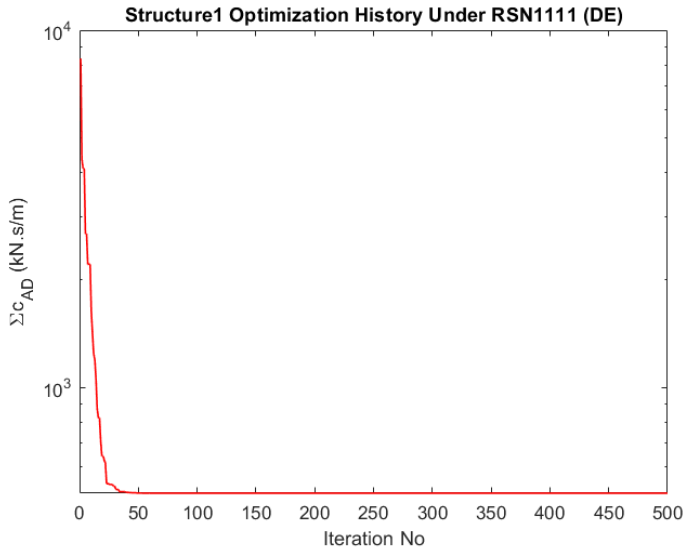

Figure 6.66 Structure1 Optimization History (DE) Under RSN1111

Optimum viscous damper (VD) distribution for Structure1 Under RSN1111 is given below in Table 6.18.

Table 6.18 Structure1 Optimum viscous damper (VD) distribution Under RSN1111

Structure1 Optimum viscous damper (VD) distribution Under RSN1111		
Story No	Added Damper PSO (kN.s/m)	Added Damper DE (kN.s/m)
1	506.225	506.225
2	0.000	0.000
3	0.000	0.000
4	0.000	0.000
Total Global Best	506.225	506.225

Comparison of maximum acceleration responses for Structure1 without VD and with optimum VD under RSN1111 is given below in Figure 6.67.

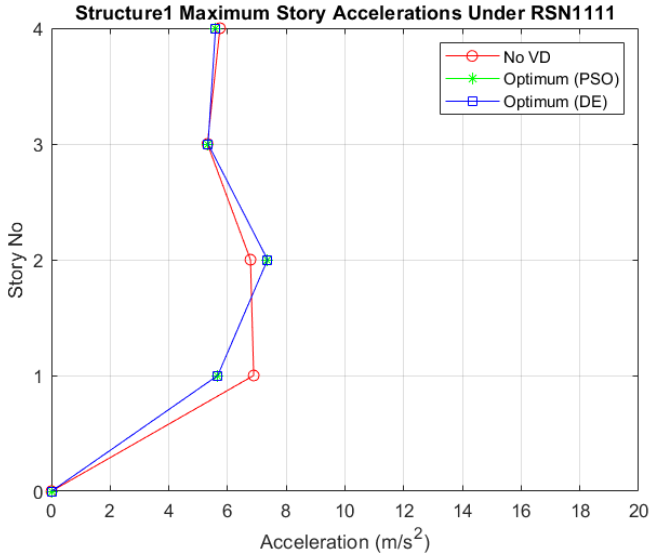

Figure 6.67 Comparison of Maximum Acceleration Responses for Structure1 With VD and Without VD Under RSN1111

Comparison of maximum velocity responses for Structure1 without VD and with optimum VD under RSN1111 is given below in Figure 6.68.

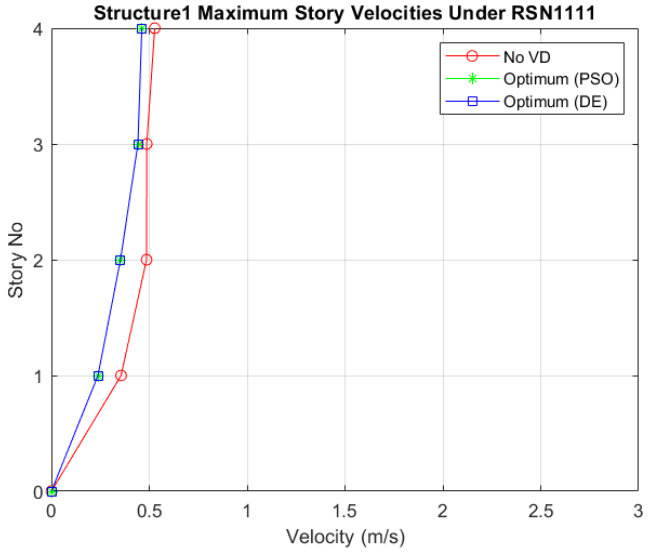

Figure 6.68 Comparison of Maximum Velocity Responses for Structure1 With VD and Without VD Under RSN1111

Comparison of maximum displacement responses for Structure1 without VD and with optimum VD under RSN1111 is given below in Figure 6.69.

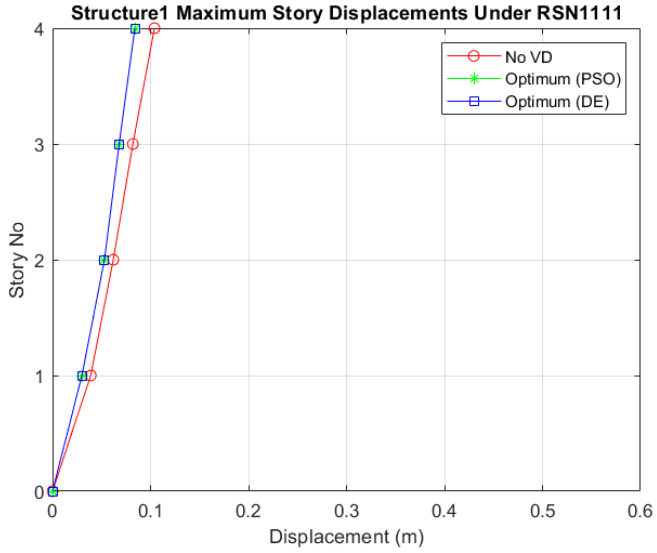

Figure 6.69 Comparison of Maximum Displacement Responses for Structure1 With VD and Without VD Under RSN1111

Comparison of peak IDR for Structure1 without VD and with optimum VD under RSN1111 is given below in Figure 6.70.

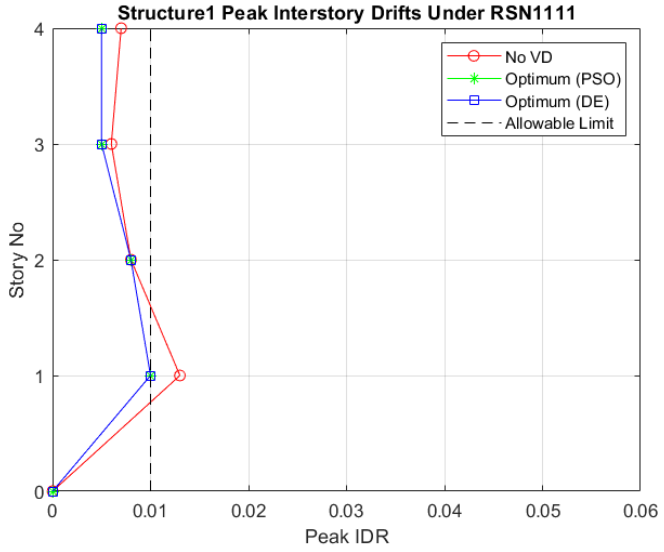

Figure 6.70 Comparison of Peak IDR for Structure1 With VD and Without VD Under RSN1111

6.3. Analysis Results for Structure2

6.3.1. Under RSN182 (PNF)

Particle Swarm Optimization (PSO) optimization history for Structure2 under RSN182 is given below in Figure 6.71.

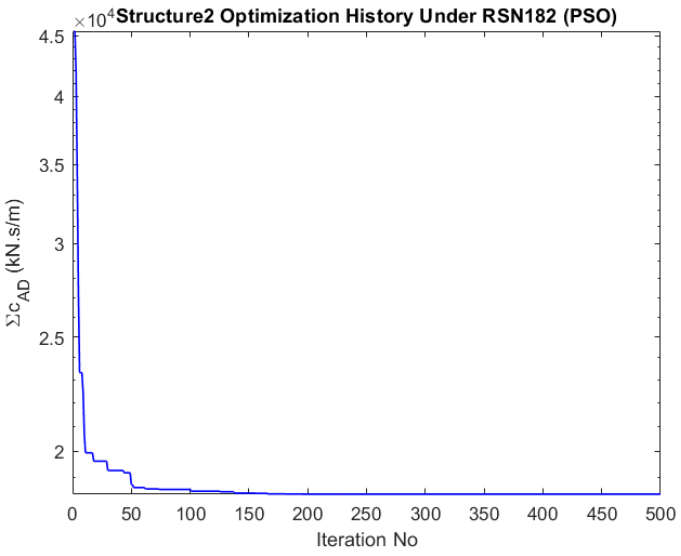

Figure 6.71 Structure2 Optimization History (PSO) Under RSN182

Differential Evolution (DE) optimization history for Structure2 under RSN182 is given below in Figure 6.72.

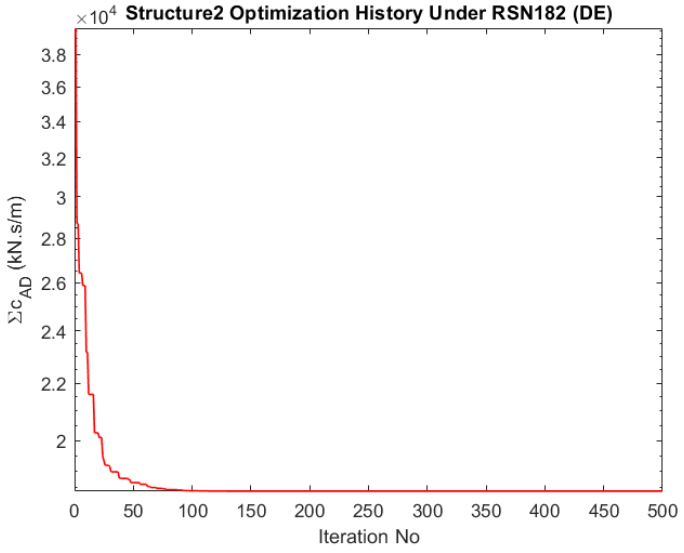

Figure 6.72 Structure2 Optimization History (DE) Under RSN182

Optimum viscous damper (VD) distribution for Structure2 Under RSN182 is given below in Table 6.19.

Table 6.19 Structure2 Optimum viscous damper (VD) distribution Under RSN182

Structure2 Optimum viscous damper (VD) distribution Under RSN182		
Story No	Added Damper PSO (kN.s/m)	Added Damper DE (kN.s/m)
1	11183.660	11198.460
2	4857.408	4873.329
3	2129.500	1925.366
4	217.628	384.701
5	0.000	0.000
6	0.000	0.000
7	0.000	0.000
Total Global Best	18388.196	18381.856

Comparison of maximum acceleration responses for Structure2 without VD and with optimum VD under RSN182 is given below in Figure 6.73.

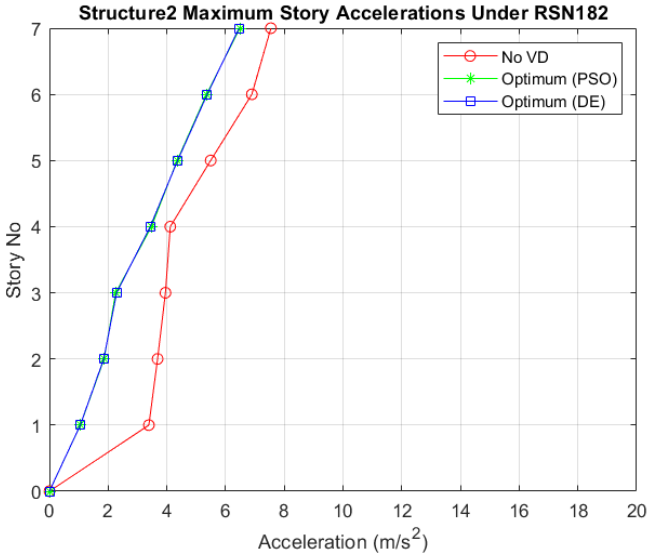

Figure 6.73 Comparison of Maximum Acceleration Responses for Structure2 With VD and Without VD Under RSN182

Comparison of maximum velocity responses for Structure2 without VD and with optimum VD under RSN182 is given below in Figure 6.74.

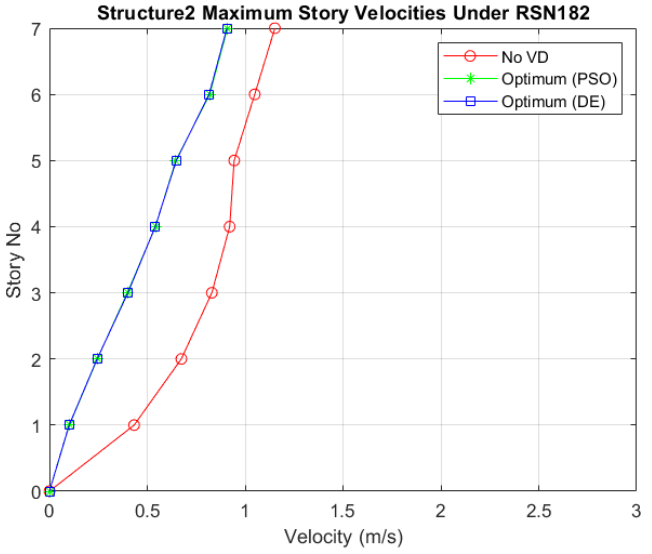

Figure 6.74 Comparison of Maximum Velocity Responses for Structure2 With VD and Without VD Under RSN182

Comparison of maximum displacement responses for Structure2 without VD and with optimum VD under RSN182 is given below in Figure 6.75.

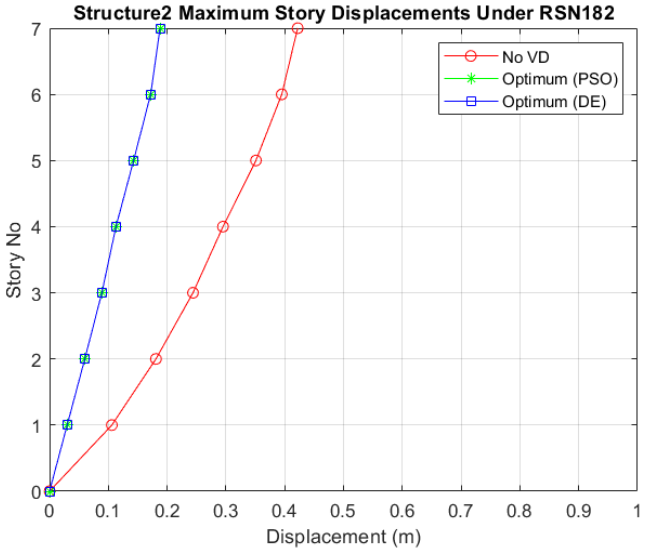

Figure 6.75 Comparison of Maximum Displacement Responses for Structure2 With VD and Without VD Under RSN182

Comparison of peak IDR for Structure2 without VD and with optimum VD under RSN182 is given below in Figure 6.76.

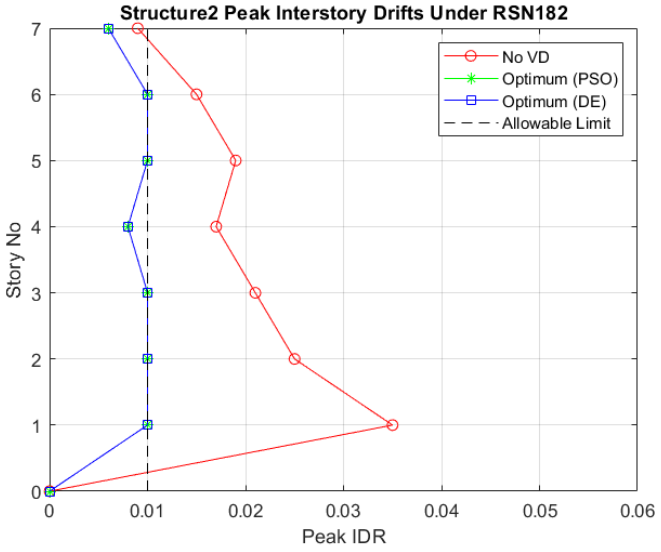

Figure 6.76 Comparison of Peak IDR for Structure2 With VD and Without VD Under RSN182

6.3.2. Under RSN821 (PNF)

Particle Swarm Optimization (PSO) optimization history for Structure2 under RSN821 is given below in Figure 6.77.

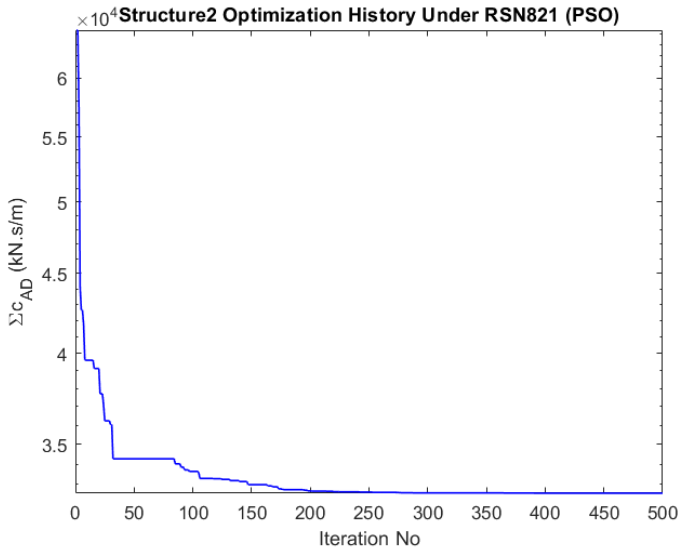

Figure 6.77 Structure2 Optimization History (PSO) Under RSN821

Differential Evolution (DE) optimization history for Structure2 under RSN821 is given below in Figure 6.78.

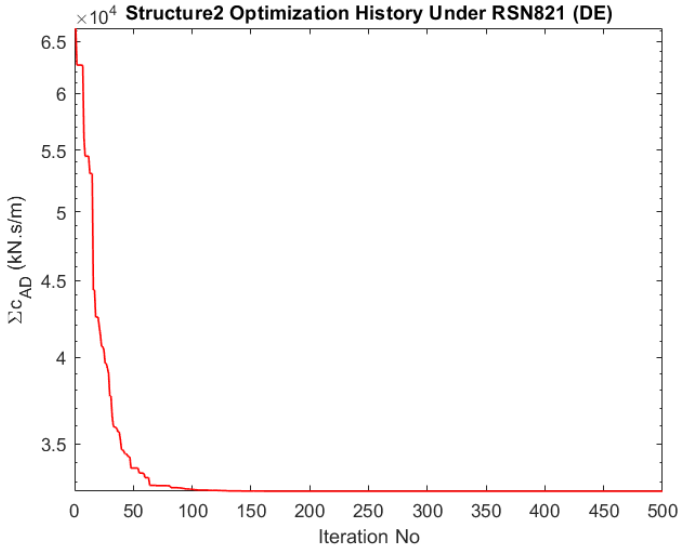

Figure 6.78 Structure2 Optimization History (DE) Under RSN821

Optimum viscous damper (VD) distribution for Structure2 Under RSN821 is given below in Table 6.20.

Table 6.20 Structure2 Optimum viscous damper (VD) distribution Under RSN821

Structure2 Optimum viscous damper (VD) distribution Under RSN821		
Story No	Added Damper PSO (kN.s/m)	Added Damper DE (kN.s/m)
1	14264.118	14260.179
2	7578.075	7710.416
3	6689.000	6772.096
4	2896.584	2592.753
5	1142.376	1219.915
6	0.000	0.000
7	0.000	0.000
Total Global Best	32570.153	32555.359

Comparison of maximum acceleration responses for Structure2 without VD and with optimum VD under RSN821 is given below in Figure 6.79.

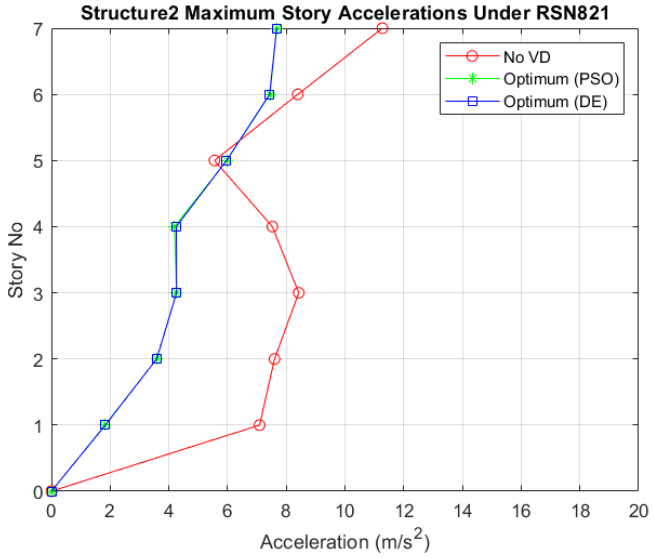

Figure 6.79 Comparison of Maximum Acceleration Responses for Structure2 With VD and Without VD Under RSN821

Comparison of maximum velocity responses for Structure2 without VD and with optimum VD under RSN821 is given below in Figure 6.80.

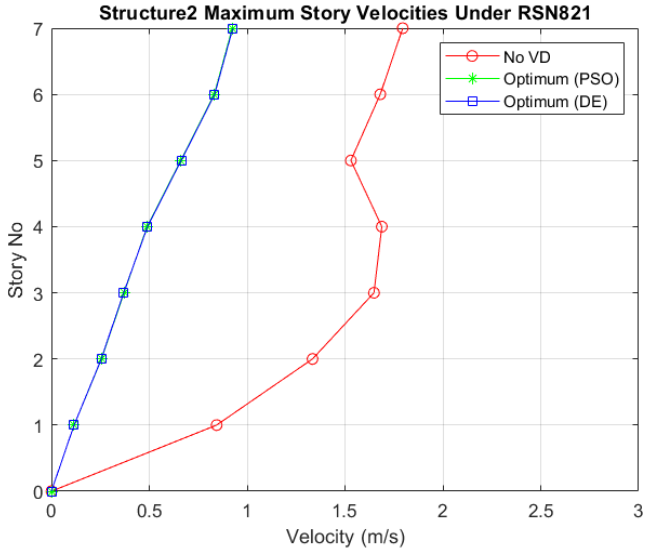

Figure 6.80 Comparison of Maximum Velocity Responses for Structure2 With VD and Without VD Under RSN821

Comparison of maximum displacement responses for Structure2 without VD and with optimum VD under RSN821 is given below in Figure 6.81.

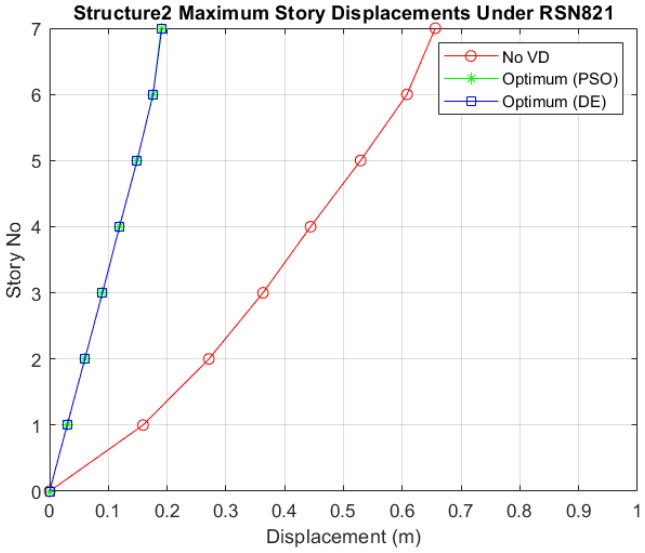

Figure 6.81 Comparison of Maximum Displacement Responses for Structure2 With VD and Without VD Under RSN821

Comparison of peak IDR for Structure2 without VD and with optimum VD under RSN821 is given below in Figure 6.82.

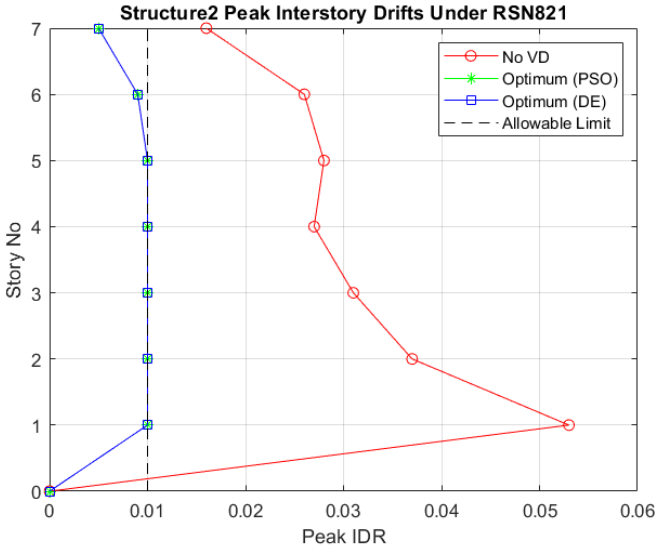

Figure 6.82 Comparison of Peak IDR for Structure2 With VD and Without VD Under RSN821

6.3.3. Under RSN1063 (PNF)

Particle Swarm Optimization (PSO) optimization history for Structure2 under RSN1063 is given below in Figure 6.83.

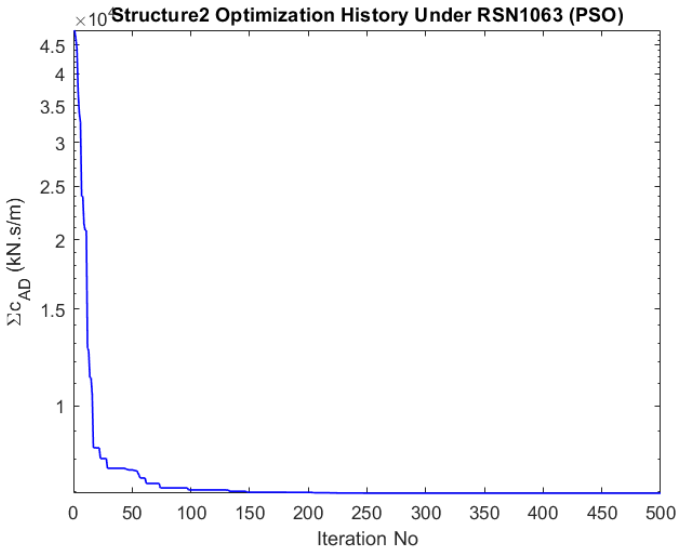

Figure 6.83 Structure2 Optimization History (PSO) Under RSN1063

Differential Evolution (DE) optimization history for Structure2 under RSN1063 is given below in Figure 6.84.

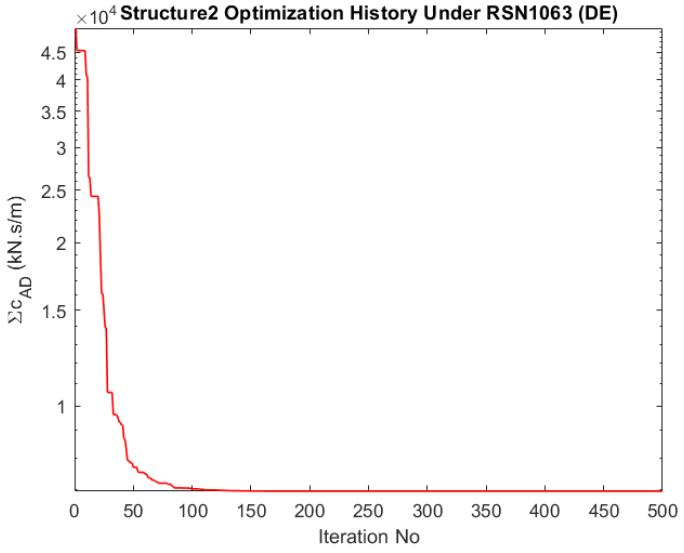

Figure 6.84 Structure2 Optimization History (DE) Under RSN1063

Optimum viscous damper (VD) distribution for Structure2 Under RSN1063 is given below in Table 6.21.

Table 6.21 Structure2 Optimum viscous damper (VD) distribution Under RSN1063

Structure2 Optimum viscous damper (VD) distribution Under RSN1063		
Story No	Added Damper PSO (kN.s/m)	Added Damper DE (kN.s/m)
1	5141.567	5223.527
2	826.592	793.617
3	256.376	258.569
4	0.000	0.000
5	0.000	0.001
6	728.374	675.839
7	0.000	0.000
Total Global Best	6952.910	6951.553

Comparison of maximum acceleration responses for Structure2 without VD and with optimum VD under RSN1063 is given below in Figure 6.85.

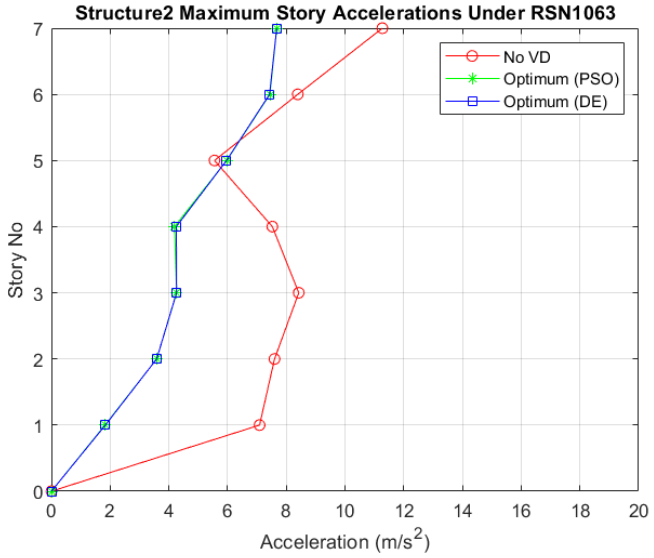

Figure 6.85 Comparison of Maximum Acceleration Responses for Structure2 With VD and Without VD Under RSN1063

Comparison of maximum velocity responses for Structure2 without VD and with optimum VD under RSN1063 is given below in Figure 6.86.

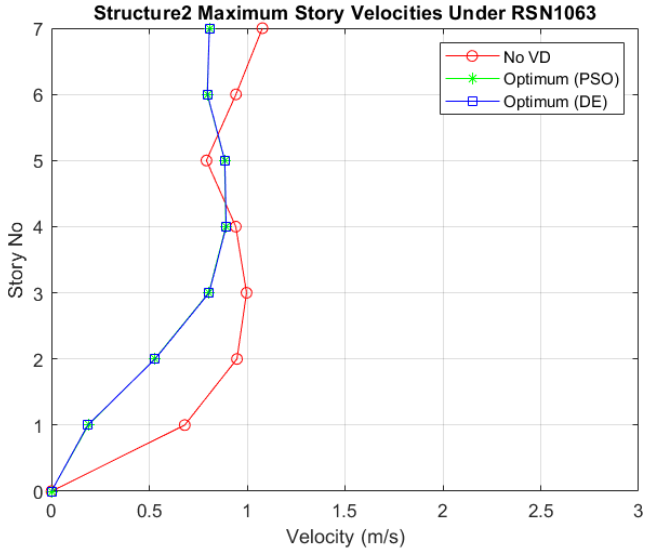

Figure 6.86 Comparison of Maximum Velocity Responses for Structure2 With VD and Without VD Under RSN1063

Comparison of maximum displacement responses for Structure2 without VD and with optimum VD under RSN1063 is given below in Figure 6.87.

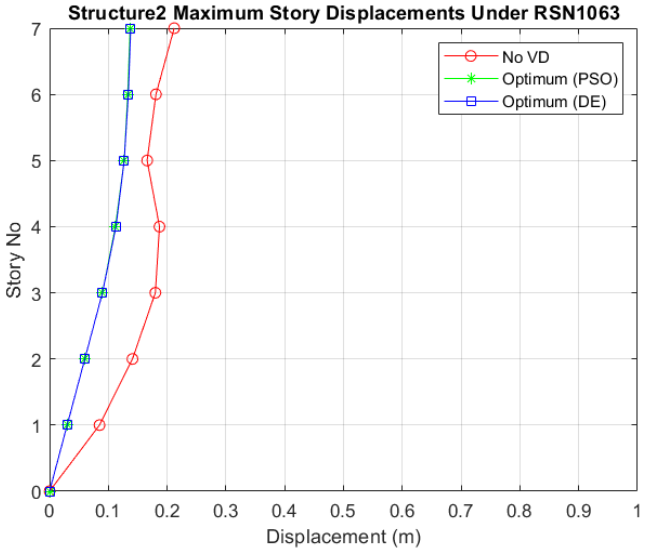

Figure 6.87 Comparison of Maximum Displacement Responses for Structure2 With VD and Without VD Under RSN1063

Comparison of peak IDR for Structure2 without VD and with optimum VD under RSN1063 is given below in Figure 6.88.

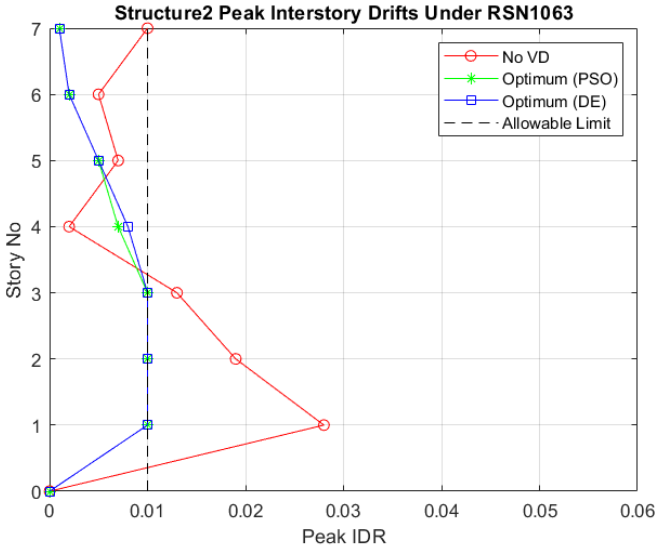

Figure 6.88 Comparison of Peak IDR for Structure2 With VD and Without VD Under RSN1063

6.3.4. Under RSN1605 (PNF)

Particle Swarm Optimization (PSO) optimization history for Structure2 under RSN1605 is given below in Figure 6.89.

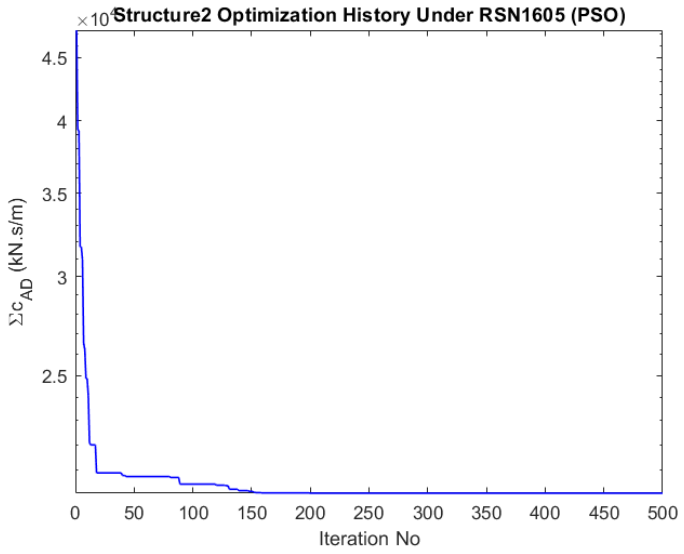

Figure 6.89 Structure2 Optimization History (PSO) Under RSN1605

Differential Evolution (DE) optimization history for Structure2 under RSN1605 is given below in Figure 6.90.

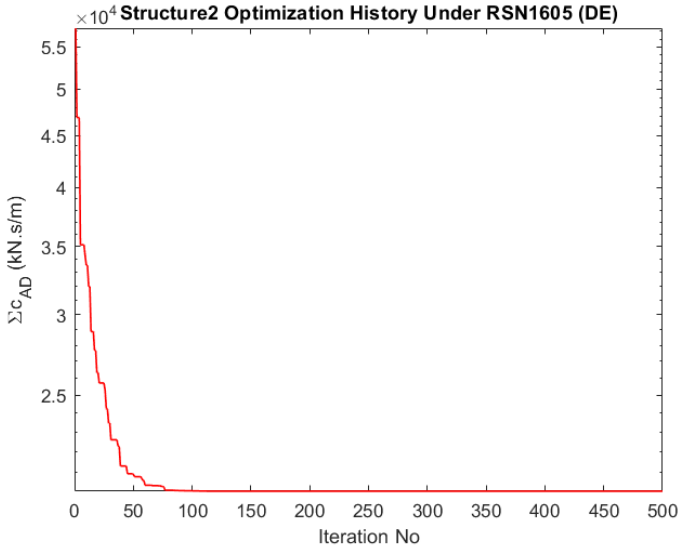

Figure 6.90 Structure2 Optimization History (DE) Under RSN1605

Optimum viscous damper (VD) distribution for Structure2 Under RSN1605 is given below in Table 6.22.

Table 6.22 Structure2 Optimum viscous damper (VD) distribution Under RSN1605

Structure2 Optimum viscous damper (VD) distribution Under RSN1605		
Story No	Added Damper PSO (kN.s/m)	Added Damper DE (kN.s/m)
1	10101.156	10101.156
2	5906.108	5906.108
3	4110.860	4110.860
4	0.000	0.000
5	0.000	0.000
6	0.000	0.000
7	0.000	0.000
Total Global Best	20118.124	20118.124

Comparison of maximum acceleration responses for Structure2 without VD and with optimum VD under RSN1605 is given below in Figure 6.91.

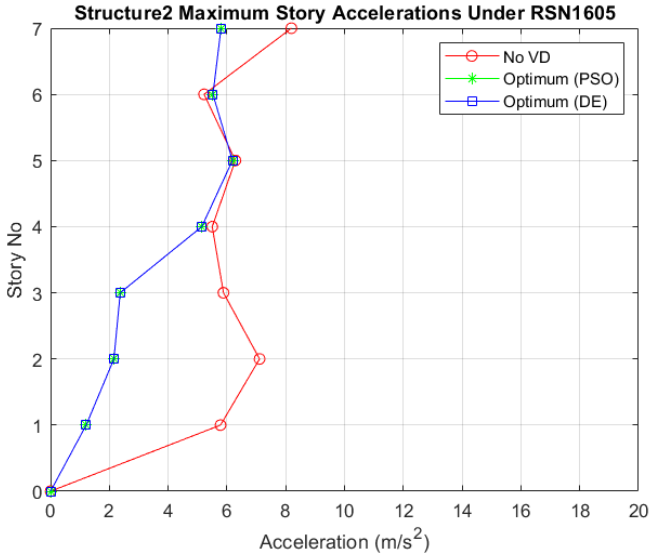

Figure 6.91 Comparison of Maximum Acceleration Responses for Structure2 With VD and Without VD Under RSN1605

Comparison of maximum velocity responses for Structure2 without VD and with optimum VD under RSN1605 is given below in Figure 6.92.

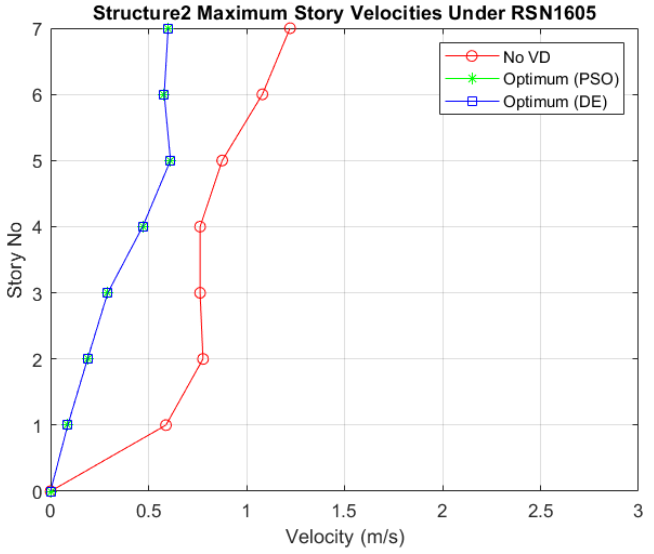

Figure 6.92 Comparison of Maximum Velocity Responses for Structure2 With VD and Without VD Under RSN1605

Comparison of maximum displacement responses for Structure2 without VD and with optimum VD under RSN1605 is given below in Figure 6.93.

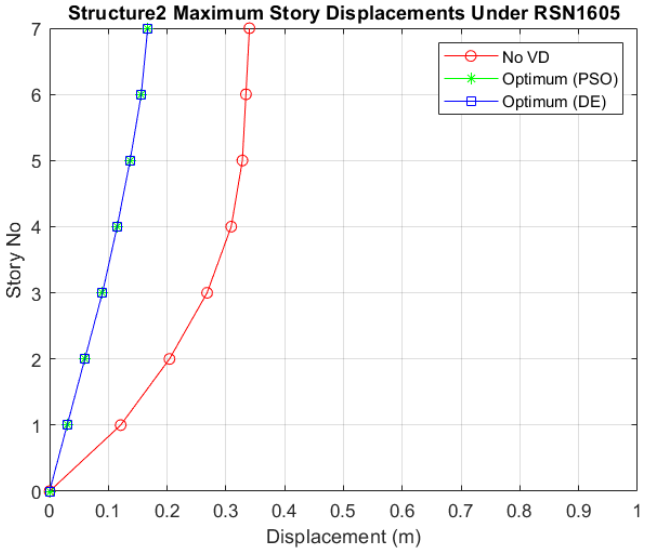

Figure 6.93 Comparison of Maximum Displacement Responses for Structure2 With VD and Without VD Under RSN1605

Comparison of peak IDR for Structure2 without VD and with optimum VD under RSN1605 is given below in Figure 6.94.

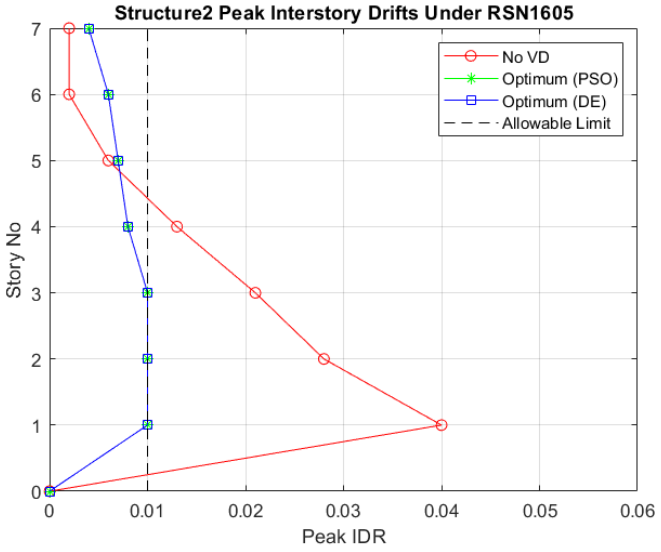

Figure 6.94 Comparison of Peak IDR for Structure2 With VD and Without VD Under RSN1605

6.3.5. Under RSN160 (NPNF)

Particle Swarm Optimization (PSO) optimization history for Structure2 under RSN160 is given below in Figure 6.95.

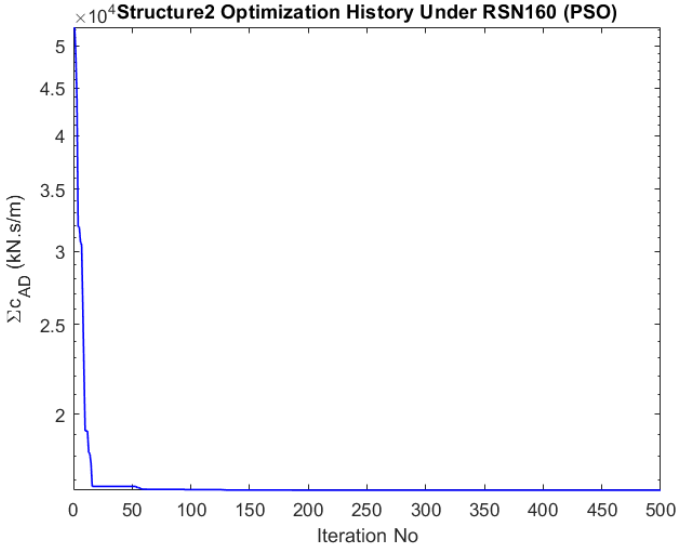

Figure 6.95 Structure2 Optimization History (PSO) Under RSN160

Differential Evolution (DE) optimization history for Structure2 under RSN160 is given below in Figure 6.96.

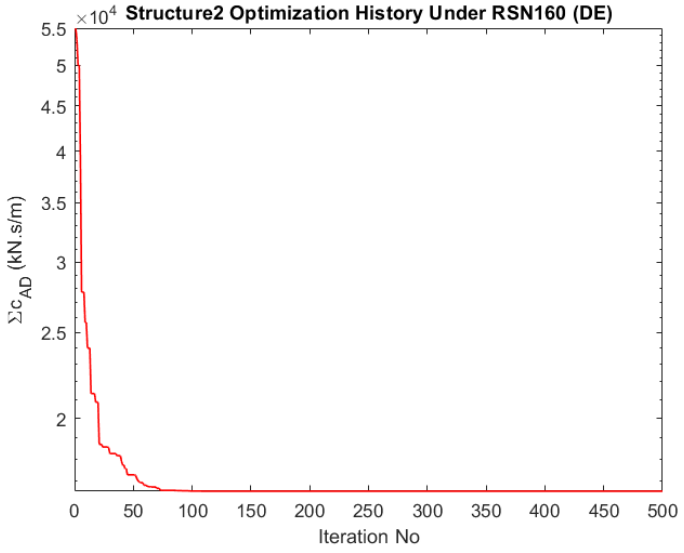

Figure 6.96 Structure2 Optimization History (DE) Under RSN160

Optimum viscous damper (VD) distribution for Structure2 Under RSN160 is given below in Table 6.23.

Table 6.23 Structure2 Optimum viscous damper (VD) distribution Under RSN160

Structure2 Optimum viscous damper (VD) distribution Under RSN160		
Story No	Added Damper PSO (kN.s/m)	Added Damper DE (kN.s/m)
1	8842.081	8842.081
2	5738.029	5738.029
3	1977.749	1977.749
4	0.000	0.000
5	0.000	0.000
6	0.000	0.000
7	0.000	0.000
Total Global Best	16557.860	16557.860

Comparison of maximum acceleration responses for Structure2 without VD and with optimum VD under RSN160 is given below in Figure 6.97.

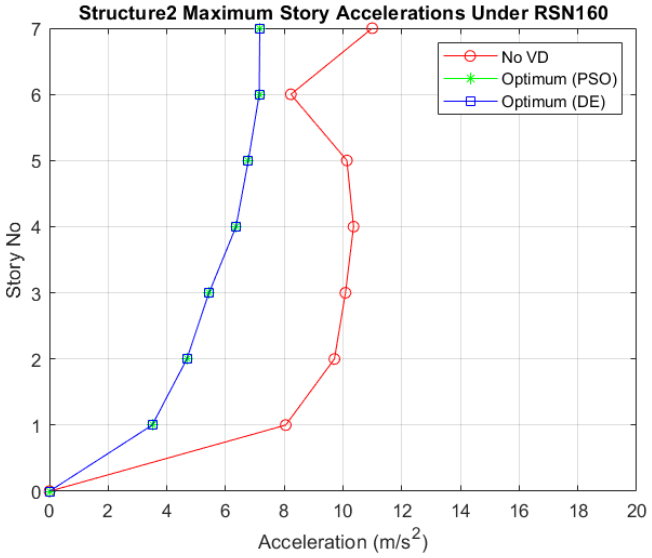

Figure 6.97 Comparison of Maximum Acceleration Responses for Structure2 With VD and Without VD Under RSN160

Comparison of maximum velocity responses for Structure2 without VD and with optimum VD under RSN160 is given below in Figure 6.98.

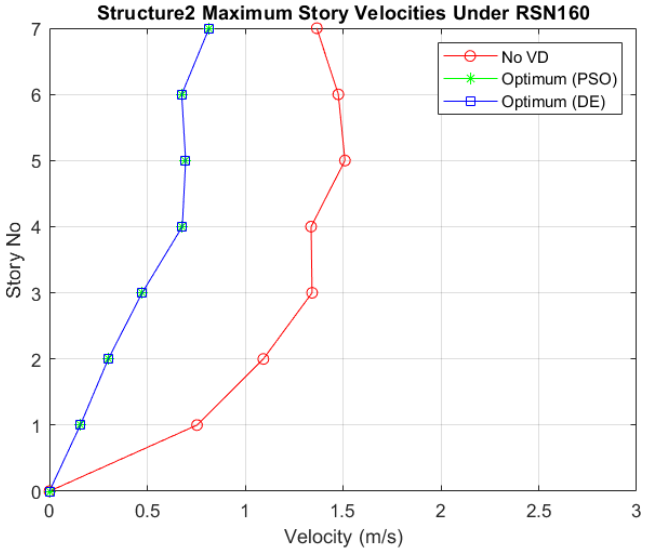

Figure 6.98 Comparison of Maximum Velocity Responses for Structure2 With VD and Without VD Under RSN160

Comparison of maximum displacement responses for Structure2 without VD and with optimum VD under RSN160 is given below in Figure 6.99.

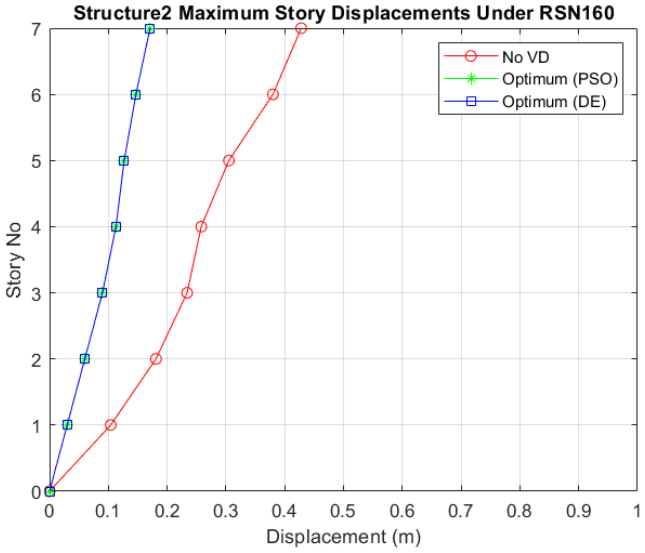

Figure 6.99 Comparison of Maximum Displacement Responses for Structure2 With VD and Without VD Under RSN160

Comparison of peak IDR for Structure2 without VD and with optimum VD under RSN160 is given below in Figure 6.100.

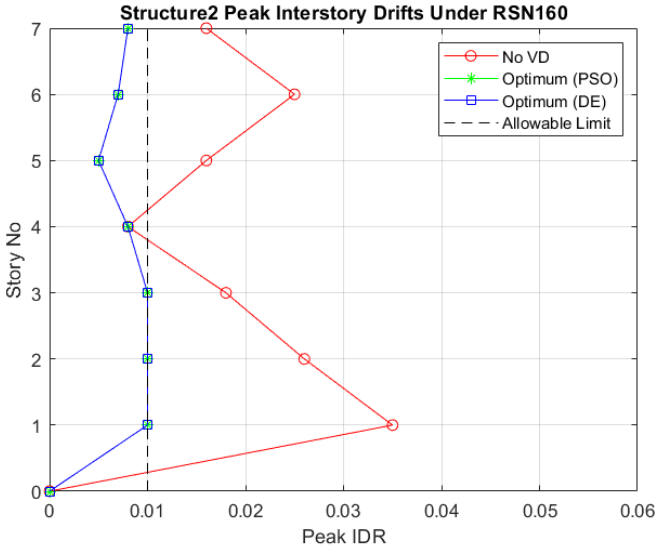

Figure 6.100 Comparison of Peak IDR for Structure2 With VD and Without VD Under RSN160

6.3.6. Under RSN496 (NPNF)

Particle Swarm Optimization (PSO) optimization history for Structure2 under RSN496 is given below in Figure 6.101.

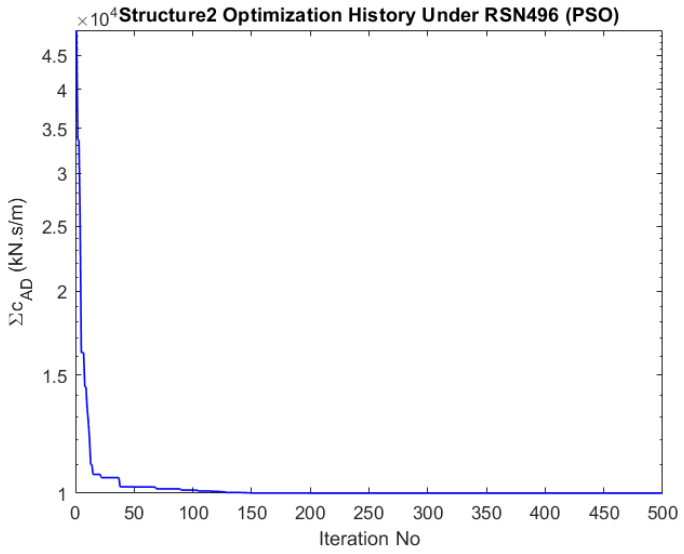

Figure 6.101 Structure2 Optimization History (PSO) Under RSN496

Differential Evolution (DE) optimization history for Structure2 under RSN496 is given below in Figure 6.102.

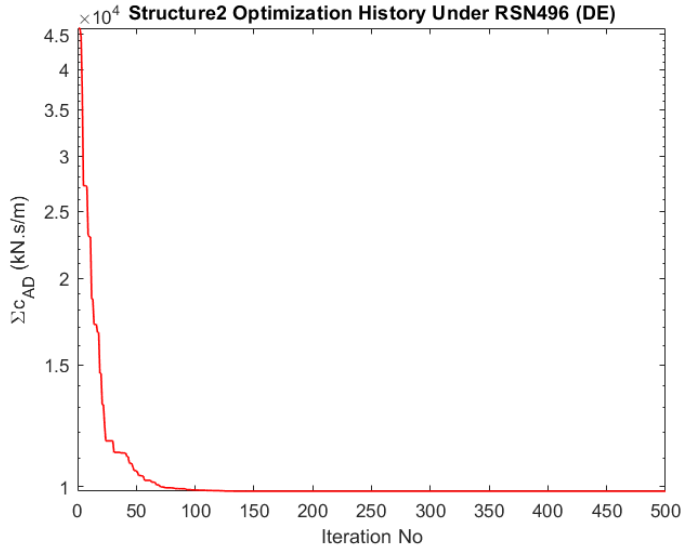

Figure 6.102 Structure2 Optimization History (DE) Under RSN496

Optimum viscous damper (VD) distribution for Structure2 Under RSN496 is given below in Table 6.24.

Table 6.24 Structure2 Optimum viscous damper (VD) distribution Under RSN496

Structure2 Optimum viscous damper (VD) distribution Under RSN496		
Story No	Added Damper PSO (kN.s/m)	Added Damper DE (kN.s/m)
1	7626.490	7589.798
2	1451.700	1338.079
3	0.000	0.000
4	0.000	85.808
5	0.000	444.269
6	907.316	396.581
7	0.000	0.000
Total Global Best	9985.506	9854.535

Comparison of maximum acceleration responses for Structure2 without VD and with optimum VD under RSN496 is given below in Figure 6.103.

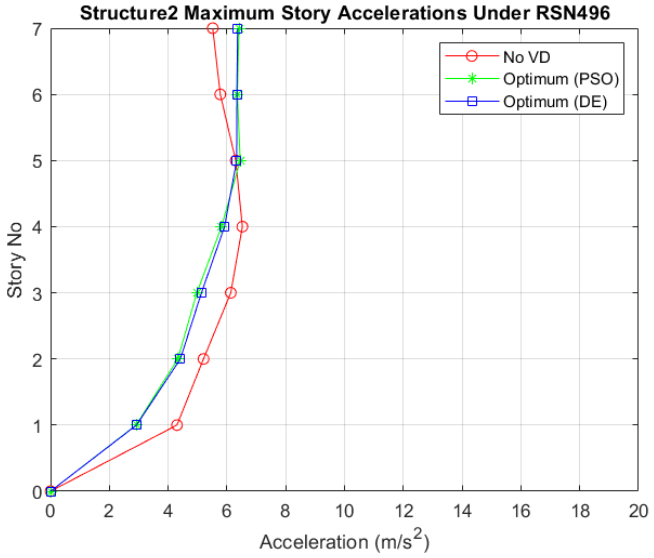

Figure 6.103 Comparison of Maximum Acceleration Responses for Structure2 With VD and Without VD Under RSN496

Comparison of maximum velocity responses for Structure2 without VD and with optimum VD under RSN496 is given below in Figure 6.104.

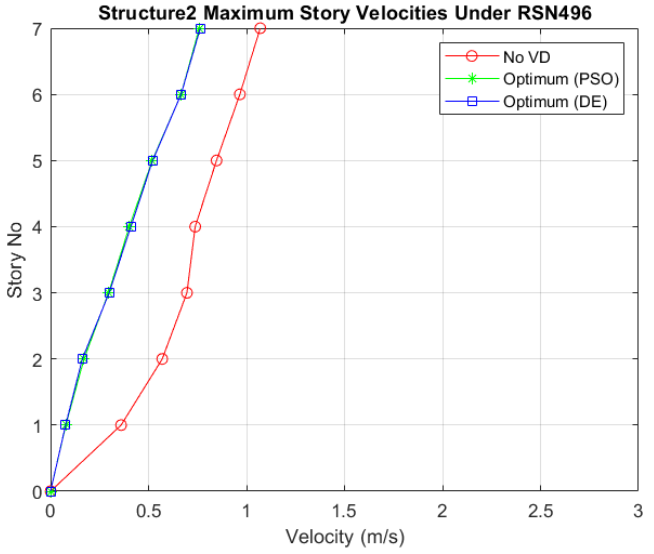

Figure 6.104 Comparison of Maximum Velocity Responses for Structure2 With VD and Without VD Under RSN496

Comparison of maximum displacement responses for Structure2 without VD and with optimum VD under RSN496 is given below in Figure 6.105.

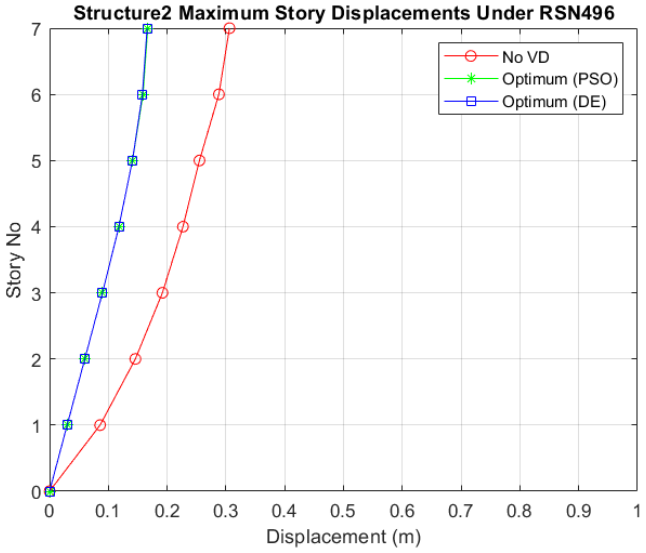

Figure 6.105 Comparison of Maximum Displacement Responses for Structure2 With VD and Without VD Under RSN496

Comparison of peak IDR for Structure2 without VD and with optimum VD under RSN496 is given below in Figure 6.106.

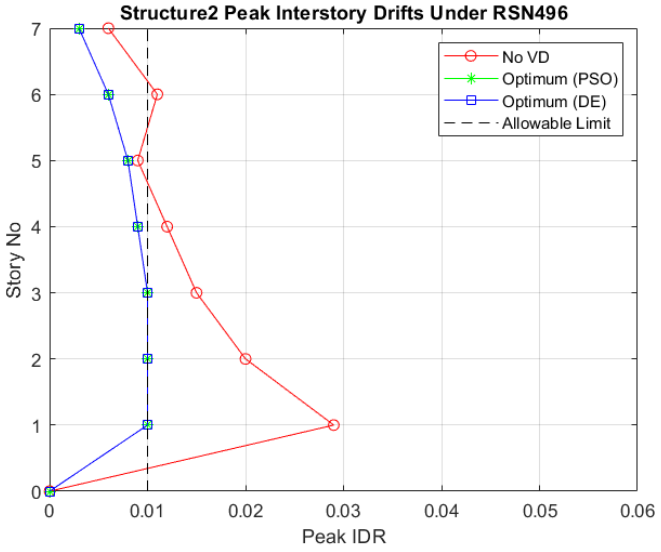

Figure 6.106 Comparison of Peak IDR for Structure2 With VD and Without VD Under RSN496

6.3.7. Under RSN741 (NPNF)

Particle Swarm Optimization (PSO) optimization history for Structure2 under RSN741 is given below in Figure 6.107.

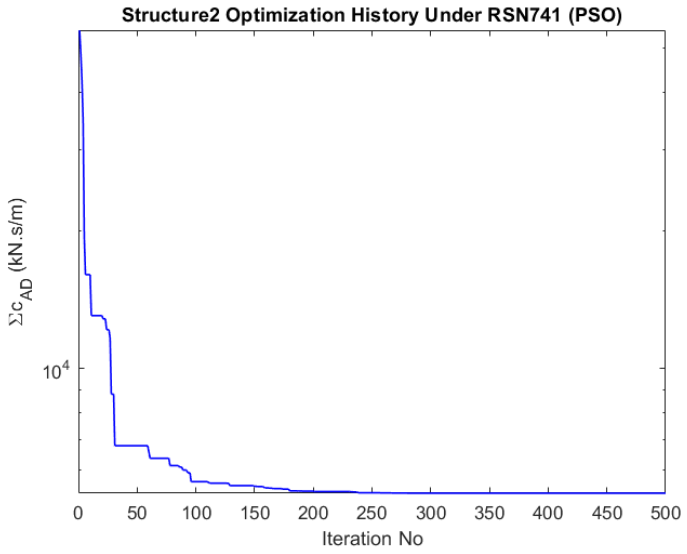

Figure 6.107 Structure2 Optimization History (PSO) Under RSN741

Differential Evolution (DE) optimization history for Structure2 under RSN741 is given below in Figure 6.108.

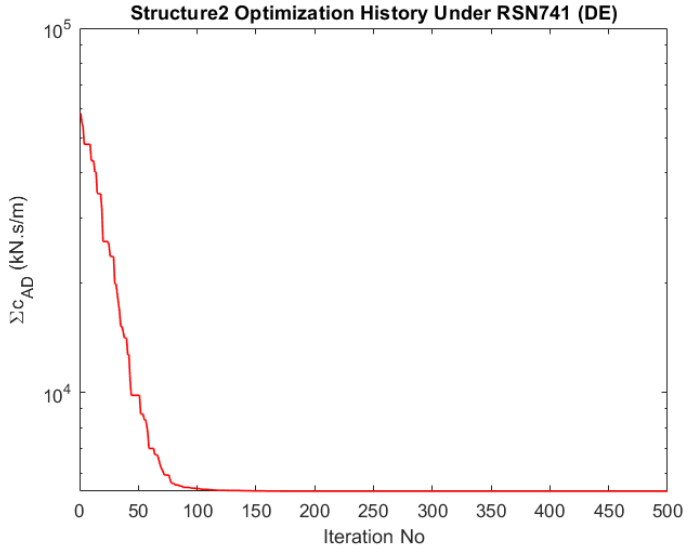

Figure 6.108 Structure2 Optimization History (DE) Under RSN741

Optimum viscous damper (VD) distribution for Structure2 Under RSN741 is given below in Table 6.25.

Table 6.25 Structure2 Optimum viscous damper (VD) distribution Under RSN741

Structure2 Optimum viscous damper (VD) distribution Under RSN741		
Story No	Added Damper PSO (kN.s/m)	Added Damper DE (kN.s/m)
1	4076.085	4076.085
2	686.871	686.871
3	0.000	0.000
4	89.389	89.389
5	494.918	494.918
6	0.000	0.000
7	0.000	0.000
Total Global Best	5347.264	5347.263

Comparison of maximum acceleration responses for Structure2 without VD and with optimum VD under RSN741 is given below in Figure 6.109.

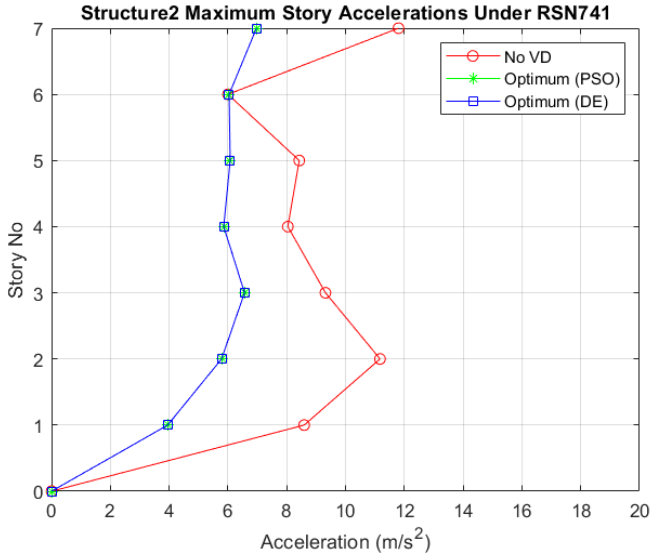

Figure 6.109 Comparison of Maximum Acceleration Responses for Structure2 With VD and Without VD Under RSN741

Comparison of maximum velocity responses for Structure2 without VD and with optimum VD under RSN741 is given below in Figure 6.110.

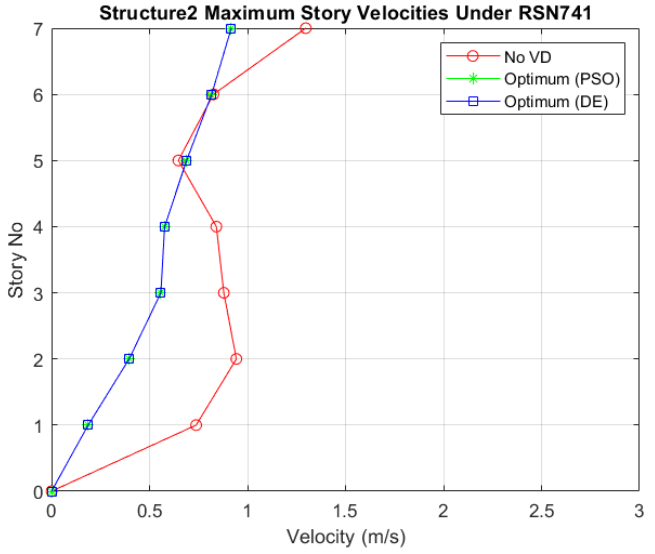

Figure 6.110 Comparison of Maximum Velocity Responses for Structure2 With VD and Without VD Under RSN741

Comparison of maximum displacement responses for Structure2 without VD and with optimum VD under RSN741 is given below in Figure 6.111.

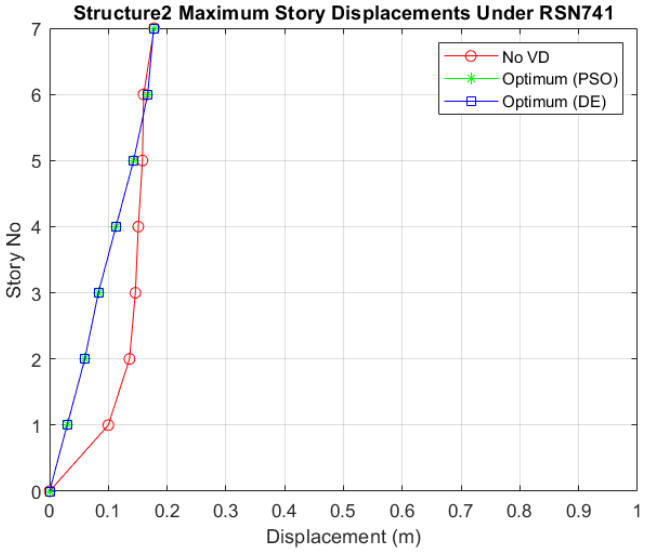

Figure 6.111 Comparison of Maximum Displacement Responses for Structure2 With VD and Without VD Under RSN741

Comparison of peak IDR for Structure2 without VD and with optimum VD under RSN741 is given below in Figure 6.112.

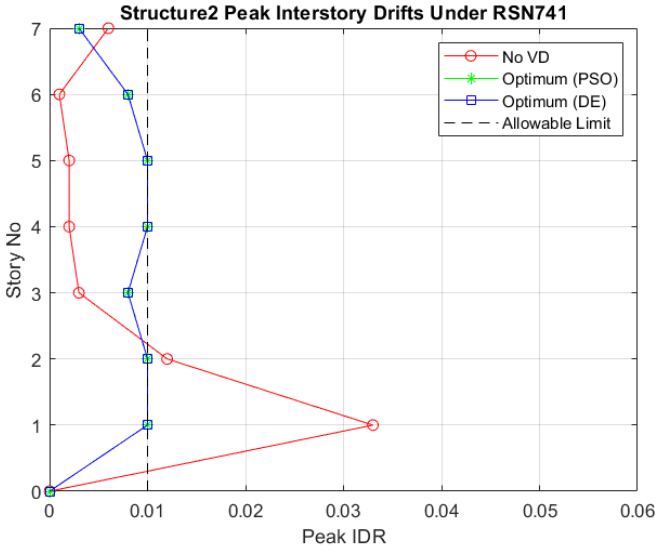

Figure 6.112 Comparison of Peak IDR for Structure2 With VD and Without VD Under RSN741

6.3.8. Under RSN1004 (NPNF)

Particle Swarm Optimization (PSO) optimization history for Structure2 under RSN1004 is given below in Figure 6.113.

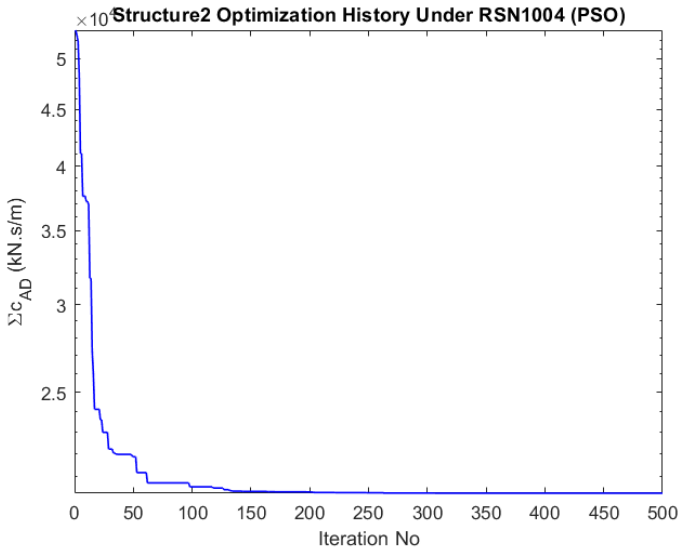

Figure 6.113 Structure2 Optimization History (PSO) Under RSN1004

Differential Evolution (DE) optimization history for Structure2 under RSN1004 is given below in Figure 6.114.

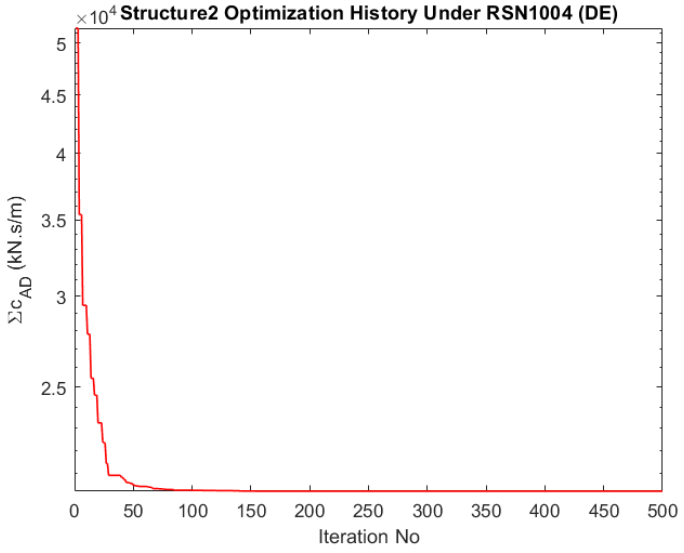

Figure 6.114 Structure2 Optimization History (DE) Under RSN1004

Optimum viscous damper (VD) distribution for Structure2 Under RSN1004 is given below in Table 6.26.

Table 6.26 Structure2 Optimum viscous damper (VD) distribution Under RSN1004

Structure2 Optimum viscous damper (VD) distribution Under RSN1004		
Story No	Added Damper PSO (kN.s/m)	Added Damper DE (kN.s/m)
1	9699.789	9696.909
2	6199.937	6198.891
3	3619.404	3595.581
4	742.052	766.582
5	0.000	0.000
6	0.000	0.000
7	0.000	0.000
Total Global Best	20261.182	20257.962

Comparison of maximum acceleration responses for Structure2 without VD and with optimum VD under RSN1004 is given below in Figure 6.115.

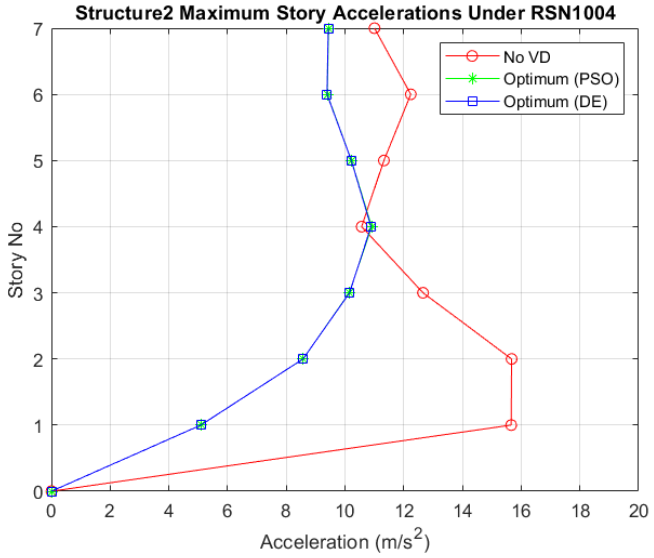

Figure 6.115 Comparison of Maximum Acceleration Responses for Structure2 With VD and Without VD Under RSN1004

Comparison of maximum velocity responses for Structure2 without VD and with optimum VD under RSN1004 is given below in Figure 6.116.

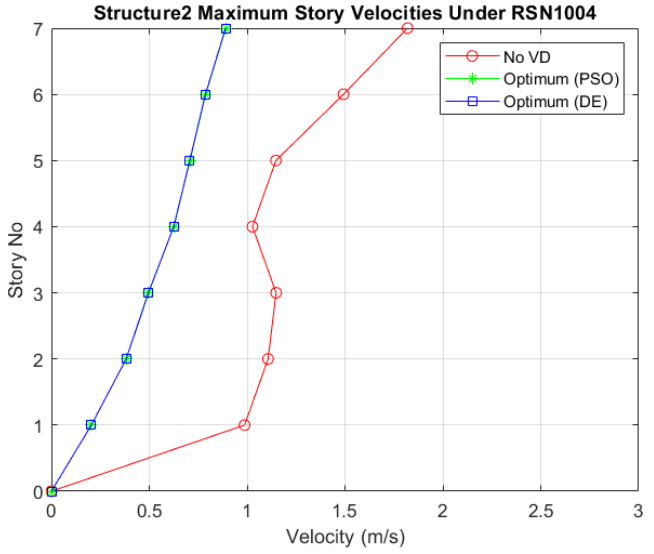

Figure 6.116 Comparison of Maximum Velocity Responses for Structure2 With VD and Without VD Under RSN1004

Comparison of maximum displacement responses for Structure2 without VD and with optimum VD under RSN1004 is given below in Figure 6.117.

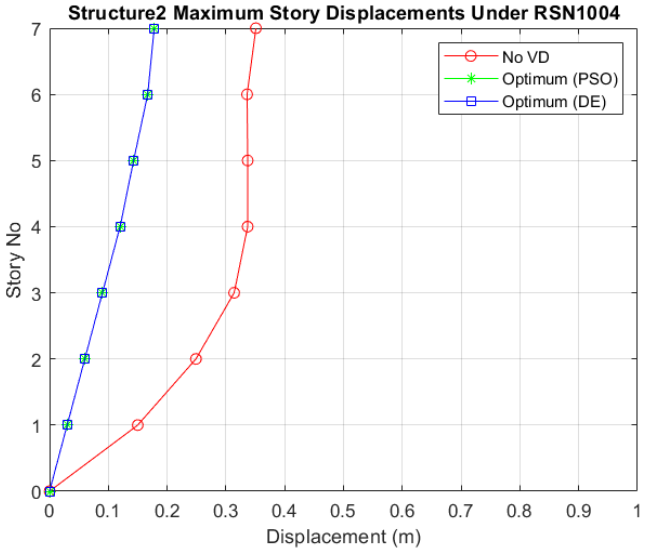

Figure 6.117 Comparison of Maximum Displacement Responses for Structure2 With VD and Without VD Under RSN1004

Comparison of peak IDR for Structure2 without VD and with optimum VD under RSN1004 is given below in Figure 6.118.

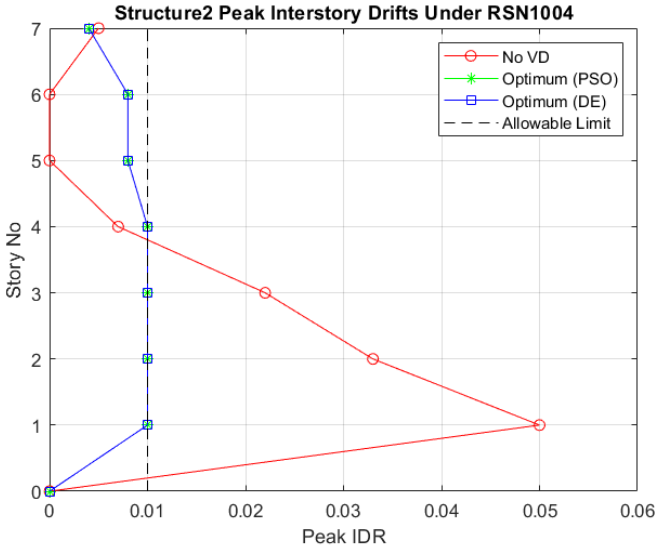

Figure 6.118 Comparison of Peak IDR for Structure2 With VD and Without VD Under RSN1004

6.3.9. Under RSN68 (FF)

Under this earthquake ground motion data, peak IDR of each story is lower than allowable limit. Because of that reason, Structure2 does not need additional VD under RSN68.

Comparison of maximum acceleration responses for Structure2 without VD and with optimum VD under RSN68 is given below in Figure 6.119.

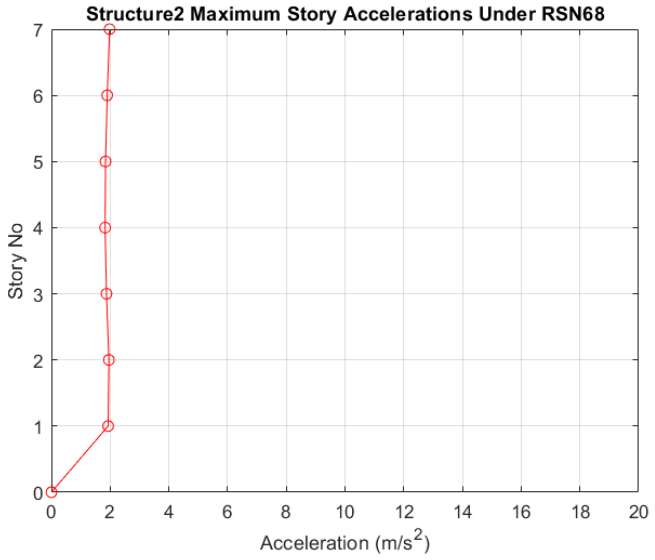

Figure 6.119 Comparison of Maximum Acceleration Responses for Structure2 With VD and Without VD Under RSN68

Comparison of maximum velocity responses for Structure2 without VD and with optimum VD under RSN68 is given below in Figure 6.120.

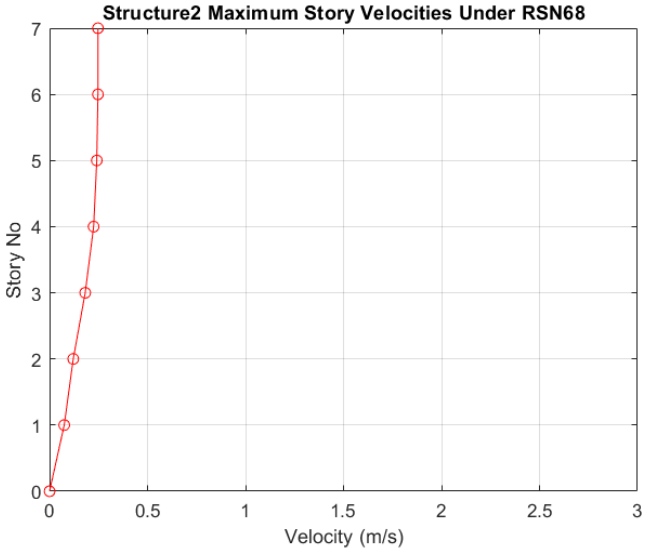

Figure 6.120 Comparison of Maximum Velocity Responses for Structure2 With VD and Without VD Under RSN68

Comparison of maximum displacement responses for Structure2 without VD and with optimum VD under RSN68 is given below in Figure 6.121.

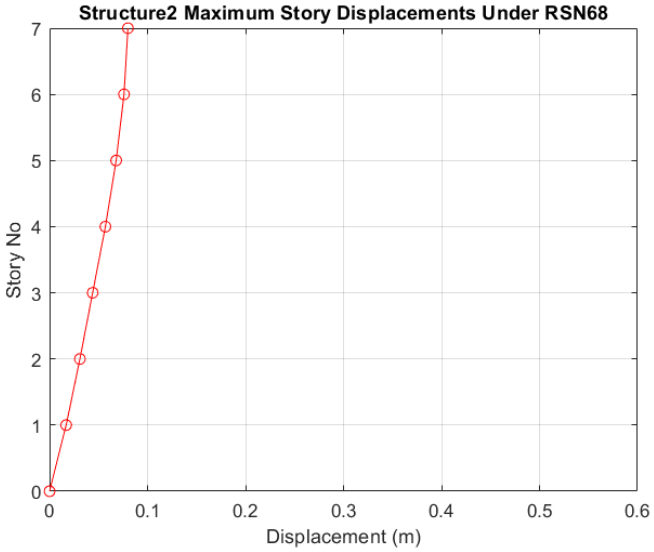

Figure 6.121 Comparison of Maximum Displacement Responses for Structure2 With VD and Without VD Under RSN68

Comparison of peak IDR for Structure2 without VD and with optimum VD under RSN68 is given below in Figure 6.122.

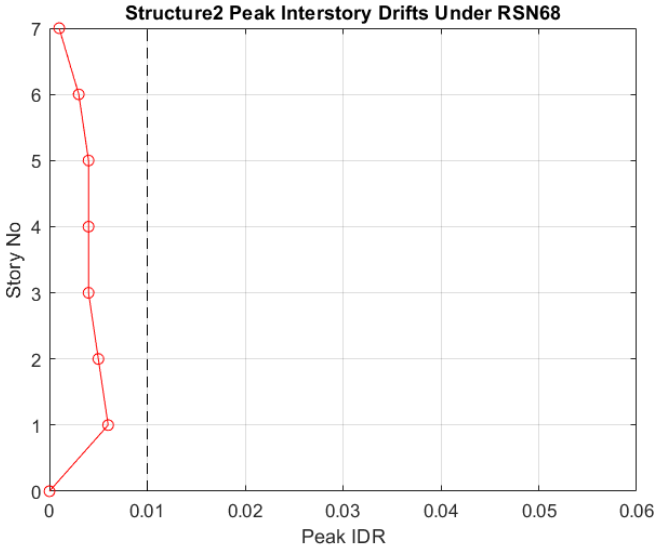

Figure 6.122 Comparison of Peak IDR for Structure2 With VD and Without VD Under RSN68

6.3.10. Under RSN752 (FF)

Particle Swarm Optimization (PSO) optimization history for Structure2 under RSN752 is given below in Figure 6.123.

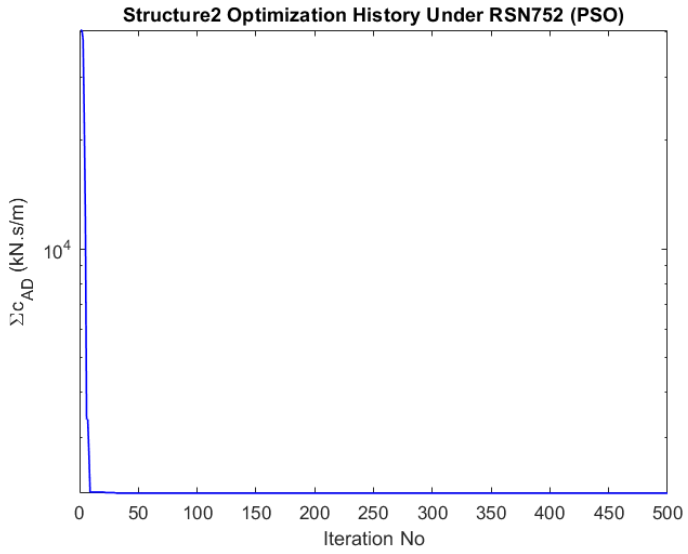

Figure 6.123 Structure2 Optimization History (PSO) Under RSN752

Differential Evolution (DE) optimization history for Structure2 under RSN752 is given below in Figure 6.124.

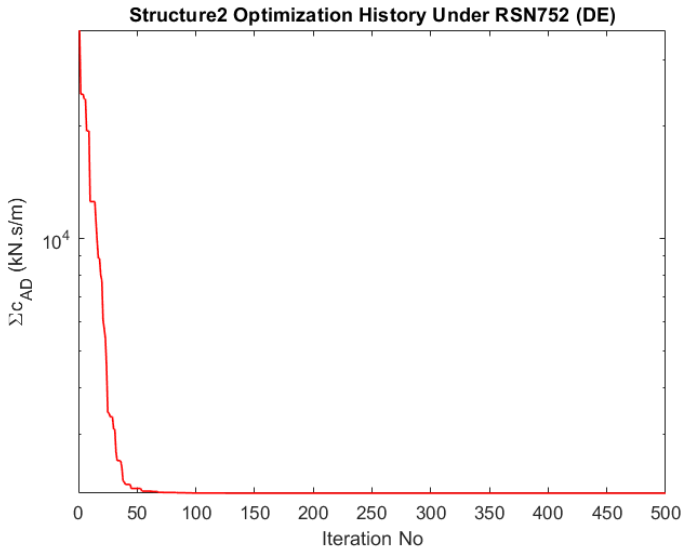

Figure 6.124 Structure2 Optimization History (DE) Under RSN752

Optimum viscous damper (VD) distribution for Structure2 Under RSN752 is given below in Table 6.27.

Table 6.27 Structure2 Optimum viscous damper (VD) distribution Under RSN752

Structure2 Optimum viscous damper (VD) distribution Under RSN752		
Story No	Added Damper PSO (kN.s/m)	Added Damper DE (kN.s/m)
1	2102.004	1906.511
2	0.000	0.000
3	0.000	0.000
4	0.000	0.000
5	0.000	0.000
6	0.000	182.664
7	0.000	0.000
Total Global Best	2102.004	2089.175

Comparison of maximum acceleration responses for Structure2 without VD and with optimum VD under RSN752 is given below in Figure 6.125.

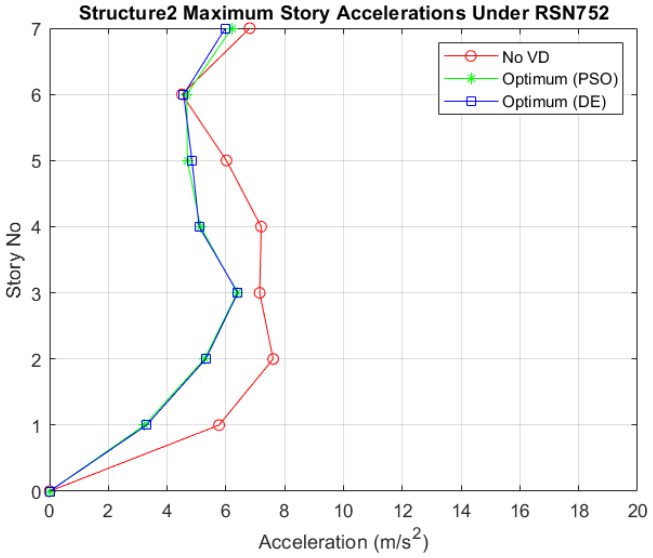

Figure 6.125 Comparison of Maximum Acceleration Responses for Structure2 With VD and Without VD Under RSN752

Comparison of maximum velocity responses for Structure2 without VD and with optimum VD under RSN752 is given below in Figure 6.126.

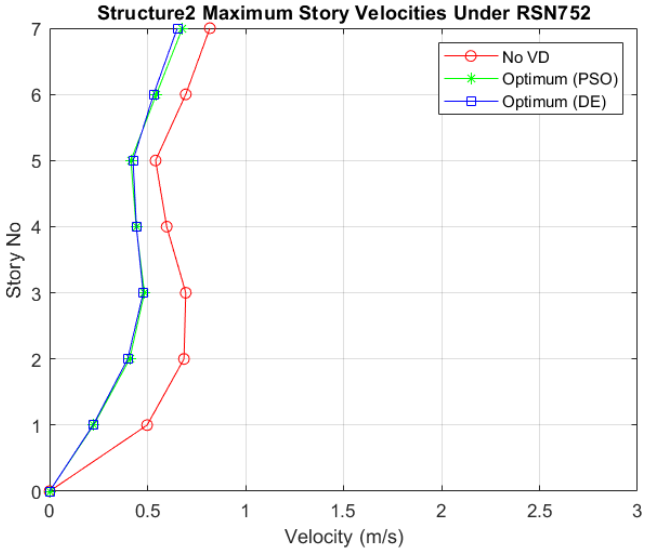

Figure 6.126 Comparison of Maximum Velocity Responses for Structure2 With VD and Without VD Under RSN752

Comparison of maximum displacement responses for Structure2 without VD and with optimum VD under RSN752 is given below in Figure 6.127.

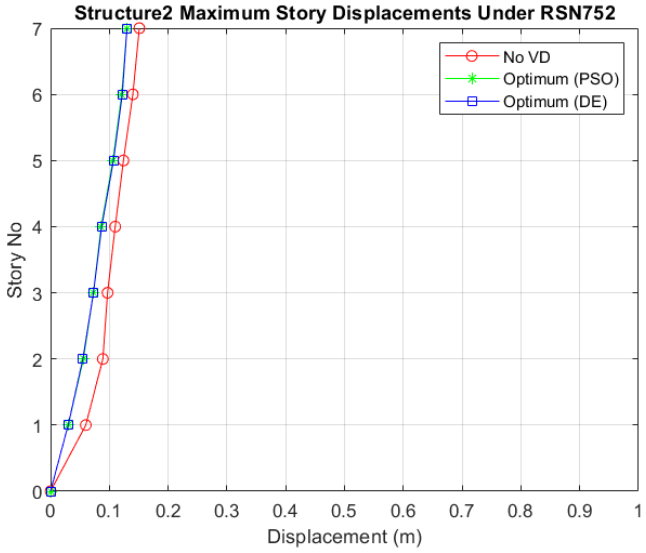

Figure 6.127 Comparison of Maximum Displacement Responses for Structure2 With VD and Without VD Under RSN752

Comparison of peak IDR for Structure2 without VD and with optimum VD under RSN752 is given below in Figure 6.128.

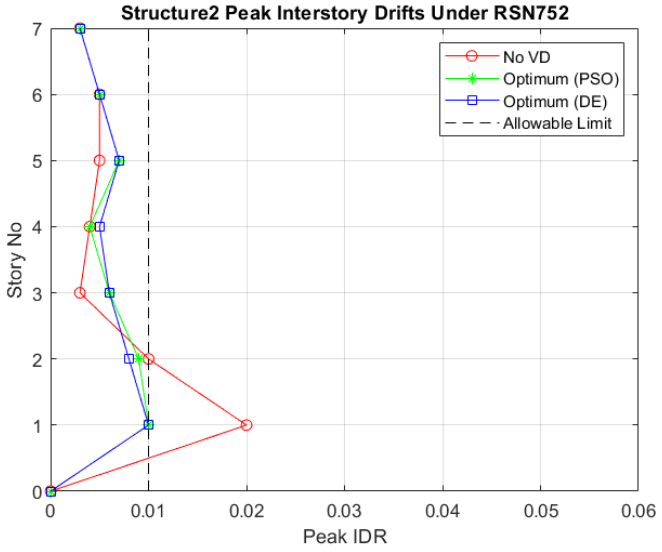

Figure 6.128 Comparison of Peak IDR for Structure2 With VD and Without VD Under RSN752

6.3.11. Under RSN953 (FF)

Particle Swarm Optimization (PSO) optimization history for Structure2 under RSN953 is given below in Figure 6.129.

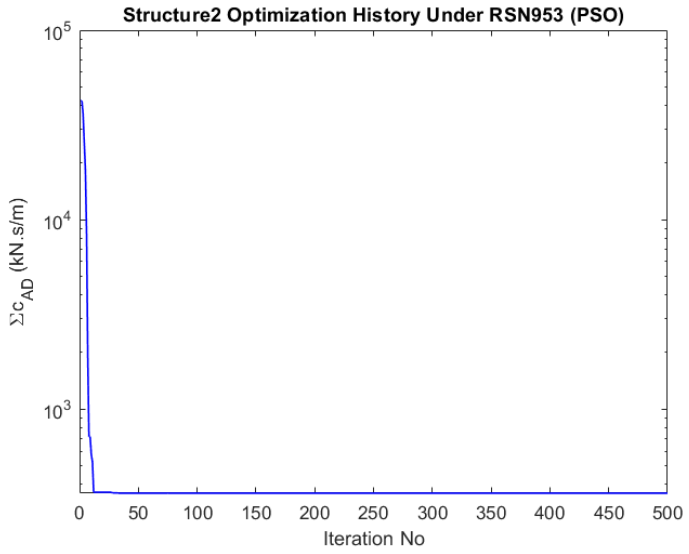

Figure 6.129 Structure2 Optimization History (PSO) Under RSN953

Differential Evolution (DE) optimization history for Structure2 under RSN953 is given below in Figure 6.130.

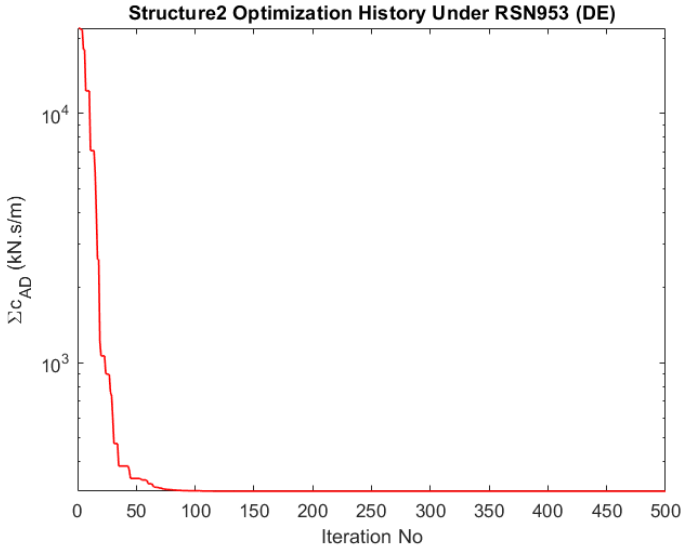

Figure 6.130 Structure2 Optimization History (DE) Under RSN953

Optimum viscous damper (VD) distribution for Structure2 Under RSN953 is given below in Table 6.28.

Table 6.28 Structure2 Optimum viscous damper (VD) distribution Under RSN953

Structure2 Optimum viscous damper (VD) distribution Under RSN953		
Story No	Added Damper PSO (kN.s/m)	Added Damper DE (kN.s/m)
1	0.000	0.000
2	0.000	0.000
3	0.000	248.265
4	0.000	0.000
5	0.000	0.000
6	359.326	57.043
7	0.000	0.000
Total Global Best	359.326	305.308

Comparison of maximum acceleration responses for Structure2 without VD and with optimum VD under RSN953 is given below in Figure 6.131.

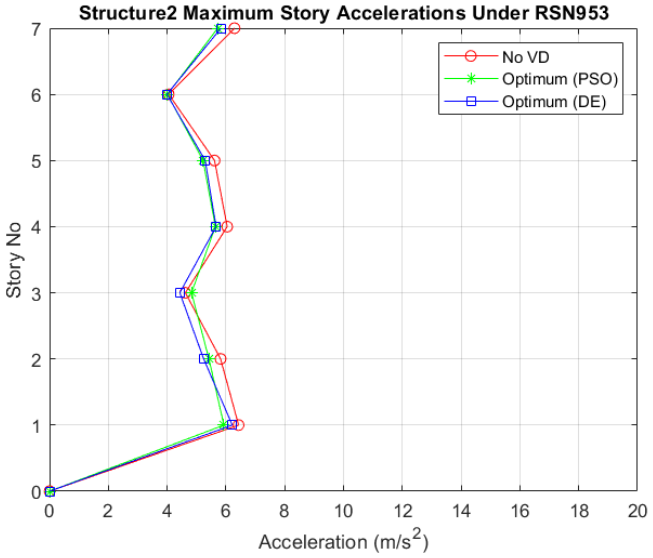

Figure 6.131 Comparison of Maximum Acceleration Responses for Structure2 With VD and Without VD Under RSN953

Comparison of maximum velocity responses for Structure2 without VD and with optimum VD under RSN953 is given below in Figure 6.132.

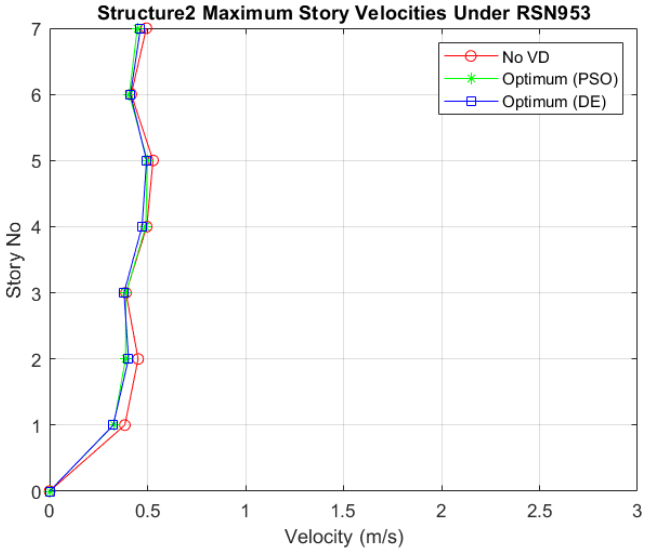

Figure 6.132 Comparison of Maximum Velocity Responses for Structure2 With VD and Without VD Under RSN953

Comparison of maximum displacement responses for Structure2 without VD and with optimum VD under RSN953 is given below in Figure 6.133.

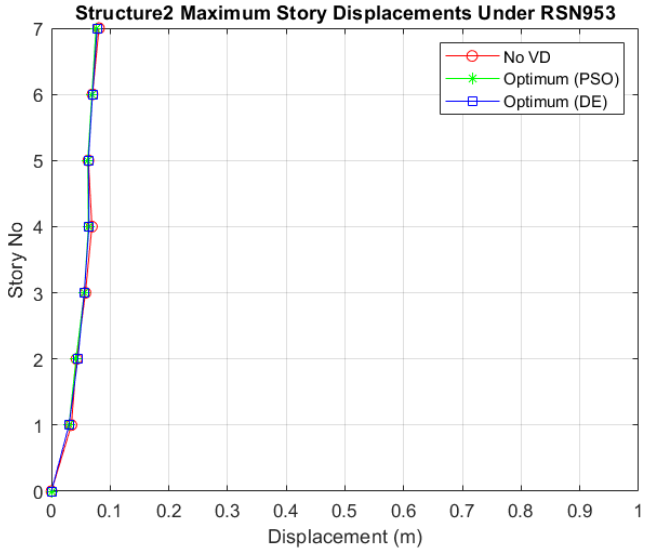

Figure 6.133 Comparison of Maximum Displacement Responses for Structure2 With VD and Without VD Under RSN953

Comparison of peak IDR for Structure2 without VD and with optimum VD under RSN953 is given below in Figure 6.134.

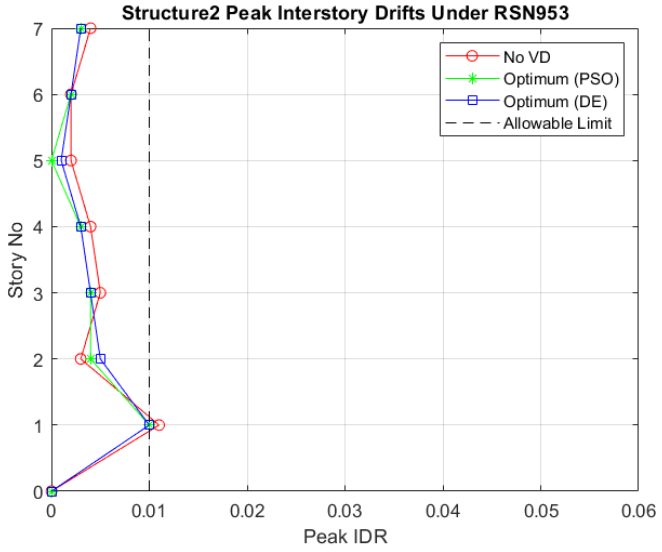

Figure 6.134 Comparison of Peak IDR for Structure2 With VD and Without VD Under RSN953

6.3.12. Under RSN1111 (FF)

Under this earthquake ground motion data, peak IDR of each story is lower than allowable limit. Because of that reason, Structure2 does not need additional VD under RSN1111.

Comparison of maximum acceleration responses for Structure2 without VD and with optimum VD under RSN1111 is given below in Figure 6.135.

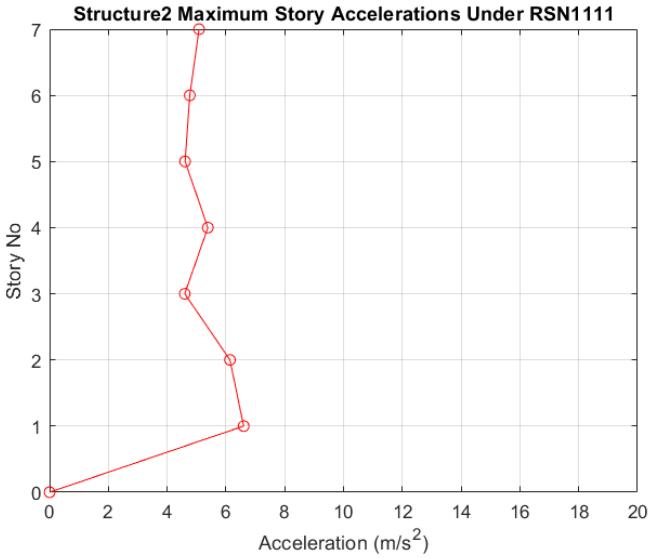

Figure 6.135 Comparison of Maximum Acceleration Responses for Structure2 With VD and Without VD Under RSN1111

Comparison of maximum velocity responses for Structure2 without VD and with optimum VD under RSN1111 is given below in Figure 6.136.

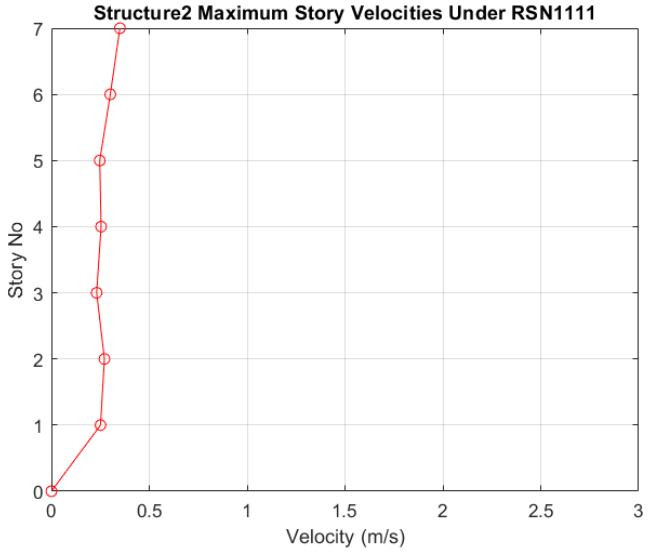

Figure 6.136 Comparison of Maximum Velocity Responses for Structure2 With VD and Without VD Under RSN1111

Comparison of maximum displacement responses for Structure2 without VD and with optimum VD under RSN1111 is given below in Figure 6.137.

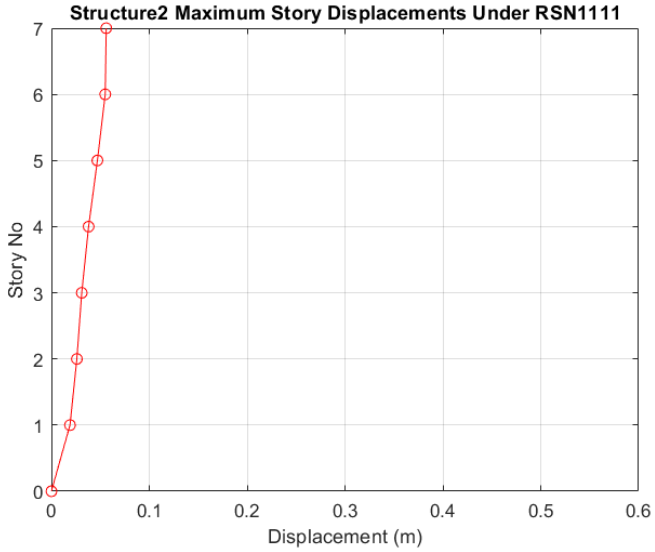

Figure 6.137 Comparison of Maximum Displacement Responses for Structure2 With VD and Without VD Under RSN1111

Comparison of peak IDR for Structure2 without VD and with optimum VD under RSN1111 is given below in Figure 6.138.

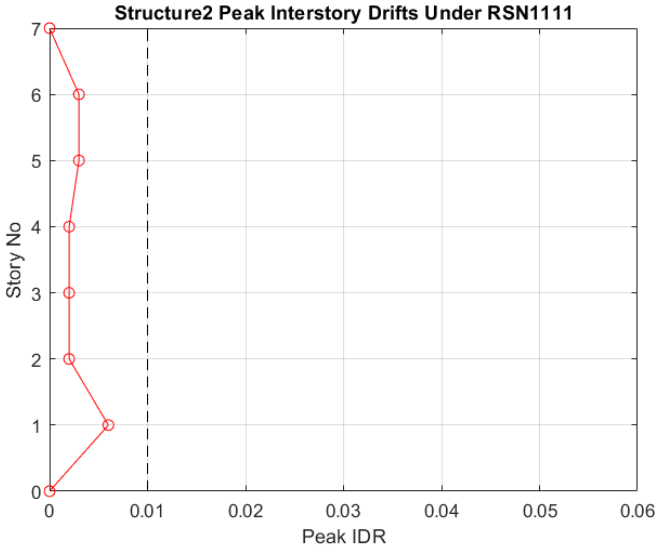

Figure 6.138 Comparison of Peak IDR for Structure2 With VD and Without VD Under RSN1111

6.4. Analysis Results for Structure3

6.4.1. Under RSN182 (PNF)

Particle Swarm Optimization (PSO) optimization history for Structure3 under RSN182 is given below in Figure 6.139.

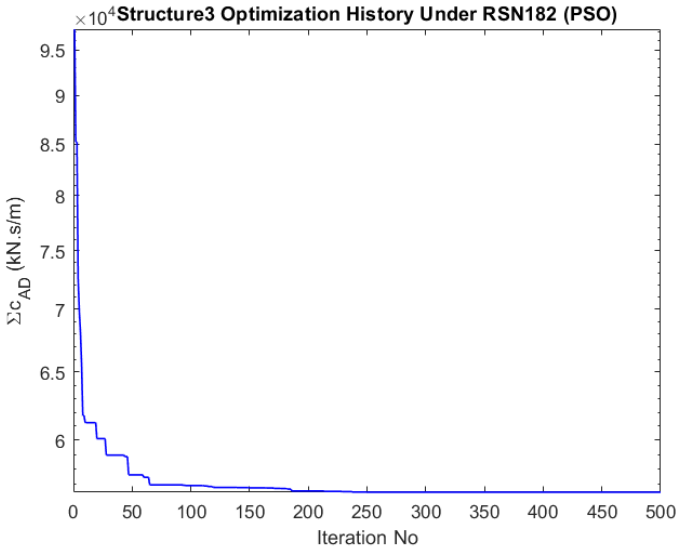

Figure 6.139 Structure3 Optimization History (PSO) Under RSN182

Differential Evolution (DE) optimization history for Structure3 under RSN182 is given below in Figure 6.140.

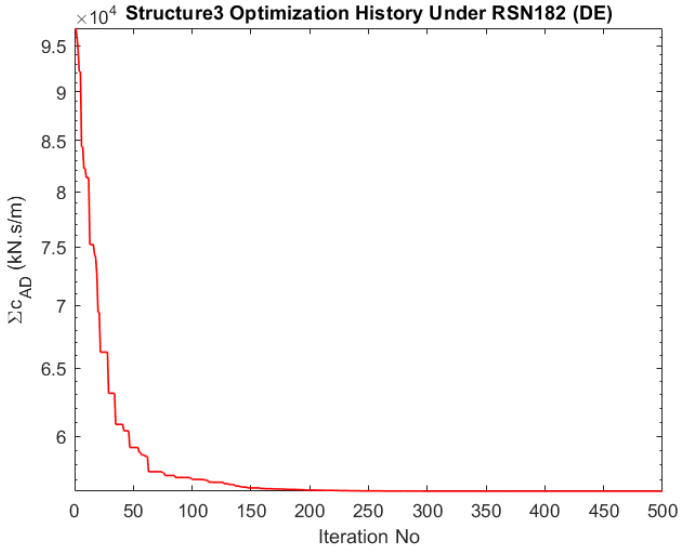

Figure 6.140 Structure3 Optimization History (DE) Under RSN182

Optimum viscous damper (VD) distribution for Structure3 Under RSN182 is given below in Table 6.29.

Table 6.29 Structure3 Optimum viscous damper (VD) distribution Under RSN182

Structure3 Optimum viscous damper (VD) distribution Under RSN182		
Story No	Added Damper PSO (kN.s/m)	Added Damper DE (kN.s/m)
1	16323.476	16049.081
2	13515.370	13173.656
3	11789.609	11404.435
4	9579.911	9109.703
5	2118.555	4737.714
6	3104.571	1774.037
7	0.000	0.000
8	0.000	0.000
9	0.000	0.000
10	0.000	0.000
Total Global Best	56431.493	56248.626

Comparison of maximum acceleration responses for Structure3 without VD and with optimum VD under RSN182 is given below in Figure 6.141.

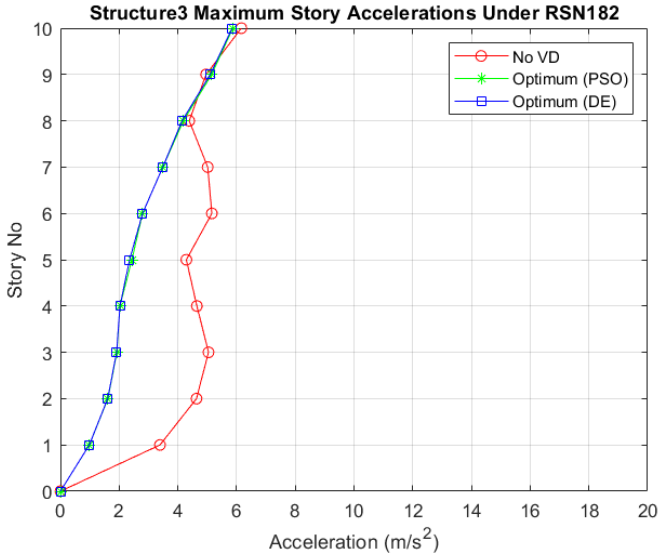

Figure 6.141 Comparison of Maximum Acceleration Responses for Structure3 With VD and Without VD Under RSN182

Comparison of maximum velocity responses for Structure3 without VD and with optimum VD under RSN182 is given below in Figure 6.142.

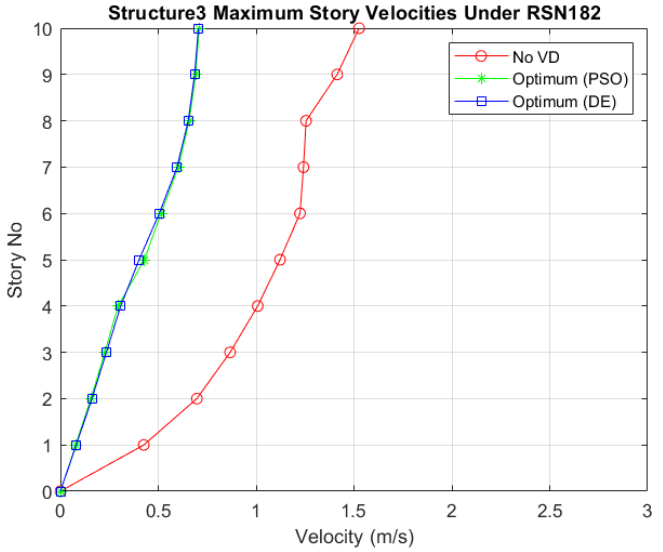

Figure 6.142 Comparison of Maximum Velocity Responses for Structure3 With VD and Without VD Under RSN182

Comparison of maximum displacement responses for Structure3 without VD and with optimum VD under RSN182 is given below in Figure 6.143.

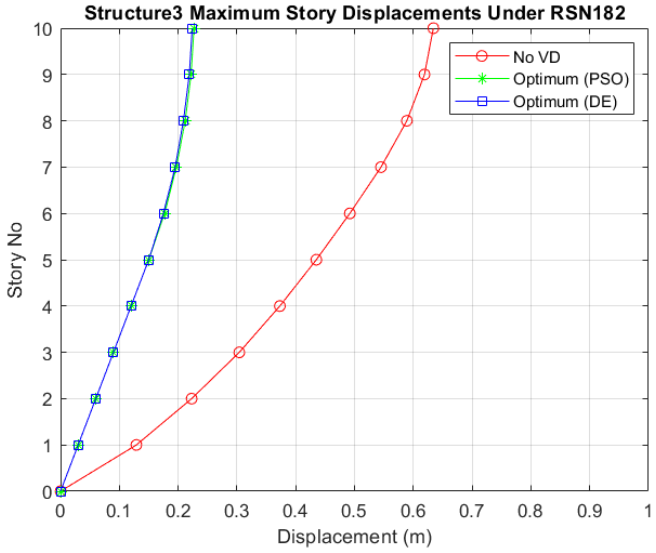

Figure 6.143 Comparison of Maximum Displacement Responses for Structure3 With VD and Without VD Under RSN182

Comparison of peak IDR for Structure3 without VD and with optimum VD under RSN182 is given below in Figure 6.144.

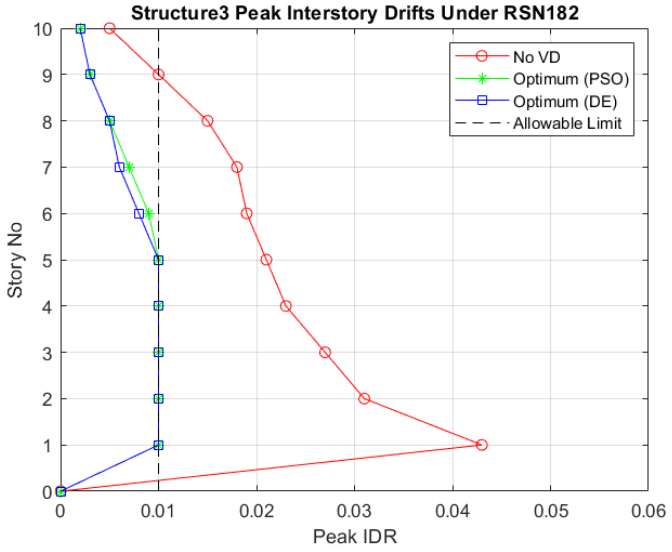

Figure 6.144 Comparison of Peak IDR for Structure3 With VD and Without VD Under RSN182

6.4.2. Under RSN821 (PNF)

Upper bound limit $2 \times 10^4(kN.sm)$ is not adequate to reduce peak IDR to allowable limit. Because of that reason upper bound limit is taken as $2.5 \times 10^4(kN.sm)$ for this specific example.

Particle Swarm Optimization (PSO) optimization history for Structure3 under RSN821 is given below in Figure 6.145.

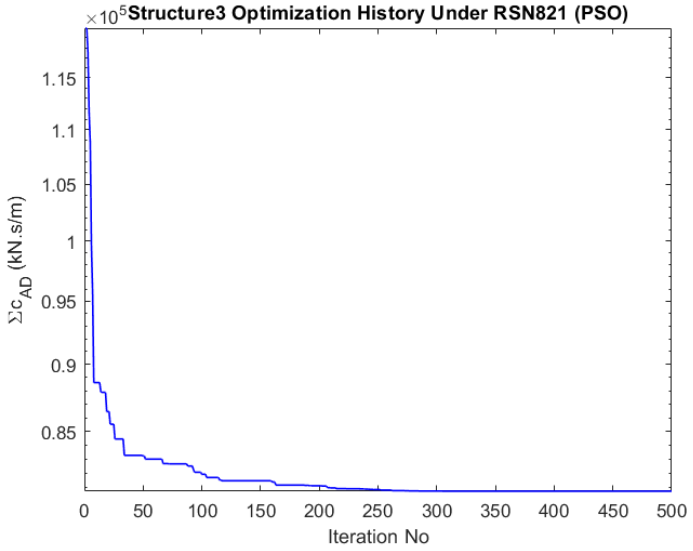

Figure 6.145 Structure3 Optimization History (PSO) Under RSN821

Differential Evolution (DE) optimization history for Structure3 under RSN821 is given below in Figure 6.146.

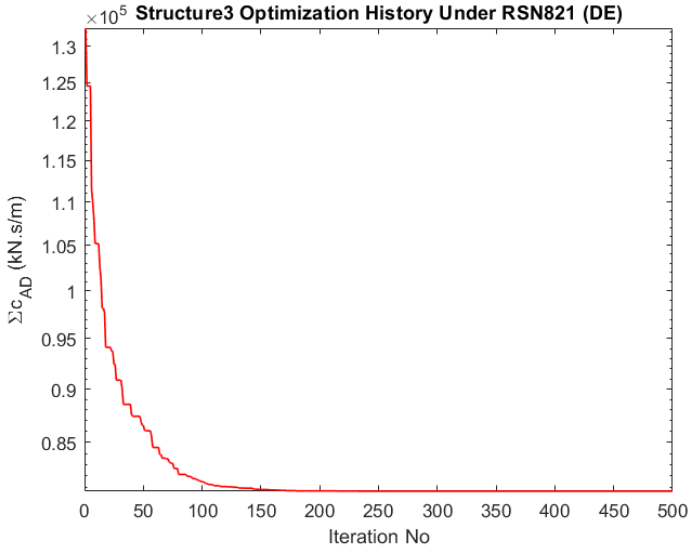

Figure 6.146 Structure3 Optimization History (DE) Under RSN821

Optimum viscous damper (VD) distribution for Structure3 Under RSN821 is given below in Table 6.30.

Table 6.30 Structure3 Optimum viscous damper (VD) distribution Under RSN821

Structure3 Optimum viscous damper (VD) distribution Under RSN821		
Story No	Added Damper PSO (kN.s/m)	Added Damper DE (kN.s/m)
1	21781.278	21915.579
2	17464.120	17629.225
3	14979.278	15155.857
4	12083.987	12285.203
5	8046.165	8368.335
6	6403.620	5304.435
7	0.000	0.000
8	0.000	0.000
9	0.000	0.000
10	0.000	0.000
Total Global Best	80758.448	80658.634

Comparison of maximum acceleration responses for Structure3 without VD and with optimum VD under RSN821 is given below in Figure 6.147.

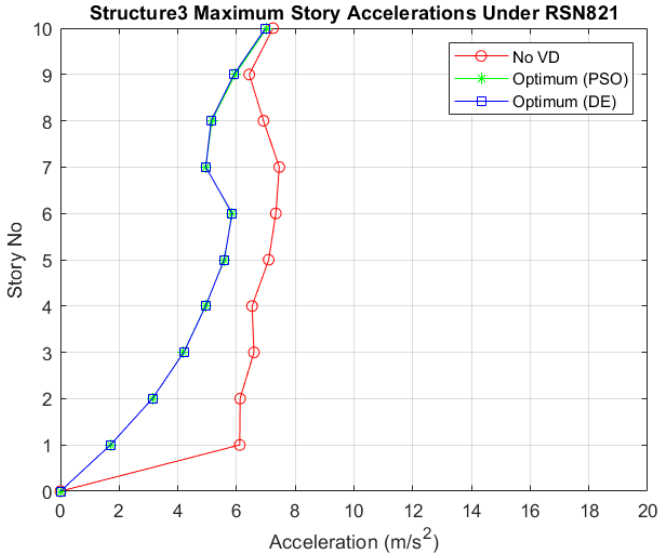

Figure 6.147 Comparison of Maximum Acceleration Responses for Structure3 With VD and Without VD Under RSN821

Comparison of maximum velocity responses for Structure3 without VD and with optimum VD under RSN821 is given below in Figure 6.148.

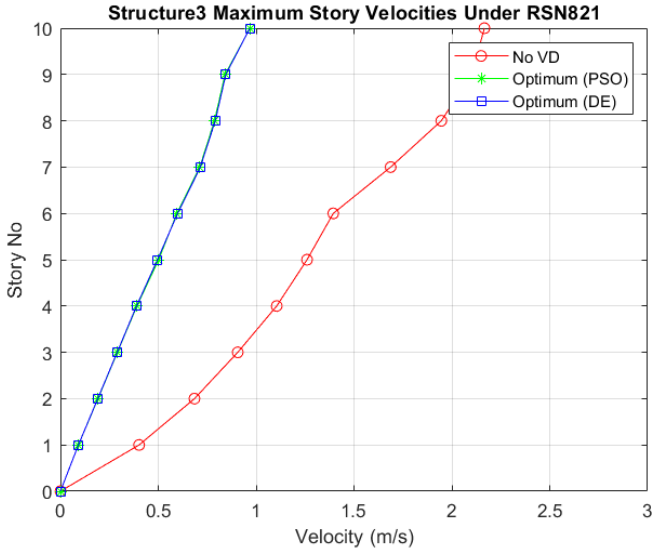

Figure 6.148 Comparison of Maximum Velocity Responses for Structure3 With VD and Without VD Under RSN821

Comparison of maximum displacement responses for Structure3 without VD and with optimum VD under RSN821 is given below in Figure 6.149.

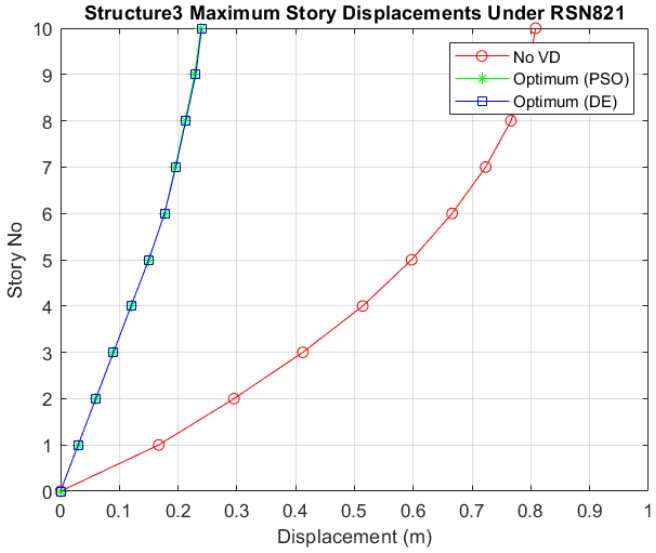

Figure 6.149 Comparison of Maximum Displacement Responses for Structure3 With VD and Without VD Under RSN821

Comparison of peak IDR for Structure3 without VD and with optimum VD under RSN821 is given below in Figure 6.150.

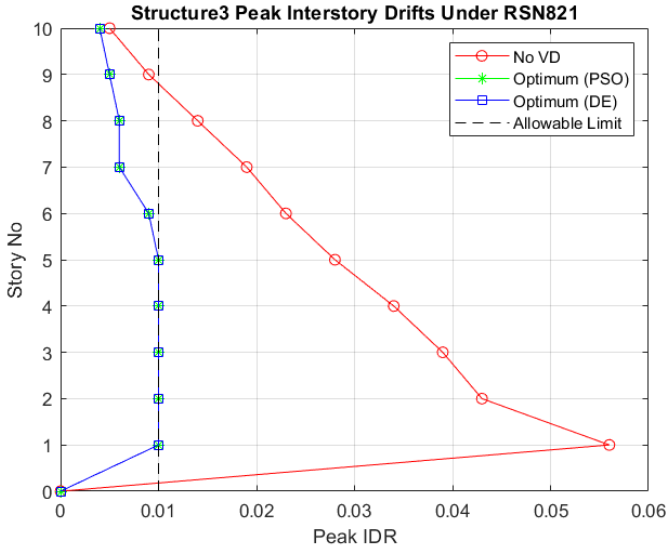

Figure 6.150 Comparison of Peak IDR for Structure3 With VD and Without VD Under RSN821

6.4.3. Under RSN1063 (PNF)

Particle Swarm Optimization (PSO) optimization history for Structure3 under RSN1063 is given below in Figure 6.151.

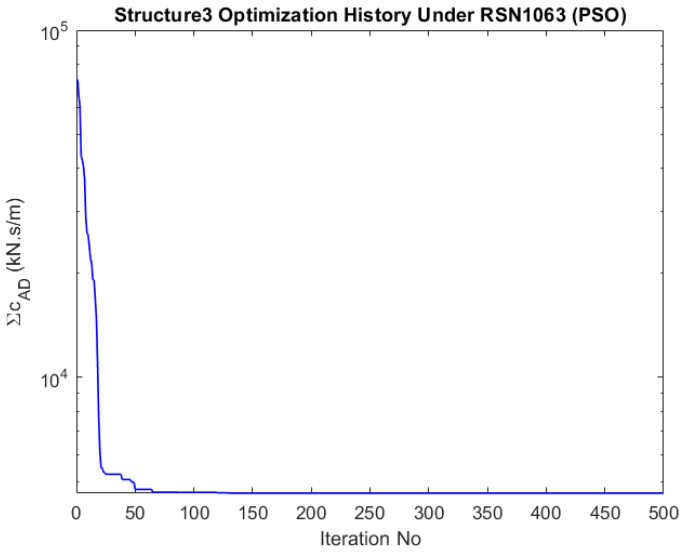

Figure 6.151 Structure3 Optimization History (PSO) Under RSN1063

Differential Evolution (DE) optimization history for Structure3 under RSN1063 is given below in Figure 6.152.

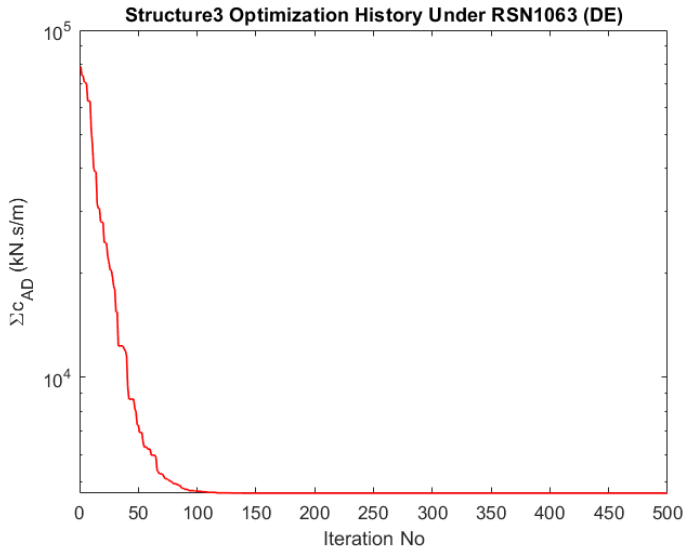

Figure 6.152 Structure3 Optimization History (DE) Under RSN1063

Optimum viscous damper (VD) distribution for Structure3 Under RSN1063 is given below in Table 6.31.

Table 6.31 Structure3 Optimum viscous damper (VD) distribution Under RSN1063

Structure3 Optimum viscous damper (VD) distribution Under RSN1063		
Story No	Added Damper PSO (kN.s/m)	Added Damper DE (kN.s/m)
1	3487.619	3487.619
2	1153.529	1153.529
3	0.000	0.000
4	0.000	0.000
5	0.000	0.000
6	0.000	0.000
7	0.000	0.000
8	0.000	0.000
9	0.000	0.000
10	0.000	0.000
Total Global Best	4641.149	4641.149

Comparison of maximum acceleration responses for Structure3 without VD and with optimum VD under RSN1063 is given below in Figure 6.153.

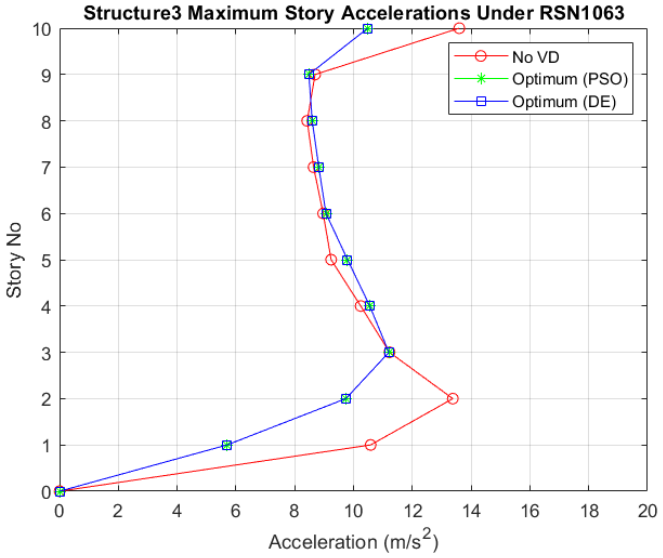

Figure 6.153 Comparison of Maximum Acceleration Responses for Structure3 With VD and Without VD Under RSN1063

Comparison of maximum velocity responses for Structure3 without VD and with optimum VD under RSN1063 is given below in Figure 6.154.

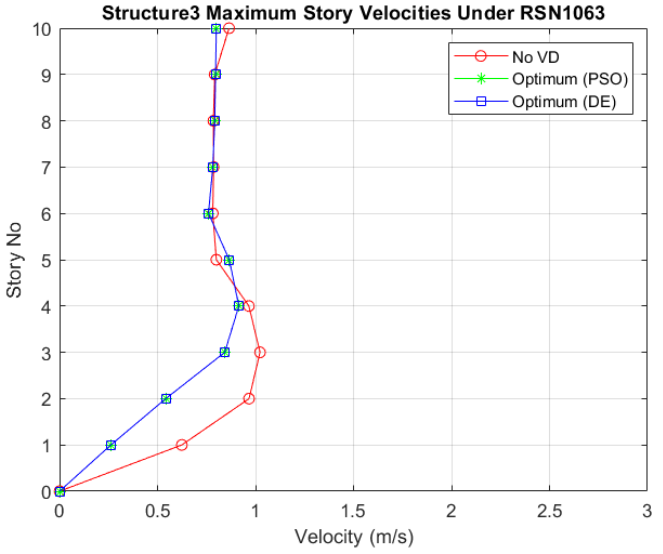

Figure 6.154 Comparison of Maximum Velocity Responses for Structure3 With VD and Without VD Under RSN1063

Comparison of maximum displacement responses for Structure3 without VD and with optimum VD under RSN1063 is given below in Figure 6.155.

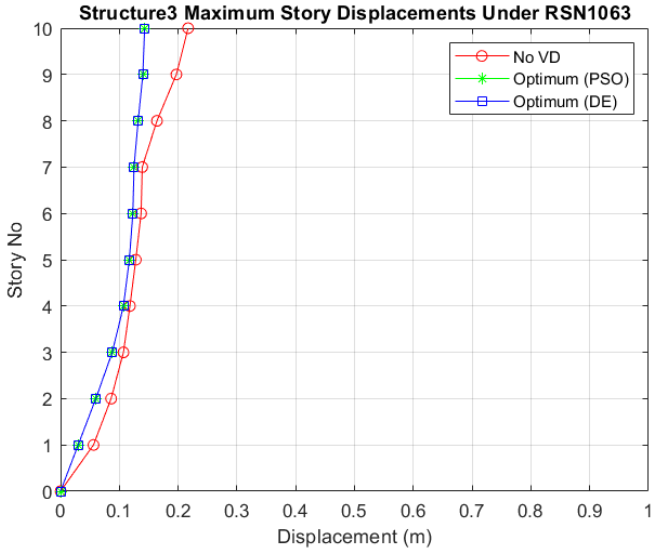

Figure 6.155 Comparison of Maximum Displacement Responses for Structure3 With VD and Without VD Under RSN1063

Comparison of peak IDR for Structure3 without VD and with optimum VD under RSN1063 is given below in Figure 6.156.

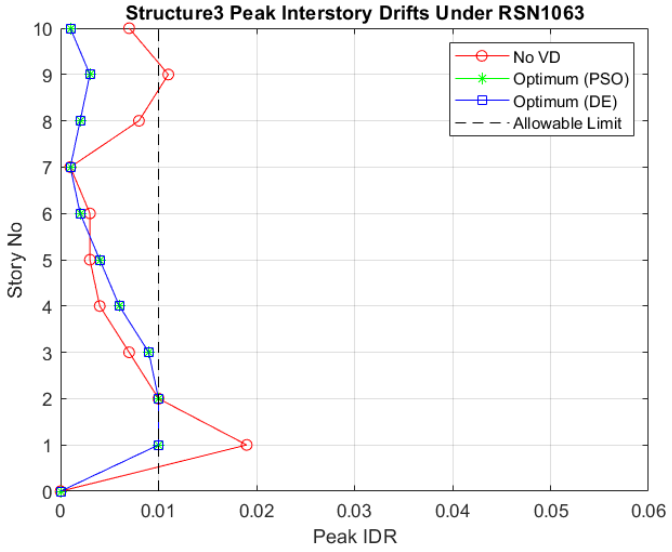

Figure 6.156 Comparison of Peak IDR for Structure3 With VD and Without VD Under RSN1063

6.4.4. Under RSN1605 (PNF)

Particle Swarm Optimization (PSO) optimization history for Structure3 under RSN1605 is given below in Figure 6.157.

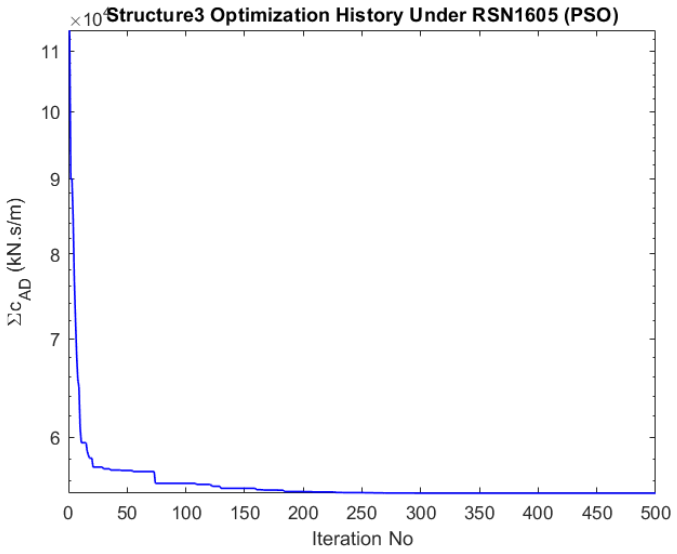

Figure 6.157 Structure3 Optimization History (PSO) Under RSN1605

Differential Evolution (DE) optimization history for Structure3 under RSN1605 is given below in Figure 6.158.

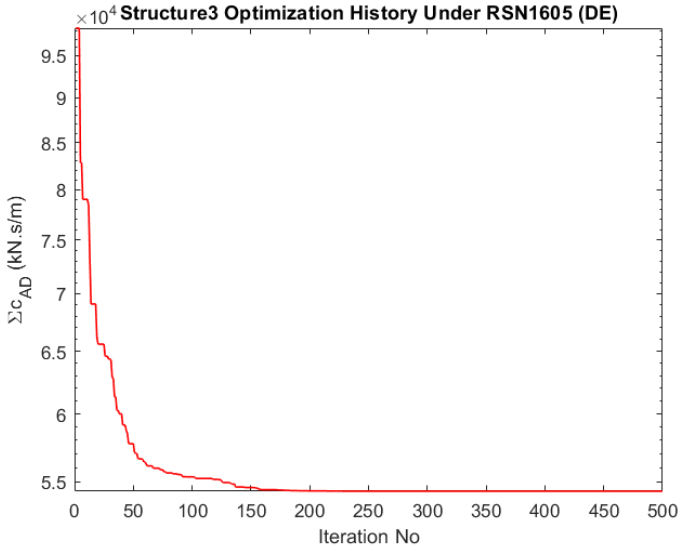

Figure 6.158 Structure3 Optimization History (DE) Under RSN1605

Optimum viscous damper (VD) distribution for Structure3 Under RSN1605 is given below in Table 6.32.

Table 6.32 Structure3 Optimum viscous damper (VD) distribution Under RSN1605

Structure3 Optimum viscous damper (VD) distribution Under RSN1605		
Story No	Added Damper PSO (kN.s/m)	Added Damper DE (kN.s/m)
1	16920.386	16878.610
2	13703.593	13673.055
3	11301.229	11248.218
4	7787.298	7647.024
5	0.000	4885.365
6	5229.708	0.000
7	0.000	0.000
8	0.000	0.000
9	0.000	0.000
10	0.000	0.000
Total Global Best	54942.214	54332.272

Comparison of maximum acceleration responses for Structure3 without VD and with optimum VD under RSN1605 is given below in Figure 6.159.

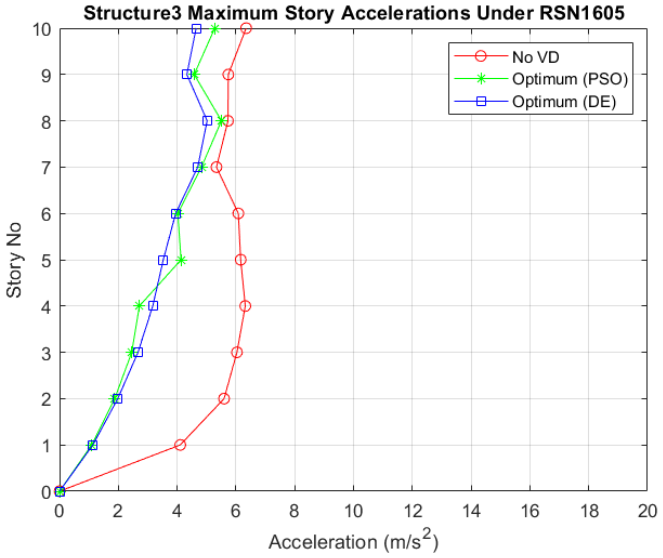

Figure 6.159 Comparison of Maximum Acceleration Responses for Structure3 With VD and Without VD Under RSN1605

Comparison of maximum velocity responses for Structure3 without VD and with optimum VD under RSN1605 is given below in Figure 6.160.

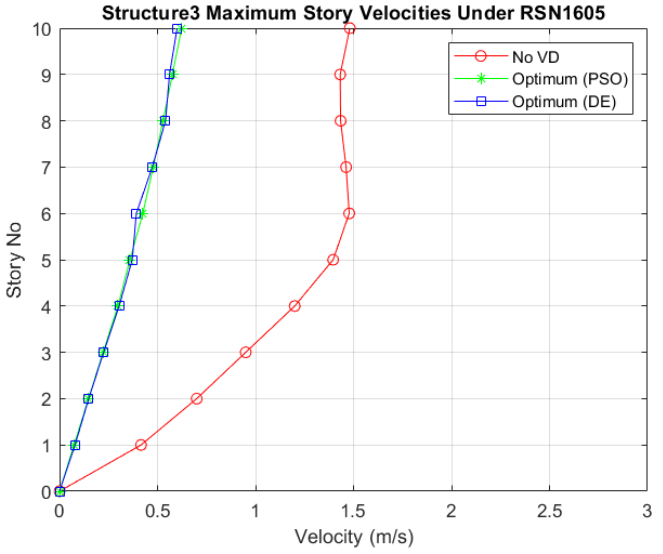

Figure 6.160 Comparison of Maximum Velocity Responses for Structure3 With VD and Without VD Under RSN1605

Comparison of maximum displacement responses for Structure3 without VD and with optimum VD under RSN1605 is given below in Figure 6.161.

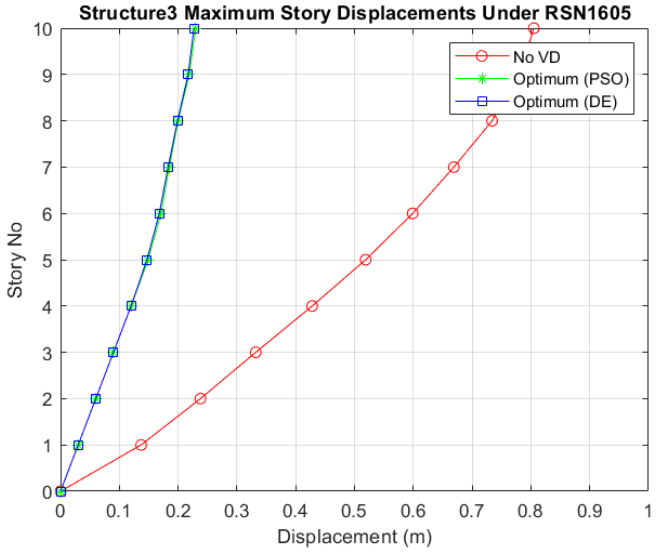

Figure 6.161 Comparison of Maximum Displacement Responses for Structure3 With VD and Without VD Under RSN1605

Comparison of peak IDR for Structure3 without VD and with optimum VD under RSN1605 is given below in Figure 6.162.

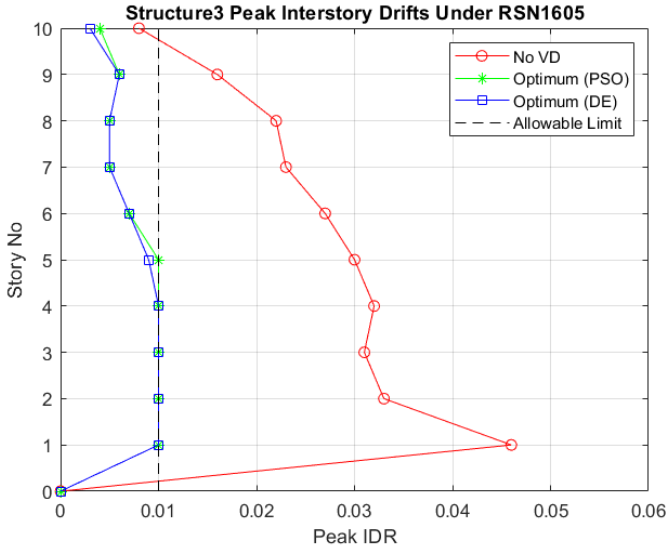

Figure 6.162 Comparison of Peak IDR for Structure3 With VD and Without VD Under RSN1605

6.4.5. Under RSN160 (NPNF)

Particle Swarm Optimization (PSO) optimization history for Structure3 under RSN160 is given below in Figure 6.163.

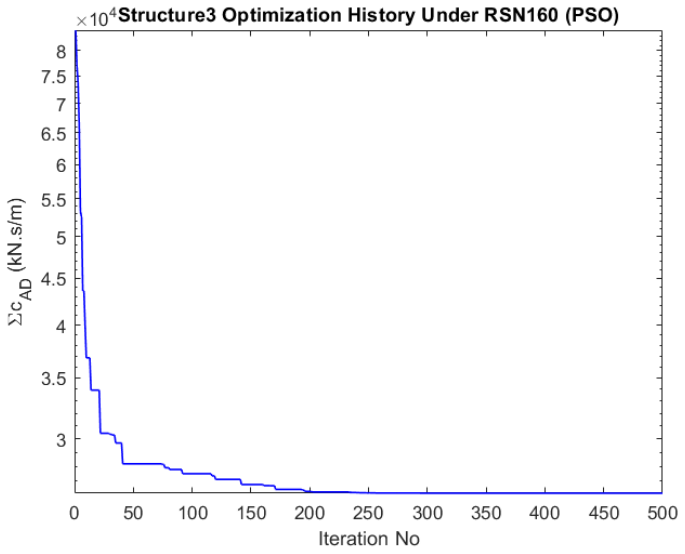

Figure 6.163 Structure3 Optimization History (PSO) Under RSN160

Differential Evolution (DE) optimization history for Structure3 under RSN160 is given below in Figure 6.164.

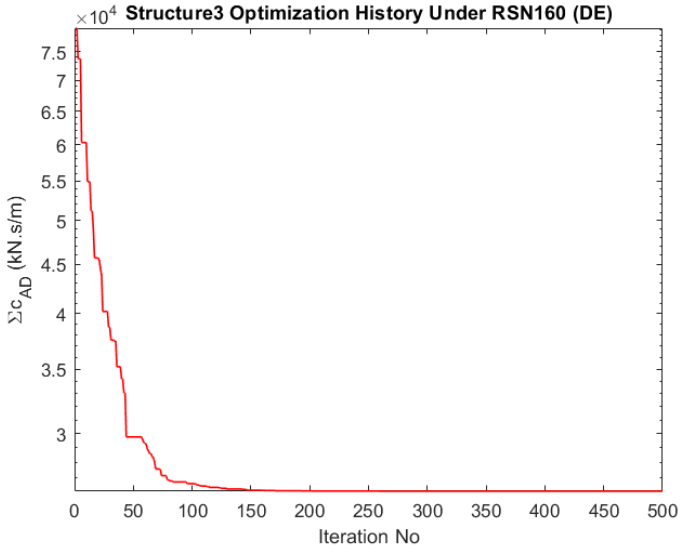

Figure 6.164 Structure3 Optimization History (DE) Under RSN160

Optimum viscous damper (VD) distribution for Structure3 Under RSN160 is given below in Table 6.33.

Table 6.33 Structure3 Optimum viscous damper (VD) distribution Under RSN160

Structure3 Optimum viscous damper (VD) distribution Under RSN160		
Story No	Added Damper PSO (kN.s/m)	Added Damper DE (kN.s/m)
1	7723.504	7658.386
2	6219.297	6145.243
3	5506.163	5424.855
4	4364.863	4268.806
5	2342.338	2203.617
6	0.000	177.514
7	0.000	0.000
8	0.000	0.000
9	0.000	242.823
10	0.000	0.000
Total Global Best	26156.165	26121.244

Comparison of maximum acceleration responses for Structure3 without VD and with optimum VD under RSN160 is given below in Figure 6.165.

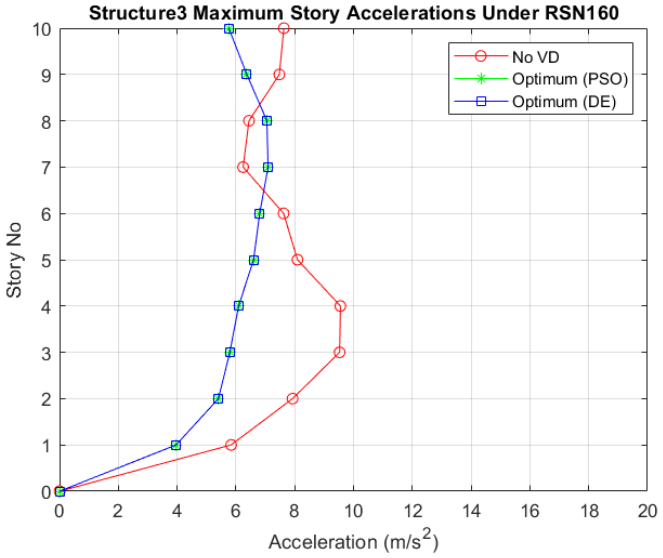

Figure 6.165 Comparison of Maximum Acceleration Responses for Structure3 With VD and Without VD Under RSN160

Comparison of maximum velocity responses for Structure3 without VD and with optimum VD under RSN160 is given below in Figure 6.166.

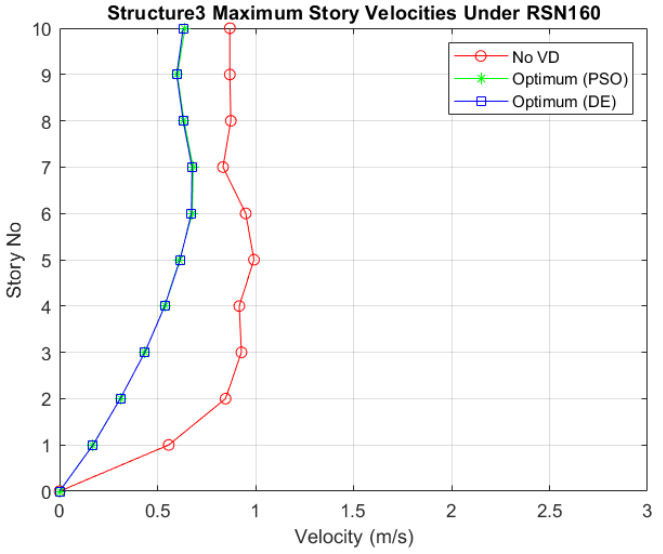

Figure 6.166 Comparison of Maximum Velocity Responses for Structure3 With VD and Without VD Under RSN160

Comparison of maximum displacement responses for Structure3 without VD and with optimum VD under RSN160 is given below in Figure 6.167.

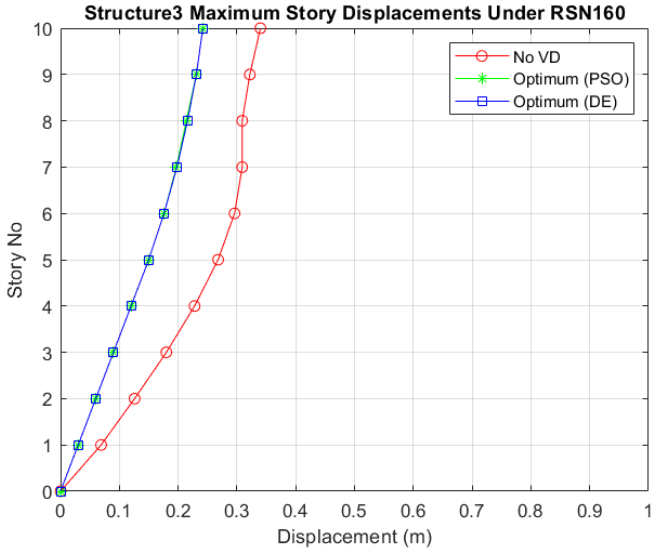

Figure 6.167 Comparison of Maximum Displacement Responses for Structure3 With VD and Without VD Under RSN160

Comparison of peak IDR for Structure3 without VD and with optimum VD under RSN160 is given below in Figure 6.168.

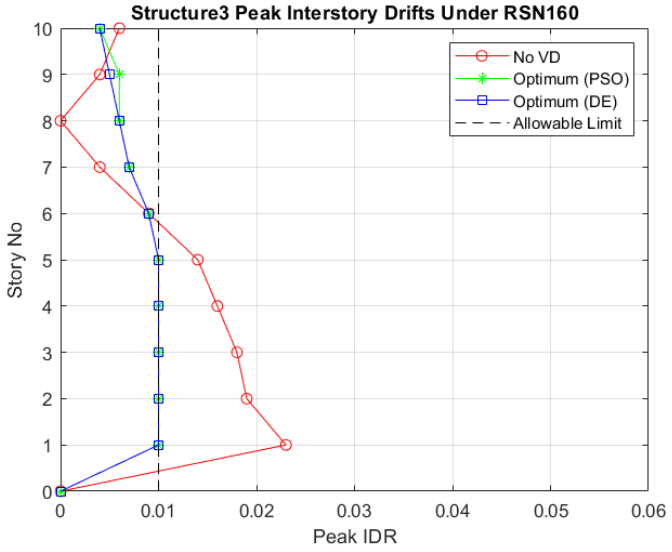

Figure 6.168 Comparison of Peak IDR for Structure3 With VD and Without VD Under RSN160

6.4.6. Under RSN496 (NPNF)

Particle Swarm Optimization (PSO) optimization history for Structure3 under RSN496 is given below in Figure 6.169.

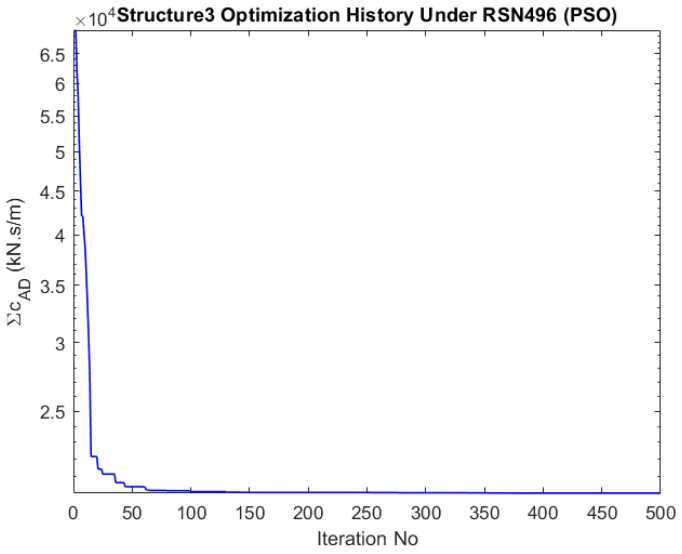

Figure 6.169 Structure3 Optimization History (PSO) Under RSN496

Differential Evolution (DE) optimization history for Structure3 under RSN496 is given below in Figure 6.170.

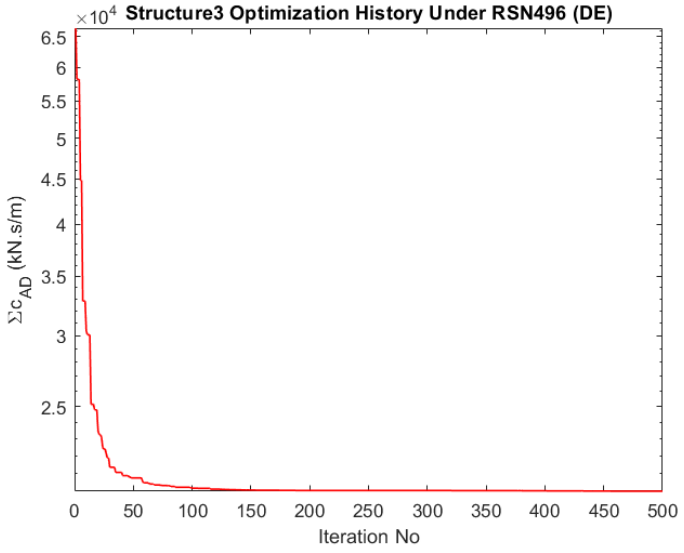

Figure 6.170 Structure3 Optimization History (DE) Under RSN496

Optimum viscous damper (VD) distribution for Structure3 Under RSN496 is given below in Table 6.34.

Table 6.34 Structure3 Optimum viscous damper (VD) distribution Under RSN496

Structure3 Optimum viscous damper (VD) distribution Under RSN496		
Story No	Added Damper PSO (kN.s/m)	Added Damper DE (kN.s/m)
1	10559.880	10559.880
2	6349.844	6349.844
3	0.000	0.000
4	0.000	0.000
5	0.000	0.000
6	0.000	0.000
7	1617.555	1617.555
8	1544.002	1544.002
9	0.000	0.000
10	0.000	0.000
Total Global Best	20071.282	20071.282

Comparison of maximum acceleration responses for Structure3 without VD and with optimum VD under RSN496 is given below in Figure 6.171.

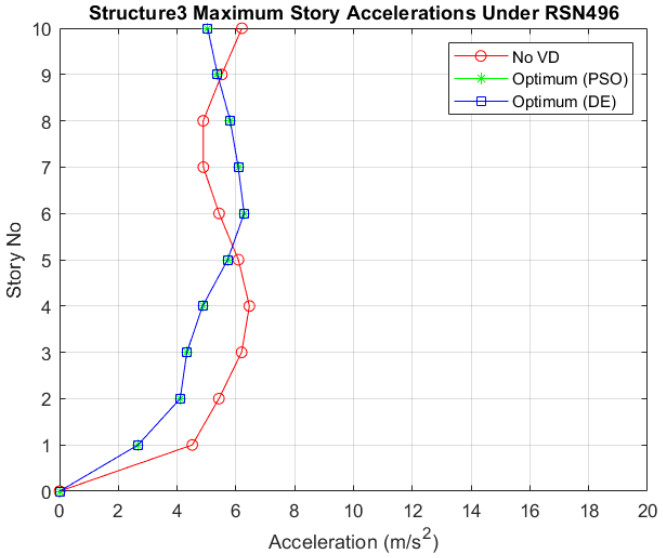

Figure 6.171 Comparison of Maximum Acceleration Responses for Structure3 With VD and Without VD Under RSN496

Comparison of maximum velocity responses for Structure3 without VD and with optimum VD under RSN496 is given below in Figure 6.172.

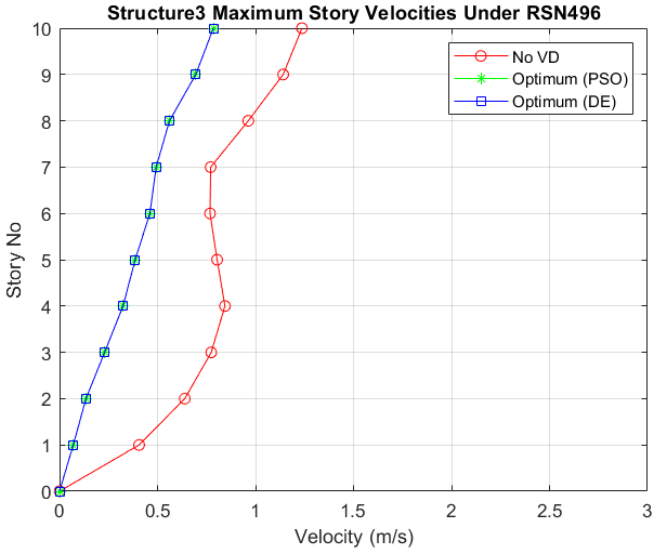

Figure 6.172 Comparison of Maximum Velocity Responses for Structure3 With VD and Without VD Under RSN496

Comparison of maximum displacement responses for Structure3 without VD and with optimum VD under RSN496 is given below in Figure 6.173.

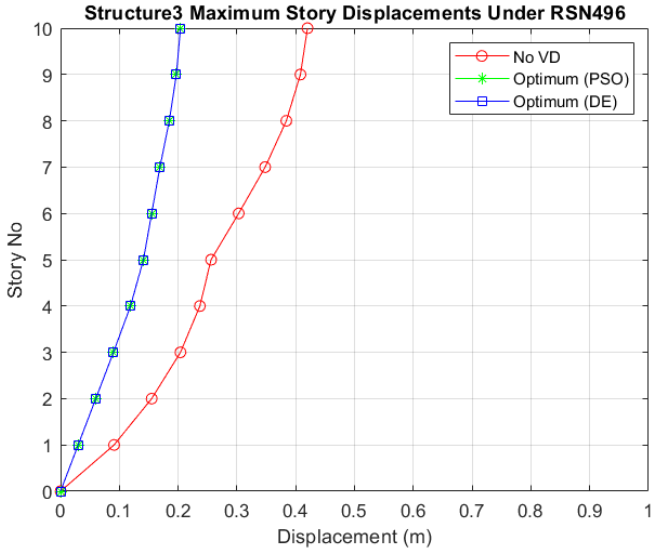

Figure 6.173 Comparison of Maximum Displacement Responses for Structure3 With VD and Without VD Under RSN496

Comparison of peak IDR for Structure3 without VD and with optimum VD under RSN496 is given below in Figure 6.174.

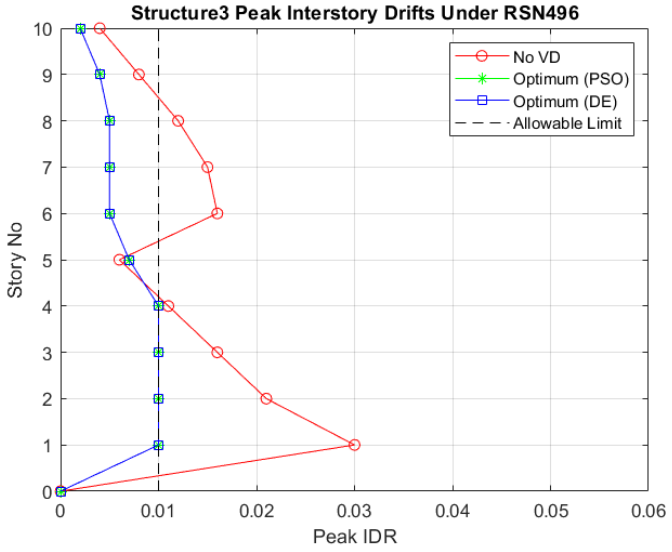

Figure 6.174 Comparison of Peak IDR for Structure3 With VD and Without VD Under RSN496

6.4.7. Under RSN741 (NPNF)

Particle Swarm Optimization (PSO) optimization history for Structure3 under RSN741 is given below in Figure 6.175.

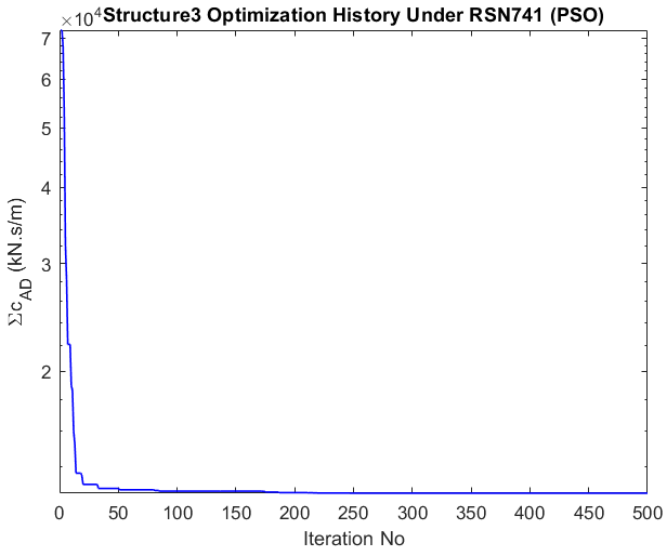

Figure 6.175 Structure3 Optimization History (PSO) Under RSN741

Differential Evolution (DE) optimization history for Structure3 under RSN741 is given below in Figure 6.176.

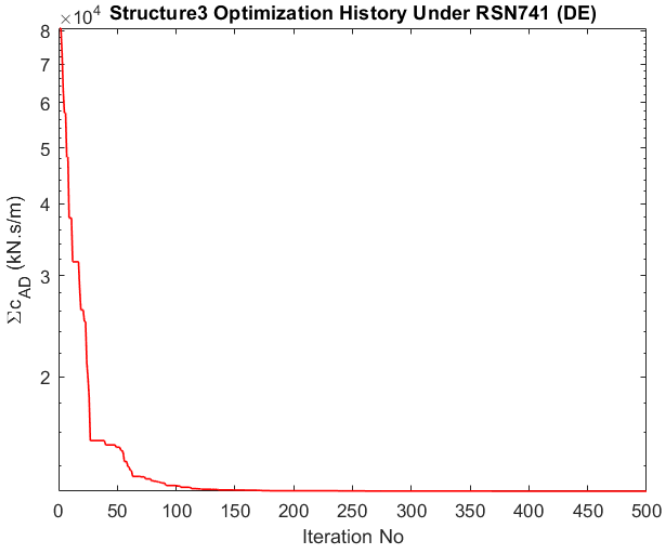

Figure 6.176 Structure3 Optimization History (DE) Under RSN741

Optimum viscous damper (VD) distribution for Structure3 Under RSN741 is given below in Table 6.35.

Table 6.35 Structure3 Optimum viscous damper (VD) distribution Under RSN741

Structure3 Optimum viscous damper (VD) distribution Under RSN741		
Story No	Added Damper PSO (kN.s/m)	Added Damper DE (kN.s/m)
1	8101.266	8192.184
2	3316.259	2800.124
3	339.362	251.033
4	0.000	0.000
5	0.000	326.232
6	0.000	433.201
7	0.000	32.160
8	386.569	386.854
9	503.710	211.688
10	0.000	0.000
Total Global Best	12647.165	12633.475

Comparison of maximum acceleration responses for Structure3 without VD and with optimum VD under RSN741 is given below in Figure 6.177.

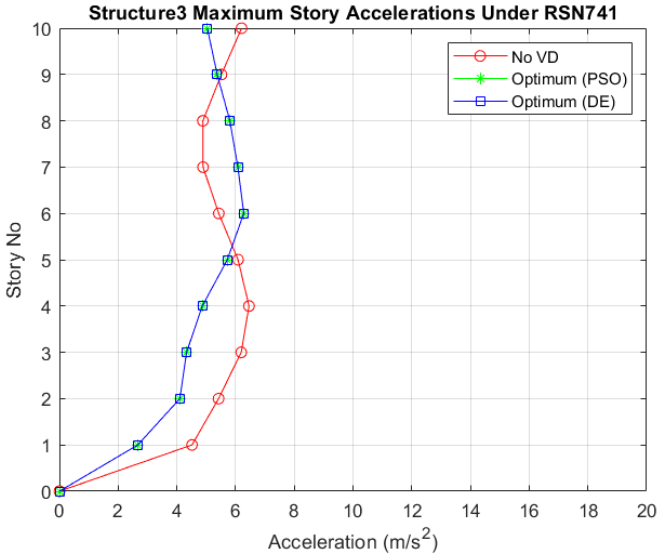

Figure 6.177 Comparison of Maximum Acceleration Responses for Structure3 With VD and Without VD Under RSN741

Comparison of maximum velocity responses for Structure3 without VD and with optimum VD under RSN741 is given below in Figure 6.178.

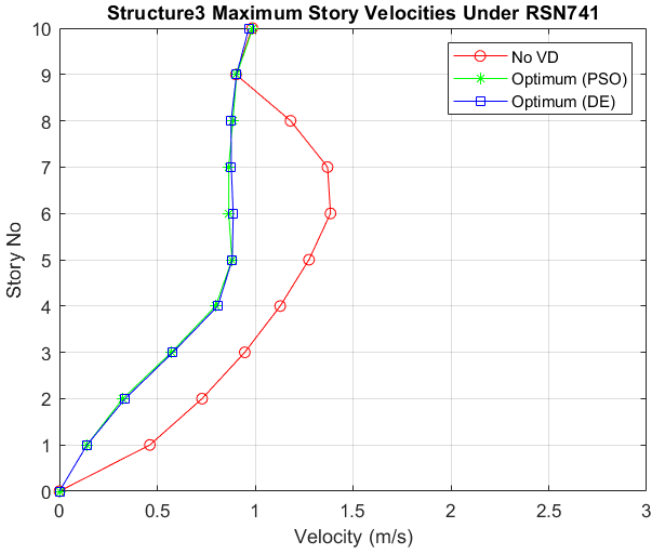

Figure 6.178 Comparison of Maximum Velocity Responses for Structure3 With VD and Without VD Under RSN741

Comparison of maximum displacement responses for Structure3 without VD and with optimum VD under RSN741 is given below in Figure 6.179.

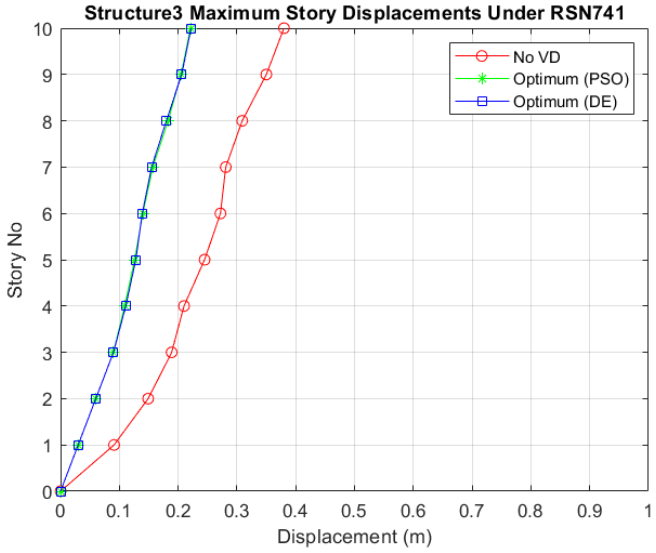

Figure 6.179 Comparison of Maximum Displacement Responses for Structure3 With VD and Without VD Under RSN741

Comparison of peak IDR for Structure3 without VD and with optimum VD under RSN741 is given below in Figure 6.180.

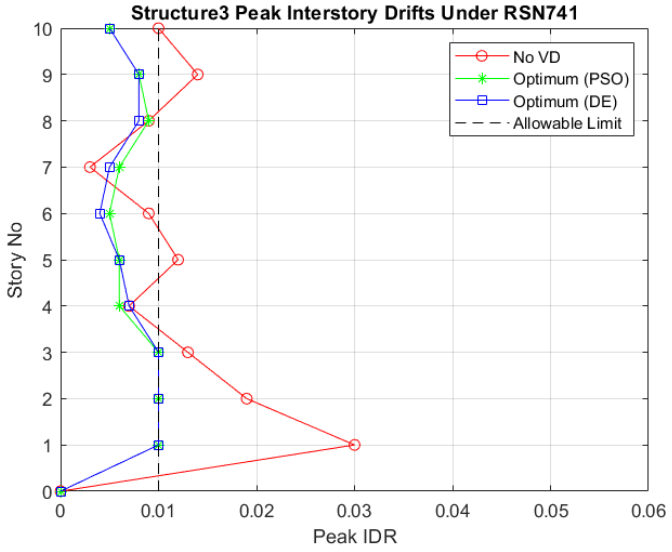

Figure 6.180 Comparison of Peak IDR for Structure3 With VD and Without VD Under RSN741

6.4.8. Under RSN1004 (NPNF)

Particle Swarm Optimization (PSO) optimization history for Structure3 under RSN1004 is given below in Figure 6.181.

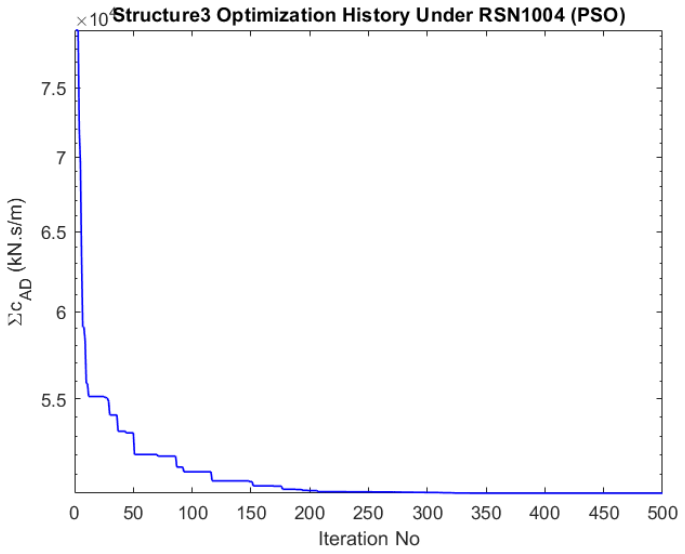

Figure 6.181 Structure3 Optimization History (PSO) Under RSN1004

Differential Evolution (DE) optimization history for Structure3 under RSN1004 is given below in Figure 6.182.

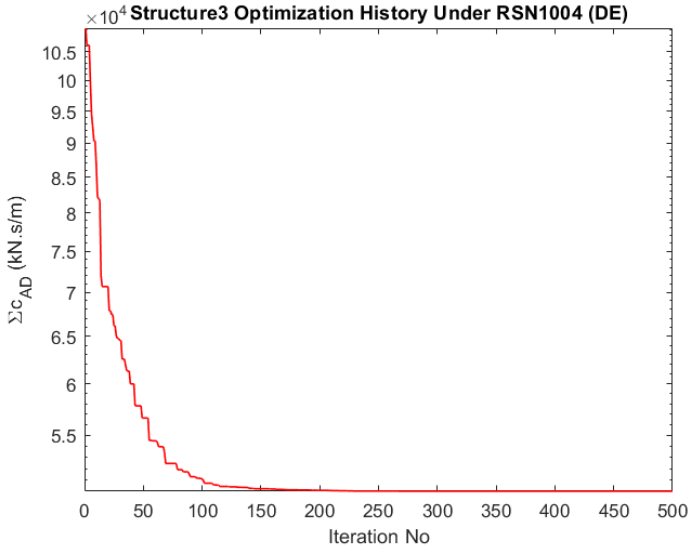

Figure 6.182 Structure3 Optimization History (DE) Under RSN1004

Optimum viscous damper (VD) distribution for Structure3 Under RSN1004 is given below in Table 6.36.

Table 6.36 Structure3 Optimum viscous damper (VD) distribution Under RSN1004

Structure3 Optimum viscous damper (VD) distribution Under RSN1004		
Story No	Added Damper PSO (kN.s/m)	Added Damper DE (kN.s/m)
1	14773.768	14775.492
2	9671.089	9671.498
3	8428.621	8430.092
4	5156.810	5140.385
5	6185.855	6190.189
6	5845.720	5848.640
7	0.000	0.041
8	0.000	0.530
9	0.000	0.011
10	0.000	0.000
Total Global Best	50061.863	50056.878

Comparison of maximum acceleration responses for Structure3 without VD and with optimum VD under RSN1004 is given below in Figure 6.183.

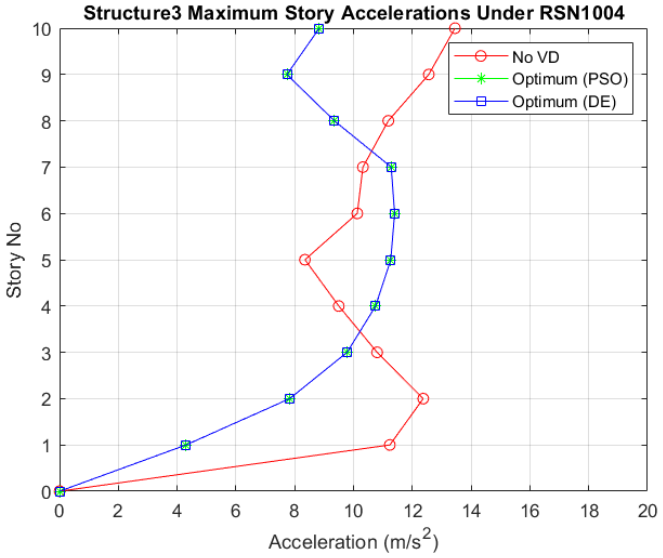

Figure 6.183 Comparison of Maximum Acceleration Responses for Structure3 With VD and Without VD Under RSN1004

Comparison of maximum velocity responses for Structure3 without VD and with optimum VD under RSN1004 is given below in Figure 6.184.

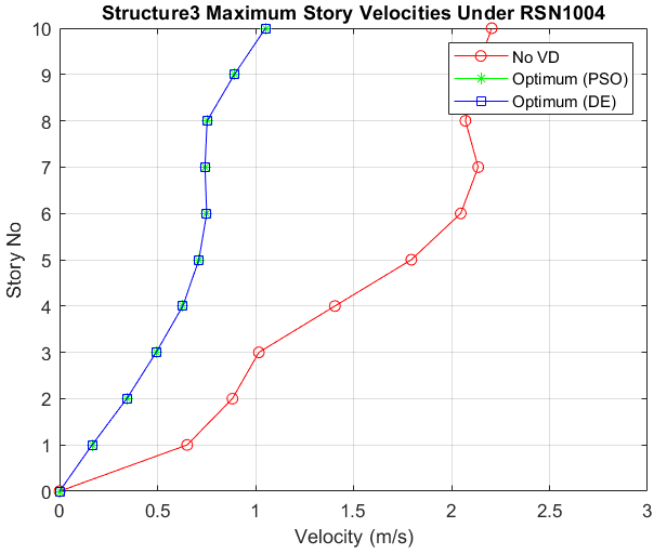

Figure 6.184 Comparison of Maximum Velocity Responses for Structure3 With VD and Without VD Under RSN1004

Comparison of maximum displacement responses for Structure3 without VD and with optimum VD under RSN1004 is given below in Figure 6.185.

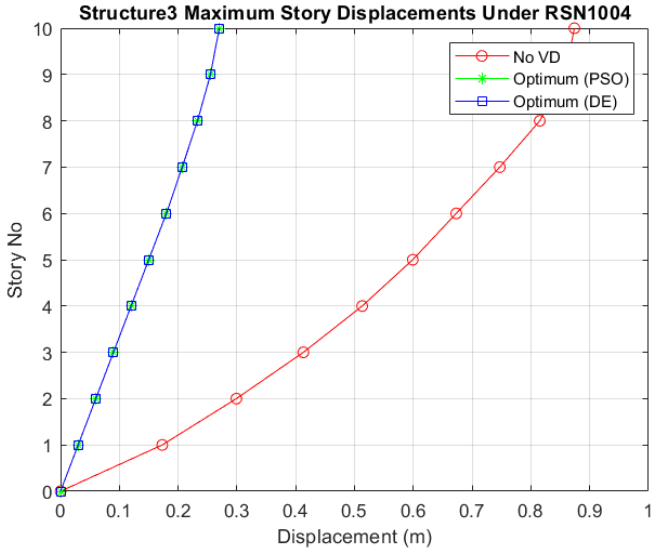

Figure 6.185 Comparison of Maximum Displacement Responses for Structure3 With VD and Without VD Under RSN1004

Comparison of peak IDR for Structure3 without VD and with optimum VD under RSN1004 is given below in Figure 6.186.

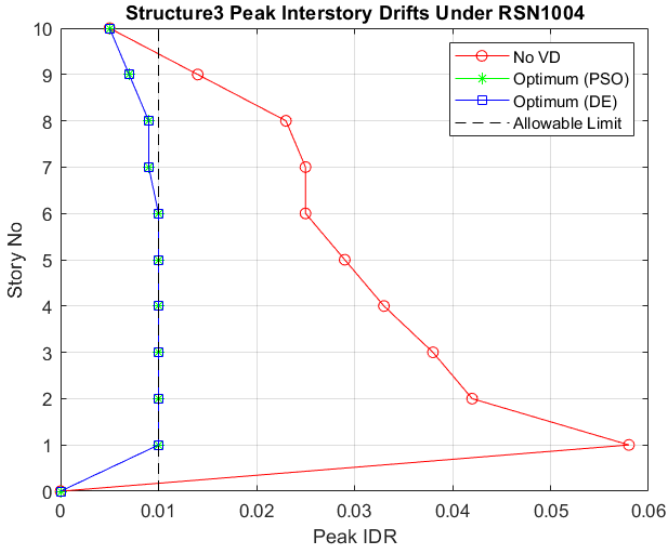

Figure 6.186 Comparison of Peak IDR for Structure3 With VD and Without VD Under RSN1004

6.4.9. Under RSN68 (FF)

Under this earthquake ground motion data, peak IDR of each story is lower than allowable limit. Because of that reason, Structure3 does not need additional VD under RSN68.

Comparison of maximum acceleration responses for Structure3 without VD and with optimum VD under RSN68 is given below in Figure 6.187.

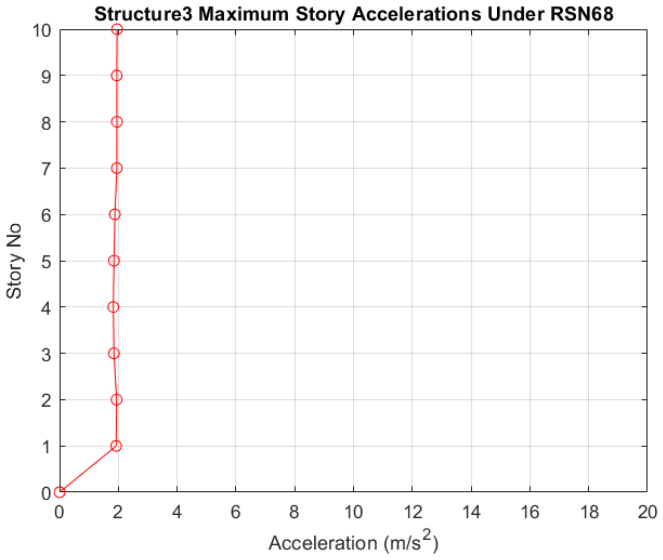

Figure 6.187 Comparison of Maximum Acceleration Responses for Structure3 With VD and Without VD Under RSN68

Comparison of maximum velocity responses for Structure3 without VD and with optimum VD under RSN68 is given below in Figure 6.188.

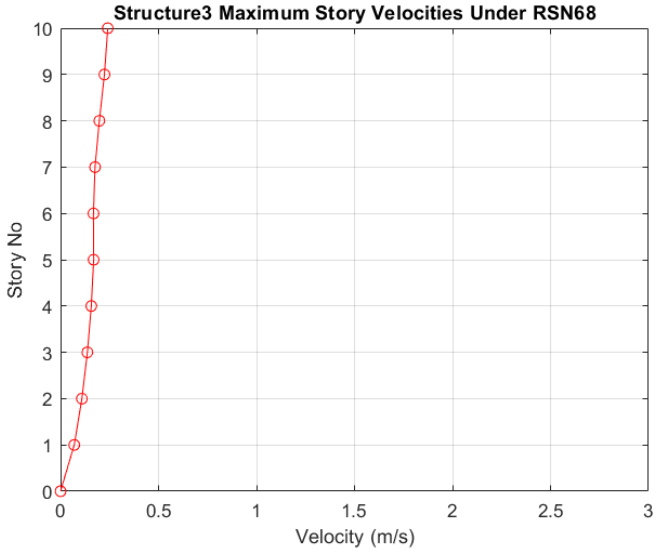

Figure 6.188 Comparison of Maximum Velocity Responses for Structure3 With VD and Without VD Under RSN68

Comparison of maximum displacement responses for Structure3 without VD and with optimum VD under RSN68 is given below in Figure 6.189.

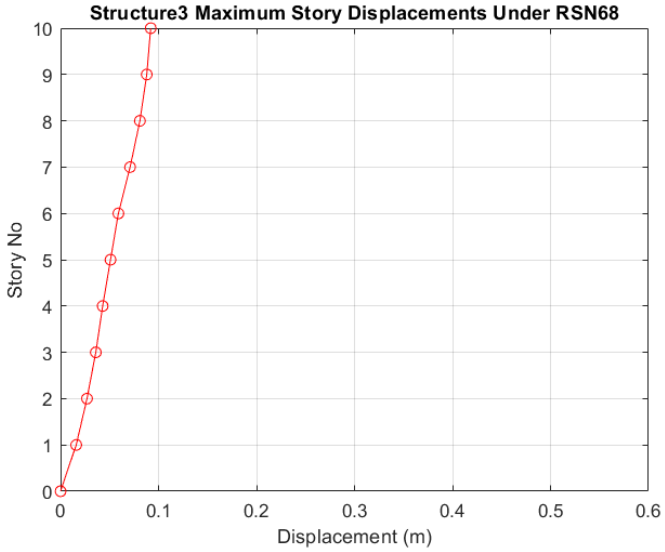

Figure 6.189 Comparison of Maximum Displacement Responses for Structure3 With VD and Without VD Under RSN68

Comparison of peak IDR for Structure3 without VD and with optimum VD under RSN68 is given below in Figure 6.190.

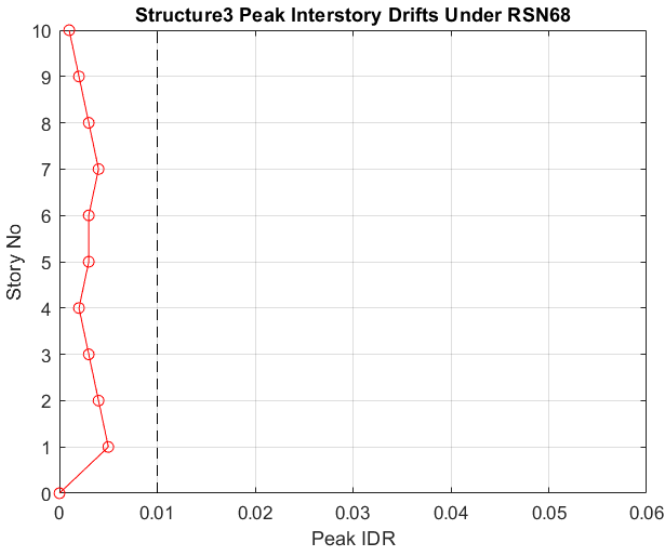

Figure 6.190 Comparison of Peak IDR for Structure3 With VD and Without VD Under RSN68

6.4.10. Under RSN752 (FF)

Under this earthquake ground motion data, peak IDR of each story is lower than allowable limit. Because of that reason, Structure3 does not need additional VD under RSN752.

Comparison of maximum acceleration responses for Structure3 without VD and with optimum VD under RSN752 is given below in Figure 6.191.

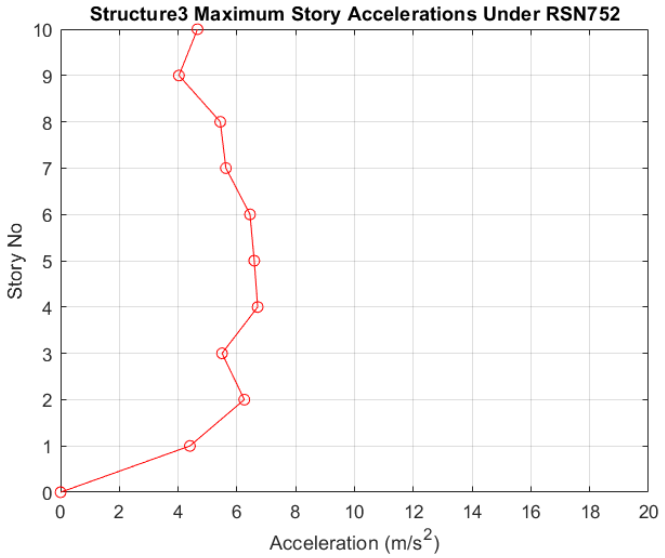

Figure 6.191 Comparison of Maximum Acceleration Responses for Structure3 With VD and Without VD Under RSN752

Comparison of maximum velocity responses for Structure3 without VD and with optimum VD under RSN752 is given below in Figure 6.192.

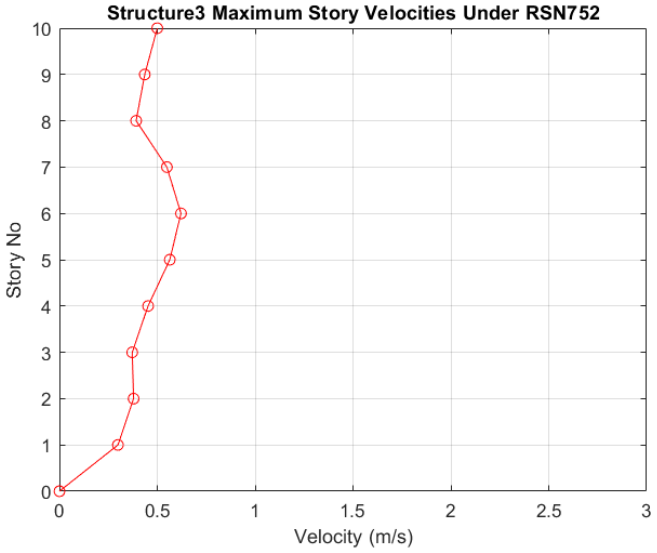

Figure 6.192 Comparison of Maximum Velocity Responses for Structure3 With VD and Without VD Under RSN752

Comparison of maximum displacement responses for Structure3 without VD and with optimum VD under RSN752 is given below in Figure 6.193.

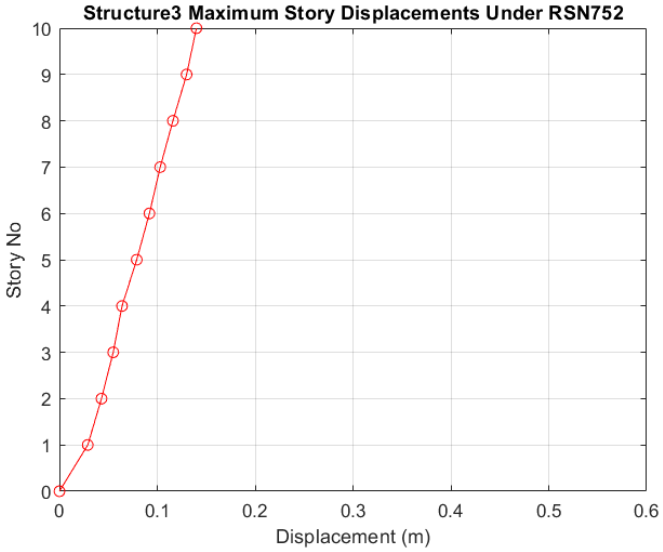

Figure 6.193 Comparison of Maximum Displacement Responses for Structure3 With VD and Without VD Under RSN752

Comparison of peak IDR for Structure3 without VD and with optimum VD under RSN752 is given below in Figure 6.194.

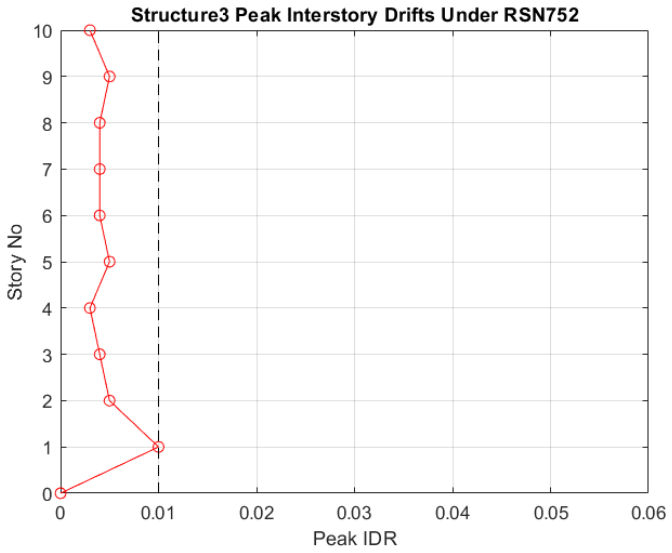

Figure 6.194 Comparison of Peak IDR for Structure3 With VD and Without VD Under RSN752

6.4.11. Under RSN953 (FF)

Under this earthquake ground motion data, peak IDR of each story is lower than allowable limit. Because of that reason, Structure3 does not need additional VD under RSN953.

Comparison of maximum acceleration responses for Structure3 without VD and with optimum VD under RSN953 is given below in Figure 6.195.

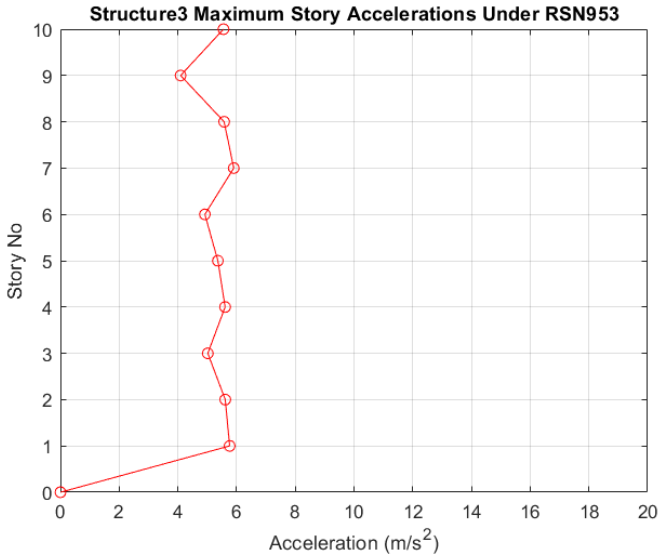

Figure 6.195 Comparison of Maximum Acceleration Responses for Structure3 With VD and Without VD Under RSN953

Comparison of maximum velocity responses for Structure3 without VD and with optimum VD under RSN953 is given below in Figure 6.196.

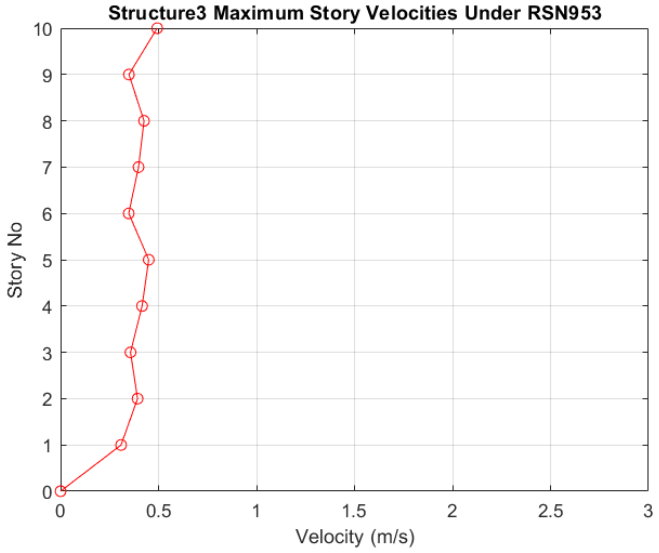

Figure 6.196 Comparison of Maximum Velocity Responses for Structure3 With VD and Without VD Under RSN953

Comparison of maximum displacement responses for Structure3 without VD and with optimum VD under RSN953 is given below in Figure 6.197.

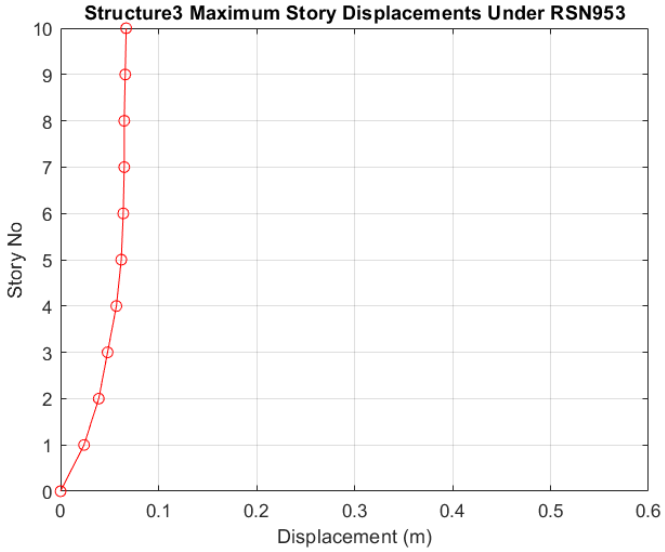

Figure 6.197 Comparison of Maximum Displacement Responses for Structure3 With VD and Without VD Under RSN953

Comparison of peak IDR for Structure3 without VD and with optimum VD under RSN953 is given below in Figure 6.198.

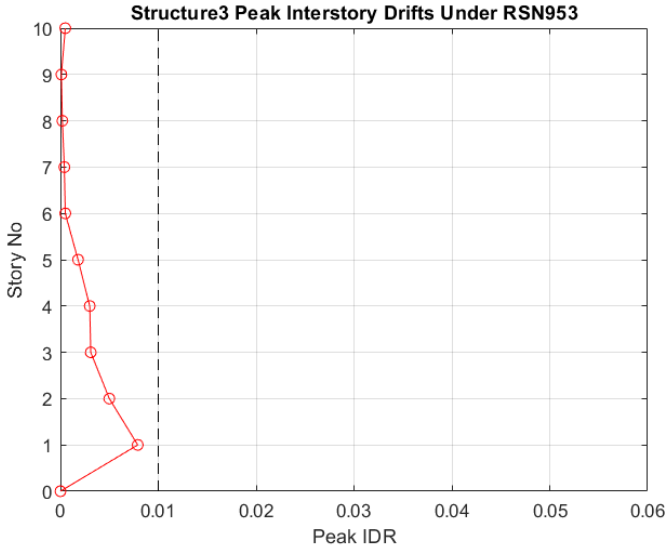

Figure 6.198 Comparison of Peak IDR for Structure3 With VD and Without VD Under RSN953

6.4.12. Under RSN1111 (FF)

Under this earthquake ground motion data, peak IDR of each story is lower than allowable limit. Because of that reason, Structure3 does not need additional VD under RSN1111.

Comparison of maximum acceleration responses for Structure3 without VD and with optimum VD under RSN1111 is given below in Figure 6.199.

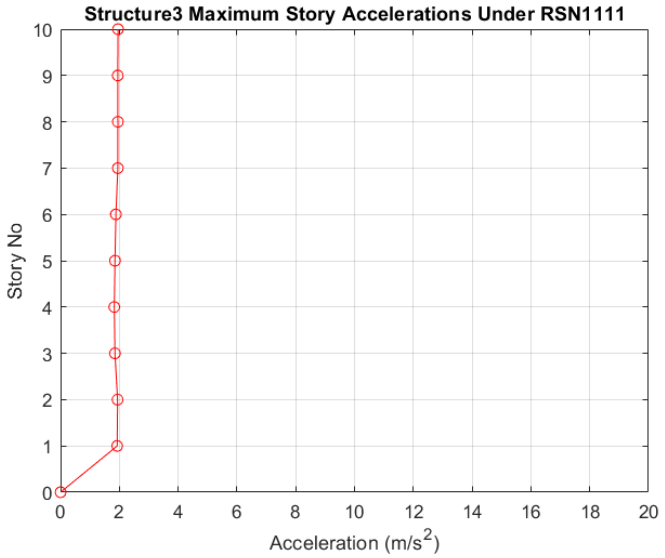

Figure 6.199 Comparison of Maximum Acceleration Responses for Structure3 With VD and Without VD Under RSN1111

Comparison of maximum velocity responses for Structure3 without VD and with optimum VD under RSN1111 is given below in Figure 6.200.

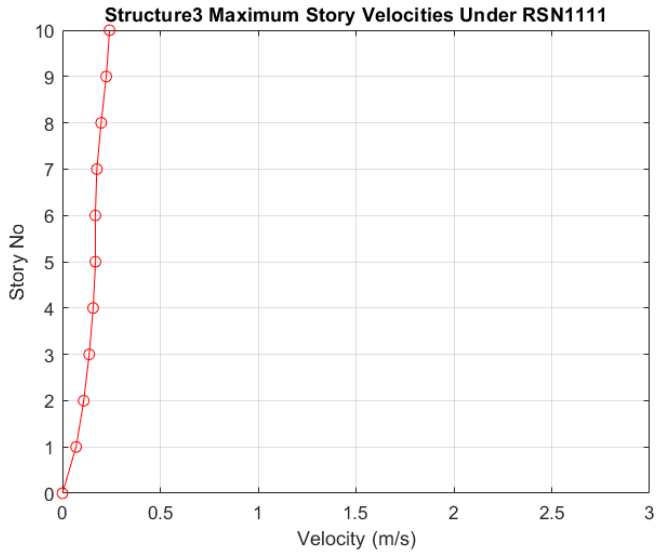

Figure 6.200 Comparison of Maximum Velocity Responses for Structure3 With VD and Without VD Under RSN1111

Comparison of maximum displacement responses for Structure3 without VD and with optimum VD under RSN1111 is given below in Figure 6.201.

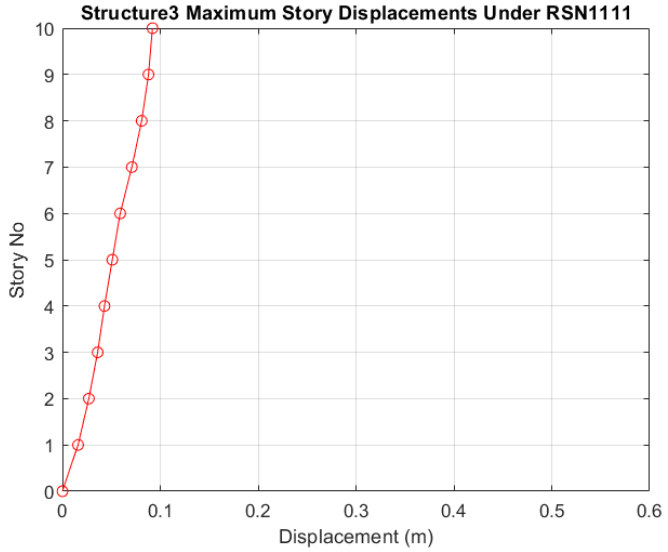

Figure 6.201 Comparison of Maximum Displacement Responses for Structure3 With VD and Without VD Under RSN1111

Comparison of peak IDR for Structure3 without VD and with optimum VD under RSN1111 is given below in Figure 6.202.

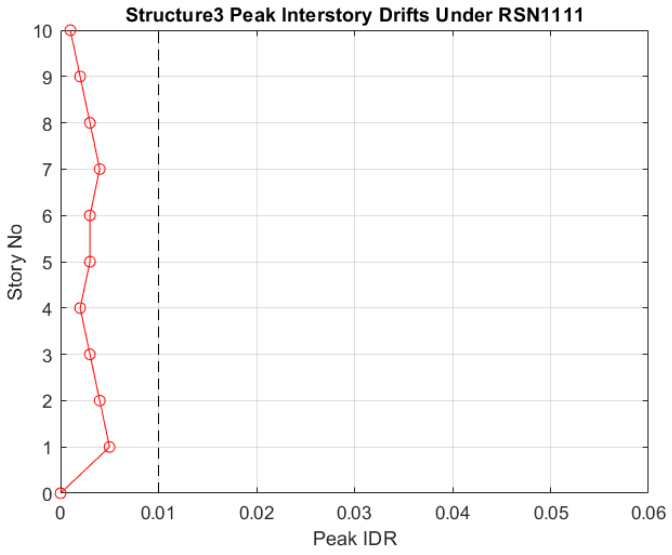

Figure 6.202 Comparison of Peak IDR for Structure3 With VD and Without VD Under RSN1111

7. CONCLUSIONS

7.1. Summary and Conclusions

In this thesis work, a methodology based on inter-story drifts was proposed to rehabilitate building structures with soft story structural irregularity with optimal viscous damper distribution by using two different meta-heuristic search algorithms. These are Differential Evolution (DE) and Particle Swarm Optimization (PSO) algorithms. Numerical examples were conducted in three different shear buildings under twelve different ground motion data. Ground motion data involve four Pulse Near Fault (PNF), four No Pulse Near Fault (NPNF), and four Far Fault (FF) records. Dynamic analyses were conducted by using Newmark-Beta linear acceleration method. Optimum viscous damper distributions were determined for three different shear buildings via DE and PSO algorithms. Dynamic analysis results consist of three main cases. These are no viscous damper, optimal viscous damper distribution via DE algorithm, and optimal viscous damper distribution via PSO algorithm. The result of dynamic analyses were compared and reported for these three cases.

Outcomes of this thesis study are given below.

- Soft story structural irregularity has a negative impact on the dynamic behavior of building structures under earthquake ground motion.
- Soft story structural irregularity increases peak IDR.
- Soft story structural irregularity causes abrupt changes in peak IDR between adjacent stories.
- Maximum dynamic responses were observed under near-fault ground motion records, particularly pulse near-fault ground motion records.
- Pulse effect has an important influence on dynamic responses of shear building and causes higher dynamic responses.

- Near source ground motion records have an important influence on optimum damper distribution problems for shear buildings with soft story structural irregularity.
- Maximum peak IDR values were observed under near-source ground motion records especially pulse near-fault ground motion records.
- Viscous dampers are remarkably effective in reducing building structures' dynamic response.
- It is possible to keep peak IDR in allowable limits with an optimal viscous damper distribution for structures with soft story structural irregularity.
- Maximum amount of damping coefficient is required under near-source ground motion records especially pulse near-fault ground motions records, due to higher dynamic responses.
- In some cases, additional viscous dampers were not required under far fault ground motions records since none of the stories exceeded the allowable peak IDR limit.
- As the decision variables increase, the optimization problem gets more challenging.
- As the decision variables increase, the gap between global best solutions that DE and PSO found is slightly increasing.
- DE and PSO algorithms can be successfully implemented to optimum viscous damper distribution problems for shear buildings with soft story structural irregularity.
- As the decision variables increase, DE founds slightly better global optimum solutions than PSO.
- It was observed that the performance of DE and PSO algorithms are close to each other; however, the performance of the DE algorithm is slightly better than the PSO algorithm.
- Proposed methodology successful in rehabilitating shear building with soft story irregularity.

- From numerical examples, it was observed that negative impacts of the soft story irregularity could be eliminated by optimal viscous damper distribution.
- Suggested procedure limits peak IDR values and reduces the dynamic response of shear building with soft story irregularity.

7.2. Recommendations for Future Studies

As already mentioned, the suggested procedure was tested on idealized shear building structures. A further study can be conducted on the optimal distribution of viscous dampers in 3D building frames. Also, in the scope of this study, linear time history analysis is utilized to analyze dynamic response under earthquake ground motions. Further research can be performed by using nonlinear time history analysis to consider the nonlinear response of the structure. Moreover, in the scope of this thesis study effect of soil-structure interaction is neglected. A further study can be conducted by considering the influence of soil-structure interaction.

REFERENCES

[1] MD Symans, FA Charney, AS Whittaker, MC Constantinou, CA Kircher, MW Johnson, and RJ McNamara. Energy dissipation systems for seismic applications: current practice and recent developments. *Journal of Structural Engineering*, 134(1):3–21, **2008**.

[2] MC Constantinou, TT Soong, and GF Dargush. Passive energy dissipation systems for structural design and retrofit. **1998**.

[3] MC Constantinou and MD Symans. *Experimental and Analytical Investigation of Seismic Response of Structures with Supplemental Fluid Viscous Dampers*. National Center for Earthquake Engineering Research Buffalo, NY, **1992**.

[4] MC Constantinou, MD Symans, P Tsopelas, DP Taylor, et al. Fluid viscous dampers in applications of seismic energy dissipation and seismic isolation. *Proceedings ATC 17*, 1:581–592, **1993**.

[5] MD Symans and MC Constantinou. Passive fluid viscous damping systems for seismic energy dissipation. *ISET Journal of Earthquake Technology*, 35(4):185–206, **1998**.

[6] MC Constantinou and IG Tadjbakhsh. Optimum design of a first story damping system. *Computers & Structures*, 17(2):305–310, **1983**.

[7] M Gürgöze and PC Müller. Optimal positioning of dampers in multi-body systems. *Journal of Sound and Vibration*, 158(3):517–530, **1992**.

[8] I Takewaki. Optimal damper placement for planar building frames using transfer functions. *Structural and Multidisciplinary Optimization*, 20(4):280–287, **2000**.

[9] JA Bishop and AG Striz. On using genetic algorithms for optimum damper placement in space trusses. *Structural and Multidisciplinary Optimization*, 28(2):136–145, **2004**.

[10] E Aydin. Optimal damper placement based on base moment in steel building frames. *Journal of Constructional Steel Research*, 79:216–225, **2012**.

[11] E Aydin, B Ozturk, and M Dutkiewicz. Analysis of efficiency of passive dampers in multistorey buildings. *Journal of Sound and Vibration*, 439:17–28, **2019**.

[12] H Cetin, E Aydin, and B Ozturk. Optimal design and distribution of viscous dampers for shear building structures under seismic excitations. *Frontiers in Built Environment*, 5:90, **2019**.

[13] E Aydin, B Ozturk, A Bogdanovic, and EN Farsangi. Influence of soil-structure interaction (ssi) on optimal design of passive damping devices. In *Structures*, volume 28, pages 847–862. Elsevier, **2020**.

[14] B Ozturk. *Seismic drift response of building structures in seismically active and near-fault regions*. Ph.D. thesis, Purdue University, **2003**.

[15] TC Graber, United States. Bureau of Land Management, and United States. Bureau of Reclamation. *FEMA 310, Seismic Evaluation of Buildings, Boise District Office Building, Boise, Ada County, Idaho*. U.S. Department of the Interior, Bureau of Reclamation, **1999**.

[16] M Ouazir, A Kassoul, A Ouazir, and B Achour. Inelastic seismic response of torsionally unbalanced structures with soft first story. *Asian Journal of Civil Engineering*, 19(5):571–581, **2018**.

[17] A.S.C. Engineers. *Minimum Design Loads for Buildings and Other Structures: ASCE Standard 7-10*. ASCE standard. American Society of Civil Engineers, **2010**.

[18] Polska. Polski Komitet Normalizacyjny. *Eurocode 8: Design of structures for earthquake resistance - Part 1: General rules, seismic actions and rules for buildings*. Polski Komitet Normalizacyjny, **2005**.

[19] *TBEC2018, Turkish Building Earthquake Code*. Republic of Turkey Disaster and Emergency Management Presidency, Ankara, **2018**.

[20] H Sezen, AS Whittaker, KJ Elwood, and KM Mosalam. Performance of reinforced concrete buildings during the august 17, 1999 kocaeli, turkey earthquake, and seismic design and construction practise in turkey. *Engineering Structures*, 25(1):103–114, **2003**.

[21] JM Jara, EJ Hernández, BA Olmos, and G Martínez. Building damages during the September 19, 2017 earthquake in Mexico City and seismic retrofitting of existing first soft-story buildings. *Engineering Structures*, 209:109977, **2020**.

[22] B Zhao, F Taucer, and T Rossetto. Field investigation on the performance of building structures during the 12 May 2008 Wenchuan earthquake in China. *Engineering Structures*, 31(8):1707–1723, **2009**.

[23] R. Villaverde. *Fundamental Concepts of Earthquake Engineering*. CRC Press, **2009**.

[24] P Mahmoodi, LE Robertson, M Yontar, C Moy, and L Feld. Performance of viscoelastic dampers in world trade center towers. In *Dynamics of Structures*, pages 632–644. ASCE, **1987**.

[25] SA Ashour and RD Hanson. Elastic seismic response of buildings with supplemental damping. report no. umce 87-1, University of Michigan. *Ann Arbor, MI*, **1987**.

[26] KC Chang, TT Soong, ML Lai, and EJ Nielsen. Viscoelastic dampers as energy dissipation devices for seismic applications. *Earthquake Spectra*, 9(3):371–387, **1993**.

[27] RL Mayes and NA Mowbray. The effect of coulomb damping on multidegree of freedom elastic structures. *Earthquake Engineering & Structural Dynamics*, 3(3):275–286, **1974**.

[28] WO Keightley. Building damping by coulomb friction. In *Proc., 6th WCEE*, pages 3043–3048. **1977**.

[29] AS Pall and R Pall. Friction-dampers for seismic control of buildings–a canadian experience. In *Eleventh World Conference on Earthquake Engineering, Acapulco, Mexico*. **1996**.

[30] NM Newmark and WJ Hall. Earthquake spectra and design. *Engineering Monographs on Earthquake Criteria*, **1982**.

[31] RW Clough and J Penzien. *Dynamics of Structures*. McGraw-Hill, **1993**.

[32] AK Chopra. *Dynamics of Structures: Theory and Applications to Earthquake Engineering*. Prentice-Hall international series in civil engineering and engineering mechanics. Prentice Hall, **2000**.

[33] R Storn and K Price. Differential Evolution–A Simple and Efficient Heuristic for Global Optimization over Continuous Spaces. *Journal of Global Optimization*, 11(4):341–359, **1997**.

[34] R Eberhart and J Kennedy. Particle swarm optimization. In *Proceedings of the IEEE International Conference on Neural Networks*, volume 4, pages 1942–1948. Citeseer, **1995**.

[35] Y Shi and R Eberhart. A modified particle swarm optimizer. In *1998 IEEE International Conference on Evolutionary Computation Proceedings. IEEE World Congress on Computational Intelligence*, pages 69–73. IEEE, **1998**.

[36] E Aydin. A simple damper optimization algorithm for both target added damping ratio and interstorey drift ratio. *Earthquakes and Structures*, 5(1):83–109, **2013**.

[37] `https://ngawest2.berkeley.edu/`.

[38] United States. Federal Emergency Management Administration. *Quantification of Building Seismic Performance Factors, FEMA P695/ June 2009*. **2009**.

[39] S Djerouni, M Abdeddaim, S Elias, and R Rupakhety. Optimum double mass tuned damper inerter for control of structure subjected to ground motions. *Journal of Building Engineering*, 44:103259, **2021**.